Multidisciplinary Structural Design and Optimization for Performance, Cost, and Flexibility

by

William David Nadir

B.S., University of California, Los Angeles, 2001

Submitted to the Department of Aeronautics and Astronautics
in partial fulfillment of the requirements for the degree of

Master of Science in Aeronautics and Astronautics

at the

MASSACHUSETTS INSTITUTE OF TECHNOLOGY

February 2005

Author . . . .
Department of Aeronautics and Astronautics
January 28, 2005

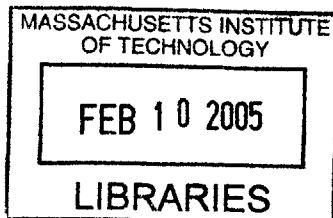Certified by . . . .
Olivier L. de Weck
Robert N. Noyce Assistant Professor of Aeronautics and Astronautics
and Engineering Systems
Thesis Supervisor

Accepted by . . . .
Jaime Peraire
Professor of Aeronautics and Astronautics
Chair, Committee on Graduate Students

Multidisciplinary Structural Design and Optimization for Performance, Cost, and Flexibility

by

William David Nadir

Abstract

Reducing cost and improving performance are two key factors in structural design. In the aerospace and automotive industries, this is particularly true with respect to design criteria such as strength, stiffness, mass, fatigue resistance, manufacturing cost, and maintenance cost. This design philosophy of reducing cost and improving performance applies to structural components as well as complex structural systems. Design for flexibility is one method of reducing costs and improving performance in these systems. This design methodology allows systems to be modified to respond to changes in desired functionality. A useful tool for this design practice is multidisciplinary design optimization (MDO). This thesis develops and exercises an MDO framework for exploration of design spaces for structural components, subsystems, and complex systems considering cost, performance, and flexibility. The structural design trade off of sacrificing strength, mass efficiency, manufacturing cost, and other "classical" optimization criteria at the component level for desirable properties such as reconfigurability at higher levels of the structural system hierarchy is explored in three ways in this thesis. First, structural shape optimization is performed at the component level considering structural performance and manufacturing cost. Second, topology optimization is performed for a reconfigurable system of structural elements. Finally, structural design to reduce cost and increase performance is performed for a complex system of structural components. A new concept for modular, reconfigurable spacecraft design is introduced and a design application is presented.

Thesis Supervisor: Olivier L. de Weck
Title: Robert N. Noyce Assistant Professor of Aeronautics and Astronautics and Engineering Systems

Acknowledgments

First, I thank my Mom for always encouraging me to try my best and do what I love. Without her encouragement I would certainly not have made it to MIT.

Second, I thank my adviser, Olivier de Weck, for believing in me, hiring me as a research assistant, funding my education, and providing insightful feedback on my research. With a busy schedule and many other graduate students to advise, he has always been very responsive to my requests and always had great ideas for me about my research. I also thank him for his contribution to the modular spacecraft design concept presented in Chapter 4.

I thank Il Yong Kim for helping me with my research, providing me with the opportunity to work on interesting projects, and allowing me to publish research papers as first author during my first year of graduate school. His guidance on my research projects was invaluable.

Thanks to everybody else that supported me during my time at MIT. Thank you Deb Howell, Paul Mitchell, Leeland Ekstrom, and Mike Rinehart for your support during my graduate career. I also thank Wilfried Hofstetter for providing much of the Mars and Moon mission architecture and vehicle conceptual design data in Chapter 4 and for his advice and other help with my research.

Thanks to Justin Wong for his contribution to the literature survey in Chapter 4. Also, thanks to Thomas Coffee for the investigation into the tiling theory associated with the modular design concept in Chapter 4.

Contents

List of Figures

14

15

List of Tables

Nomenclature

Abbreviations

AWJ	Abrasive Waterjet
AWS	Adaptive Weighted Sum
CAD	Computer Aided Design
CAE	Computer Aided Engineering
CAM	Computer Aided Manufacturing
CM	Command Module
CNC	Computer Numerically Controlled
DARPA	Defense Advanced Research Projects Agency
DFX	Design for Flexibility
DSM	Design Structure Matrix
ESM	Extended Service Module
ERV	Earth Return Vehicle
FEA	Finite Element Analysis
FEM	Finite Element Modeling
GUI	Graphical User Interface
IAP	Independent Activities Period
IMLEO	Initial Mass in Low Earth Orbit
ISS	International Space Station
JWST	James Webb Space Telescope
LCC	Life Cycle Cost
LEO	Low Earth Orbit
LLO	Low Lunar Orbit

LMO	Low Mars Orbit
MAGLEV	Magnetic Levitation
MAV	Mars Ascent Vehicle
MDO	Multidisciplinary Design Optimization
MIT	Massachusetts Institute of Technology
NASA	National Aeronautics and Space Administration
NASA-DRM	NASA Design Reference Mission
NURBS	Non-Uniform Rational B-Spline
OASIS	Orbital Aggregation and Space Infrastructure Systems
OM	Orbital (Maneuvering) Module
RCS	Reaction Control System
SM	Service Module
SOI	Sphere of Influence
TEI	Trans-Earth Injection
TM	Transfer Module
TMI	Trans-Mars Injection
TSH	Transfer and Surface Habitat

Symbols

a	Edge length of octahedron
b	Edge length of truncated octahedron
C	Abrasive waterjet (AWJ) cutting speed estimation constant
C_{man}	Total manufacturing cost, \$
d_m	Mixing tube diameter of the AWJ cutting machine, in
d_o	AWJ cutter orifice diameter, in
D_{cs}	Truncated octahedron circumsphere diameter, m
D_{hex}	Truncated octahedron hexagonal face insphere diameter, m
D_{sq}	Truncated octahedron square face insphere diameter, m
E	AWJ cutter error limit
f_a	Abrasive factor for abrasive used in AWJ cutter
f_{ECLS}	Environmental control and life support system recovery factor
f_s	Design variable scaling factor
h	Thickness of material machined by AWJ, cm
H	Hessian matrix
J	Objective function
l_i	Curve length of constant cut speed section, in
L_j	Step length for j^{th} step along cut curve
m	Number of curves being optimized in the structure
$\dot{m}_{cons}$	Consumables mass flow rate, kg/crew/day
M	Mass, kg
M_a	AWJ abrasive flow rate, lb/min
n	Number of modules
n_i	Number of control points for the ith curve
n_{lc}	Number of loading cases considered
n_{max}	Loading case number with maximum vertical deflection constraint value
N_{crew}	Number of crew
$N_{i,k}$	NURBS basis function of degree k for i_{th} knot
N_m	Machinability Number

23

OC	Overhead cost for machine shop, \$/hr
P_i	Knot coordinates for i_{th} NURBS control point
P_w	AWJ water pressure, ksi
q	AWJ cutting quality
R	Arc section cut radius for AWJ cutter, in
S_i	Total number of steps along i_{th} cutting curve
Δt_{man}	Manned duration, days
u	AWJ cutting speed, in/min
u_{as}	AWJ arc section cutting speed approximation, in/min
u_{max}	AWJ maximum linear cutting speed approximation, in/min
V	Volume, m^3
ΔV	Velocity change, m/s
w_i	Width of ith truss element, in
x	Vector of X-coordinate design variables
$x^{(j)}$	Vector of element cross-sectional areas of jth length, cm^2
X	Vector of design variables, cm^2
y	Vector of Y-coordinate design variables
Y	Configuration of structural elements
α	Objective function weighting factor
δ	Deflection, mm
σ	Stress, Pa
Θ	Revolution angle, deg
μ_j	Design reconfigurability for a structural system of j design elements

Chapter 1

Introduction

1.1 Motivation

Structures play a vital role in the everyday lives of people. Structures are used in transportation vehicles for the delivery of goods and services which improve productivity. For example, structures play a critical role in the automotive and aerospace industries. Modern transportation and communication systems make significant use of the products provided by these industries.

Although these systems each make use of structures, they have different constraints imposed upon their respective vehicle structural designs (see Figure 1-1). For example, the automotive industry is generally not required to design vehicle structures as efficiently as aircraft and spacecraft. This is due to the fact that people generally want affordable cars, which reduces the amount of money invested in structural design per automobile sold. Aircraft manufacturers, on the other hand, require higher structural mass efficiency because aircraft are expensive and their customer, the airline industry, wants to fill aircraft with as many paying customers (payload mass), as opposed to structural mass, as possible. Spacecraft manufacturers, dealing with customers concerned with high launch costs, design mass efficient structures to minimize launch mass. However, payload mass efficiency for transportation spacecraft is lower than automobiles and aircraft because transportation spacecraft require massive complex equipment and fuel tank structures for mission success. Transportation

spacecraft are significantly more expensive than both aircraft and spacecraft due to costly customized structural design, vehicle complexity, and lower production volume.
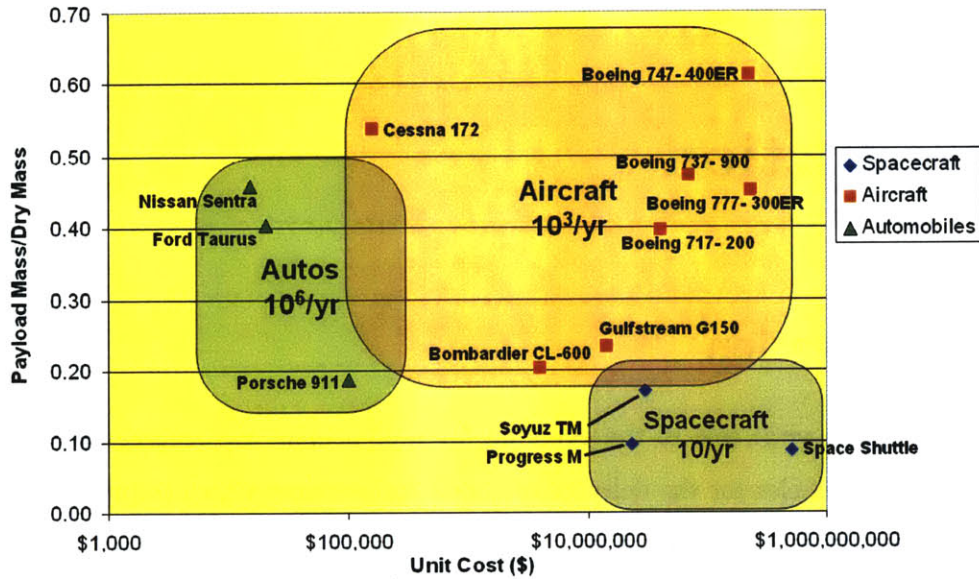
Figure 1-1: Payload mass efficiency versus production cost per unit and production rate for the automobiles, aircraft, and spacecraft. Approximate production rate volumes are listed.

For the automobiles, aircraft, and spacecraft, the structural portion of these vehicles can be divided into systems, subsystems, and components. Examples of these are shown in Figure 1-2.

To be profitable, it is critical to investigate the cost versus performance trade off and how it can be improved for structures at the system, subsystem, and component level. This is accomplished in this thesis using the methods of multidisciplinary design optimization (MDO) and design for flexibility, a component of design for changeability.
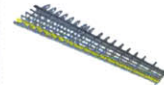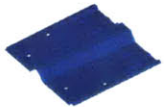
	Automobile	Aircraft	Spacecraft
System			
Subsystem	Body-in-white	Wing structure	Bus structure
Component	Floor pan	Wing spar	Bracket

Figure 1-2: Examples of structural systems, subsystems, and components for the automotive, aircraft, and spacecraft industries.

1.2 Design for Changeability

One level above design for flexibility, design for changeability [38], presented by Fricke *et. al.* in 2000, can be incorporated into the design process to enhance the capability of a design to perform better during its lifetime while being subjected to a uncertain dynamic, evolving environment. The goal of this enhanced system performance is to improve profitability and/or sustainability.

There are four aspects of changeability. These are flexibility, agility, robustness, and adaptability. These four components of changeability can characterize the ability of a system to be either adapted or to react to changes [71]. The definitions provided by Fricke *et. al.* of these changeability aspects are explained below and illustrated in Figure 1-3.

- **Flexibility:** the property of a system to be changed easily and without undesired effects.

- **Agility:** the property of a system to implement necessary changes rapidly.

- **Robustness** characterizes systems which are not affected by changing environments.

• **Adaptability** characterizes a system's capability to adapt itself to changing environments to deliver its intended functionality.

Attributes of DFC	Flexibility	Agility	Robustness	Adaptability
Basic				
Ideality/Simplicity	strong	strong	strong	strong
Independence	strong	strong	strong	strong
Modularity/Encapsulation	strong	strong	strong	strong
Extending				
Integrability	strong			intermediate
Autonomy	light			strong
Scalability	intermediate	strong		light
Non-Hierarchical Integration		strong		light
Decentralization		strong		strong
Redundancy	intermediate		strong	
Reliability			strong	
Anticipation		strong		strong
Incorporation of Agents		strong		strong

Legend: ■ := strong support ◪ := intermediate support □ := light support + := useful interrelation − := harmful interrelation

Figure 1-3: The four aspects of changeability [38] (left side) and the Attribute-Principles-Correlation Matrix [71] (right side).

Flexibility is a prerequisite to agility, as shown in Figure 1-3 (left-hand side). This is because a system will not have the ability to implement changes rapidly (agility) if it has no ability to implement changes at all (flexibility). In addition, robustness is a prerequisite to adaptability because a system cannot be adaptable if it has no ability to be insensitive to changing environments (robustness).

1.2.1 Enabling Design Principles

Several design principles can be incorporated in the design process to allow for the embedment of changeability. These design principles, detailed by Fricke *et. al.*, can be separated into two categories: basic and extending principles [38]. Basic principles support all four aspects of design for changeability, while extending principles support only specific aspects of design for changeability. These enabling design principles are defined below.

Basic Principles

- **Ideality/Simplicity:** ideality is defined as the ratio of a system's sum of useful functions to the system's sum of harmful effects. An ideal system would be composed of only useful functions.

- **Independence:** changing a design parameter in a system does not affect any related design parameter and thus not the proper operation of related functions. A design parameter represents the physical embodiment of a function's solution (i.e. a physical component).

- **Modularity/Encapsulation:** the clustering of the functions of a system into various modules while minimizing the coupling between the modules and maximizing the cohesion among the modules. This design principle is discussed in greater detail in Section 4.3.

Extending Principles

In addition to the three basic enabling design principles of changeability, nine extending principles have been defined by Fricke [38]. These extending principles are integrability, autonomy, scalability or self-similarity, non-hierarchical integration, decentralization, redundancy, reliability, anticipation, and incorporation of agents (see Figure 1-3 right-hand side).

1.2.2   Design for Flexibility

In the context of structural design, flexibility is the most applicable aspect of changeability to be considered in the design process. This aspect of changeability is used in this thesis rather than the more general concept of design for changeability or other changeability aspects. Agility is not used because it implies a changeability time constraint and the structural design examples considered in this paper are not subjected to a time constraint in order to respond to a changing environment. Although design for robustness can be used to design systems to successfully weather changes that

29

occur during system development or operation [86], robustness is not included in the structural design formulations in the design examples in this thesis.

Flexibility is defined in this paper as being composed of three main aspects: reconfigurability, platforming, and extensibility. The definitions of these terms are listed below and the concepts are illustrated in Figure 1-4. In the figure, the connectivity of the elements are also shown in a design structure matrix (DSM), first presented by Steward [78].

- **Reconfigurability** is defined as the property of a system to allow interconnections between its components, modules, or parts to be changed easily and without undesired effects.

- **Platforming:** a system composed of a set of common components, modules, or parts from which a stream of derivative products can be created easily and without undesired effects [60].

- **Extensibility** is defined as the property of a system to be able to enhance or increase its capabilities by incorporating additional components, modules, or parts easily and without undesired effects.
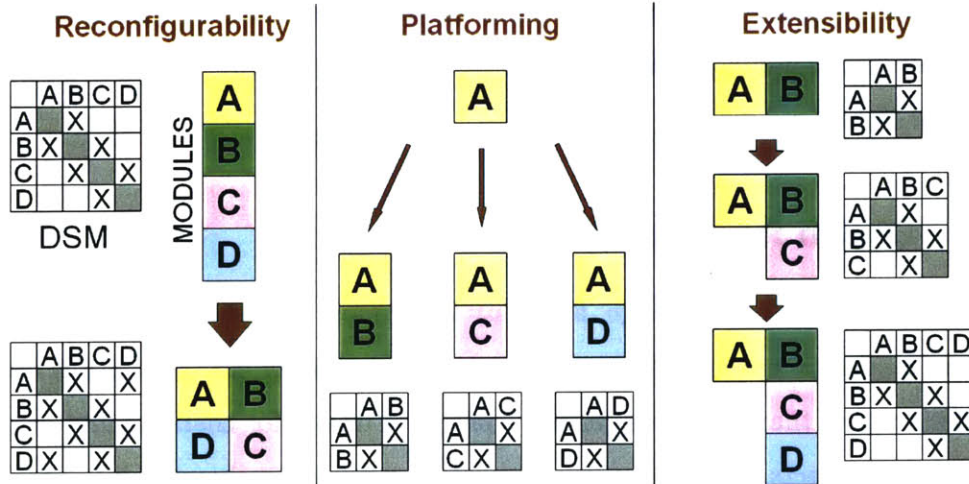
Figure 1-4: The aspects of flexibility [23].

30

1.2.3 The Other "ilities"

In addition to design for changeability and flexibility, other "ilities" exist which are considered during the structural design process. These design philosophies include manufacturability, reconfigurability, and extensibility. The goal of these design philosophies is to enhance affordability and ultimately sustainability and/or profitability.

Manufacturability

Manufacturability is defined as the ease of which a component, subsystem, or system can be manufactured. Rais-Rohani and Huo [69] define manufacturability in the context of aerospace structures design. Their definition includes constraints on material, shape, size, process, assembly, and factors that account for compatibility and complexity. In their multidisciplinary design optimization framework for MAGLEV vehicles, Tyll *et. al.* used geometric constraints on the range of shapes possible for the vehicle [82]. This is satisfactory because certain manufacturing processes place limits on the degree of curvature of a part, for example. In this MDO example for MAGLEV vehicles, aerodynamics, structures, cost, and geometry were considered in order to design an economically viable MAGLEV transportation system.

Reconfigurability

Reconfigurability, as defined in Section 1.2.2, is the property of a system to be changed in order to respond well to future uncertainties. In complex aerospace systems such as satellite constellations, the benefits of designing for reconfigurability are evident. After the economic failures of global satellite telephone systems such as Iridium [37] and Globalstar [29], it has been shown that the ability of the constellation to be reconfigured after initial construction and operation may have economic benefits. de Weck *et. al.* [26] addressed future market uncertainties which affect demand for global satellite telephone services by designing a satellite constellation to be deployed in stages. Although there is a cost for incorporating reconfigurability into the system,

this allows for minimization of a economic impacts of significantly lower than expected demand and also provides for the growth of the system to take advantage of higher than expected demand after the service is operational.

Extensibility

On January 14, 2004, President George W. Bush presented to the nation a bold new initiative [17] to "explore space and extend a human presence across our solar system ... using existing programs and personnel." With this new space exploration initiative came a mandate from the White House to "implement a *sustained* and *affordable* human and robotic program." Given tight annual budget constraints compared to that of the Apollo program [31, 18], the system used by NASA to carry out these exploration activities must be affordable in order to allow the program to be sustainable given political, social, and economic uncertainty.

In order to achieve a sustainable space exploration system, it has been proposed by MIT's spring 2004 16.89 Space Systems Engineering class that extensibility should be incorporated into the design process. An extensible space exploration system involves modular components which can be used in increasingly complex manned missions to the moon and more complex manned missions to Mars. This extension of the capabilities from one mission to another by reusing components in different vehicle configurations rather than designing a new space exploration system for each mission could reduce program costs significantly. Figure 1-5 shows how a flexible system can adapt to changing needs.

1.3 Multidisciplinary Design Optimization

Multidisciplinary design optimization is a powerful design tool used throughout this thesis. According to Sobieszczanski-Sobieski [77], multidisciplinary optimization is a methodology for the design of systems where the interaction between several disciplines must be considered, and where the designer is free to significantly affect the system performance in more than one discipline. With this design framework,

32
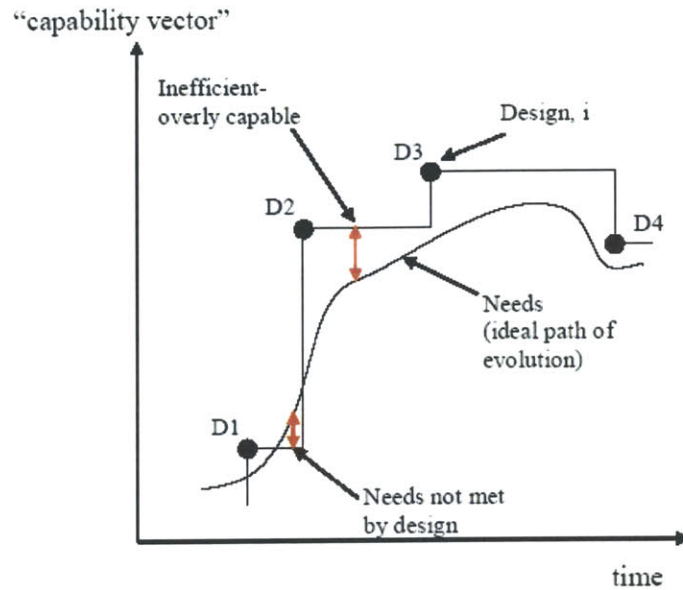
Figure 1-5: Change in system need and capability versus time [32].

complex systems can be designed while considering many different disciplines which may each drive a design in a different direction. Disciplines such as fluid mechanics, structural mechanics, aerodynamics, cost modeling, and controls can affect a system design in a complex, interrelated manner that may not be fully understood by the designer.

An example of how MDO can be applied to aerospace systems can be found from work involving the optimization of aircraft considering both structures and aerodynamics. Grossman *et al.* in 1988 [41] performed integrated structural design considering these two disciplines and found that the integrated, multidisciplinary design approach in all cases resulted in superior designs to a more traditional sequential design approach. Wakayama and Kroo in 1994 [85] also considered both structures and aerodynamics when performing wing planform optimization using an integrated design approach.

1.3.1 Historical Perspective of Multidisciplinary Design Optimization for the Aerospace Industry

The need for and corresponding evolution of MDO can be explained in the context of the evolution of the aerospace industry. In 1903, the Wright Flyer made its first manned, powered flight. After that groundbreaking moment in aerospace history, successively more capable aircraft were designed, built, and flown with the goal of increased performance.

However, in the early 1970s, a downturn in the airline industry principally due to the world oil shock of 1973 and heavy airline regulation set the stage for dramatic changes in aircraft design. Several major developments, including the emergence of successful computer-aided design (CAD) and airline degregulation [1], contributed to this design and procurement policy shift. This design and policy shift involved balancing objectives such as performance, life-cycle cost, reliability, maintainability, vulernability, and other "ilities." This change, enacted to help reduce life cycle cost, resulted in a dramatic increase in design requirements (see Figure 1-6) considered in aeronautical vehicle design [62, 28]. These changes spurred competition among airlines, drove down prices, and further cemented this shift in aircraft design and procurement policy.

This change in the goals of aerospace vehicle design was primarily driven by the control of life-cycle costs. This is due to the fact that poor design decisions made during the concept development stage of the design process are costly to change. Many authors agree that design decisions made during this early design stage can determine approximately 50-80% of total costs in the concept development design stage (see Figure 1-7) [62, 70, 11].

Due to an increasingly competitive global marketplace, companies have been forced to change how they design their products in order to remain profitable. The consideration of performance and design aspects such as reliability and manufacturability allows engineers to design products which satisfy requirements necessary for companies to maintain profitability. Multidisciplinary design optimization helps
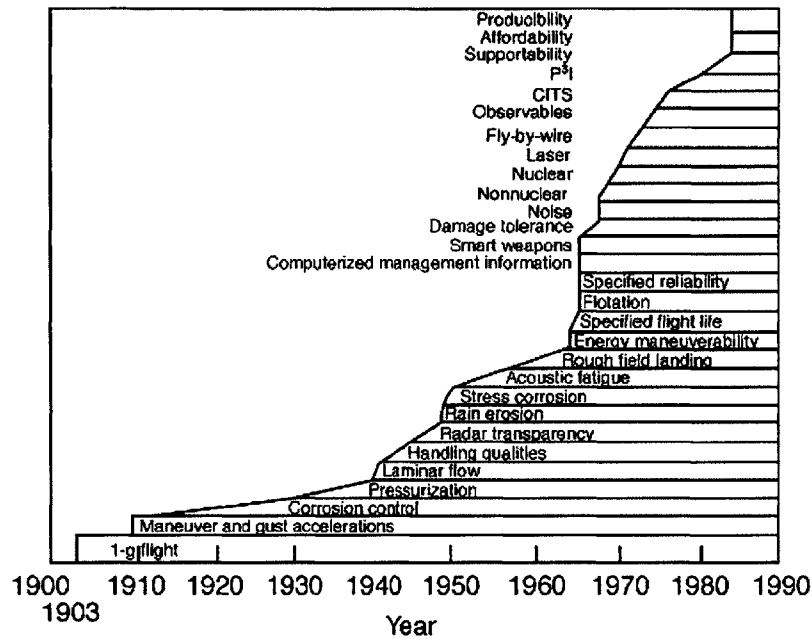
Figure 1-6: Increase in aircraft design requirements over time [62].

accomplish this by balancing a multitude of conflicting objectives.

1.3.2 The Need for Multidisciplinary Design Optimization

The ability of the engineer to consider many disciplines concurrently is important to the success of a design. Using mathematical tools and methodologies to consider these disciplines is essential to the cost-effectiveness of the design. The goal of the balanced design approach of MDO is to increase design freedom and knowledge about the design throughout the design process.

More design knowledge and freedom needs to be gained earlier and throughout the design process. This increased design knowledge and freedom, made possible through the use of MDO techniques, can be used by engineers to make more prudent design decisions (see Figure 1-8). In addition, a larger percentage of the budget will be allocated based on better information than designers usually have at that stage of the design process.

As stated by Jilla and Miller in 2004 [49], during the conceptual design phase,

Life cycle-cost committed versus incurred by life-cycle phase
(Ballistic missile system)
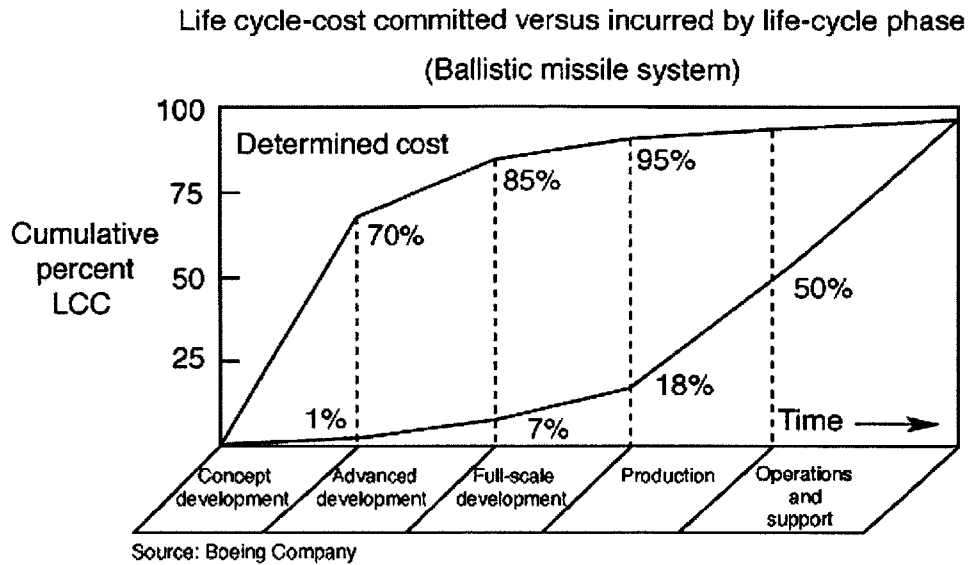
Figure 1-7: Life-cycle cost committed versus incurred life-cycle phase [62].

an improperly explored tradespace can result in an optimal design solution being overlooked, greatly increasing the life-cycle cost of the system. This is because modifications required to integrate and properly operate the system during the latter stages of the design process are more expensive to implement [11]. The use of MDO can help fully explore a tradespace by considering relevant disciplines for a design problem and account for the positive and negative interactions between them.

1.4 Components, Subsystems, and Systems

The definitions used for components, subsystems, and systems in this thesis are defined in this section. These definitions are:

- **Components:** an object, possibly part of a system, which can not be separated into smaller components without destroying the functionality of the object.

- **Subsystems:** a division of a system that has the characteristics of a system.

- **Systems:** a set of interrelated elements which perform a function, whose func-

36

100% Conceptual 100% Preliminary 100% Detailed 100%

Knowledge about design

Goal

Aerodynamics
Propulsion
Structures
Controls
Manufacturing
Supportability
Cost

Goal

Design freedom

Time into design process
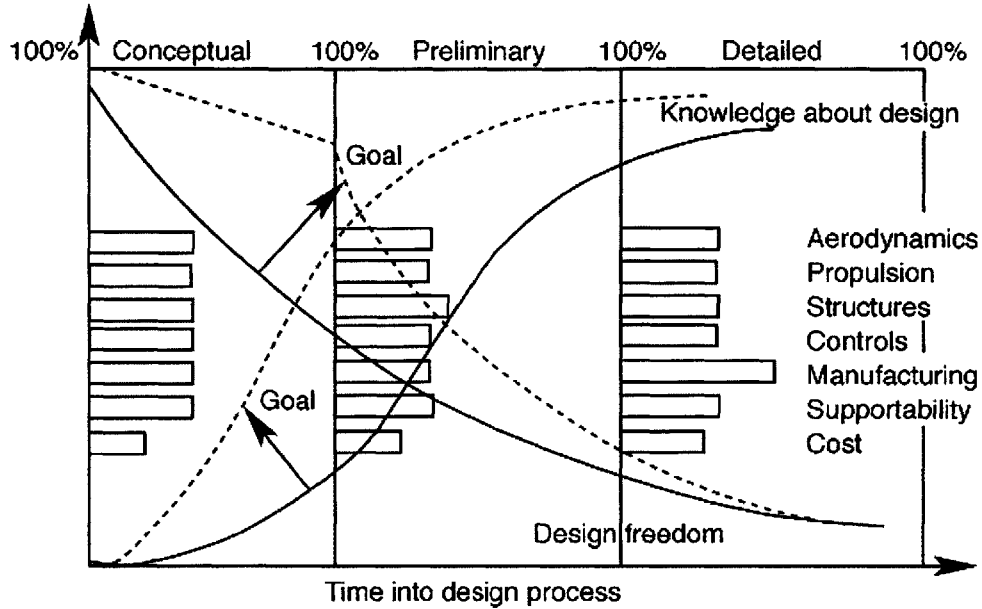
Figure 1-8: Design process reorganized to gain information earlier and retain design freedom longer [62].

tionality is greater than the sum of the parts [22].

1.5 Thesis Objectives and Overview

The goal of this thesis is to show the benefits and penalties associated with concurrent structural design for performance, cost, and flexibility for components, subsystems, and complex systems.

1.5.1 Component Design

The main objectives for component design are to minimize mass and cost while satisfying structural performance constraints. For small-scale component design, as is studied in this chapter, even small cost and performance savings are important for products with mass production potential. For example, in the automotive industry, due to the high volume of products sold, a fraction of a percent in cost savings can lead to dramatic cost savings.

37

1.5.2 Subsystem Design

For the subsystem design chapter of this thesis, the main objective is to minimize manufacturing cost for a system of simple components. Structural reconfigurability of this system of structural components is used as a means for achieving this manufacturing cost savings. Combining reconfigurability with design optimization provides the subsystem with the ability to satisfy several design requirements with an efficient design. This design approach has the potential to provide additional cost savings due to a potential reduction in inventory size as well as resulting learning curve manufacturing benefits.

1.5.3 Complex System Design

The objective of the system design chapter of this thesis is to improve the affordability of complex space systems with the introduction of modularity and reconfigurability into the design process. This concept can help enable extensible space system design. An extensible space exploration system is one in which many different, increasingly complex missions can be successfully completed while using as many common components as is feasible. This commonality and upgradability should allow for cost savings in the areas of non-recurring and recurring engineering activities.

1.5.4 Thesis Overview

An overview of this thesis is illustrated in Figure 1-9. This "road map" shows the interconnectivity between the thesis chapters.

Chapter 2, focused on component design optimization, introduces the trade off between cost and performance for structural design. The objectives for this chapter are enumerated in Section 1.5.1. The models created to illustrate this trade off are presented. The optimization method and framework used to perform this analysis is detailed. Design and objective space results are shown to highlight the cost and performance trade off.

Chapter 3 presents the benefits of adding design flexibility attributes into struc-

Chapter 1: Introduction
- Motivation
- Design for Changeability
- Multidisciplinary Design Optimization
- Thesis Objectives and Outline

Chapter 2: Component Design
- Literature survey
- Optimization model and framework
- Results

Chapter 3: Subsystem Design
- Literature survey
- Optimization model and framework
- Results

Chapter 4: System Design
- Literature survey
- The truncated octahedron
- Evaluation of metrics
- Structural design application

Chapter 5: Conclusion
- Design recommendations
- Flexible structural design process
- Future work

Appendix
- A: Engineering education
- B: Launch vehicle data

Figure 1-9: Thesis road map.

tural subsystem optimization. The goals of this chapter are in Section 1.5.2. More specifically, reconfigurability is incorporated into the design process to see what cost benefits are possible from this design practice. Similar to Chapter 2, the computer models, optimization framework, and optimization method used are discussed. Results are presented which enumerate the various cost benefits from incorporating the reconfigurability aspect of design for flexibility into the structural design optimization process.

In Chapter 4, a new concept for modular, reconfigurable spacecraft design is presented. This structural design concept is shown to have potential to improve space system design. Metrics are detailed which are used to compare this design concepts with other alternatives. The design potential from this concept is illustrated. In addition, a space system structural design example is presented which incorporates design

39

for flexibility in order to design a more extensible, affordable architecture which is more sustainable with respect to budgetary limitations.

In Appendix A, the importance of engineering education is stressed by including a paper detailing a new undergraduate design course in the Department of Aeronautics and Astronautics at MIT. This course deals with the concepts of multidisciplinary design and optimization and investigates the trade off between structural performance and manufacturing cost as they have been developed in this thesis. This course combines design theory, lectures and hands-on activities to teach the design stages from conception to implementation. Activities include hand sketching, CAD, CAE, CAM, design optimization, rapid prototyping, and structural testing. The learning objectives, pedagogy, required resources and instructional processes as well as results from a student assessment are discussed. This paper is included as a supplement because (1) I worked as a teaching assistant for the course and helped create the project and (2) "systems thinking" in structural design must begin with engineering education.

Appendix B includes specifications data used in Chapter 4 for launch vehicle selection.

1.6 Chapter 1 Summary

Chapter 1 provided the motivation for considering cost, performance, and flexibility in structural design. The definitions of design flexibility were presented. The reasoning for using a multidisciplinary design optimization approach was also discussed. The goals and outline of the thesis were detailed.

Chapter 2

Structural Component Shape Optimization Considering Performance and Manufacturing Cost

This chapter presents multidisciplinary optimization for structural components considering structural performance and manufacturing cost. The optimization model, framework, theory, and results for this research are presented and discussed.

2.1 Introduction

Typical structural design optimization involves the optimization of important structural performance metrics such as stress, mass, deformation, or natural frequencies. This structural design method often does not consider an important factor in structural design: manufacturing cost. In this research, manufacturing cost is an important performance metric in addition to typical structural performance metrics. The weighted sum method, a method for combining several objectives into a single objective [94], commonly used in multidisciplinary design optimization, is used to observe the trade off between manufacturing cost and structural performance. Two exam-

41

ples are presented which exhibit this trade off. Both examples involve optimization of two-dimensional metallic structural parts: a generic part and a bicycle frame-like part.

While it is not possible to construct a manufacturing cost model that represents all manufacturing processes, the scope of this research has been limited to one manufacturing process: rapid prototyping using an abrasive water jet (AWJ) cutter. Although AWJ cutting is the only manufacturing process considered, this framework is generalizable to other manufacturing processes provided that realistic parametric cost models of the manufacturing process can be made and verified.

2.2 Literature Survey

The aim of structural optimization is to determine the values of structural design variables which minimize an objective function chosen by the designer for a structure while satisfying given constraints. Structural optimization may be subdivided into shape optimization and topology optimization. For shape optimization, the theory of shape design sensitivity analysis was established by Zolésio [99] and Haug [44]. Bendsøe and Kikuchi [16] proposed the homogenization method for structural topology optimization by introducing microstructures and applied it to a variety of problems [79]. Yang et al. [93] proposed artificial material and used mathematical programming for topology optimization. Kim and Kwak [51] first proposed design space optimization, in which the number of design variables and layout change during the course of optimization.

Structural shape optimization has been performed along with an estimation of manufacturing cost by Chang and Tang [20]. This work involved optimization of a three-dimensional part in order to reduce mass and manufacturing cost for the special application of the fabrication of a mold or die. However, manufacturing cost was not included in either the objective or constraint function, as is done in this thesis. Park et al. [64] performed optimization of composite structural design considering mechanical performance and manufacturing cost. This work focused on the optimal

stacking sequence of composite layers as well as the optimal injection gate location to be used in the composite material manufacturing process. However, as in the work by Chang and Tang, Park *et. al.* did not perform multidisciplinary optimization including manufacturing cost.

The weighted sum method is a popular method for handling objective functions with more than one objective. Objective functions with many different linear combinations of the individual objectives are optimized in order to obtain a Pareto front. Zadeh [94] performed early work on the weighted sum method. In addition, Koski [52] used the weighted sum method for the application of multicriteria truss optimization.

The standard method for determining manufacturing cost for the AWJ manufacturing process is presented by Zeng and Kim [96] as well as Singh and Munoz [75]. To estimate manufacturing cost, Zeng and Kim use the cutting speed of the water jet cutter to estimate manufacturing time via the required cutting length and layout. Manufacturing time is then multiplied by an overhead cost factor for the specific AWJ cutting machine considered.

AWJ cutting speed prediction models have been presented by Zeng and Kim [98]. Zeng and Kim developed a widely accepted AWJ cutting speed prediction model. In addition, Zeng developed the theory behind AWJ cutting process [95]. Zeng, Kim, and Wallace [97] conducted an experimental study to determine the machinability numbers of engineering materials used in water jet machining processes.

For the purposes of this chapter, the AWJ cutting speed model presented by Zeng and Kim is used. The Zeng and Kim model has been used by Singh and Munoz to predict AWJ cutting speed and is also used, in part, in Omax water jet CAM software [6], [5].

While other researchers have performed structural shape optimization and investigated manufacturing cost, a lack of research exists for true multidisciplinary optimization considering both structural performance and manufacturing cost at the same time. This chapter presents multidisciplinary structural shape optimization considering both structural performance and manufacturing cost.

43

2.3   Structural Optimization Model

This section presents the structural optimization model used for this research. Design assumptions, variables, objectives, and constraints are presented.

2.3.1   Modeling Assumptions

Several assumptions are made in the models for simplification. These are:

- The cuts made by the abrasive waterjet cutter for the simple structural optimization example are closed curves.

- The cuts can not disappear or join together.

- The cuts can not intersect each other or the structural part boundary unless they define the part boundary.

These models were developed to investigate the trade off between structural performance and manufacturing cost by incorporating a manufacturing cost model into a multiobjective optimization framework. These assumptions allowed for an exploration of the design space within a reasonable amount of time. More advanced models can be developed to allow for hole generation or merging.

2.4   Optimization Framework

This section presents the optimization framework used to obtain an "optimal" structural design which meets the given design requirements. The gradient-based optimization algorithm used in this framework is discussed. Details of the software modules used in the simulation are presented.

2.4.1   Flow Chart

The optimal structural design for the given range of design requirements is determined using an optimization approach shown in Figure 2-1. A gradient-based optimizer is

44

combined with a finite element analysis software module and an abrasive waterjet manufacturing cost estimation module to determine the "optimal" design solution.

The initial design, defined from X coordinates, Y coordinates, and geometrical parameters, is input to the system and the objective function is evaluated using finite-element analysis and the manufacturing cost estimation model. Structural performance evaluation using finite-element analysis is performed using the ANSYS software package [7]. Rather than perform structural optimization and then off-line manufacturing cost evaluation, manufacturing cost and structural performance are both calculated simultaneously for each design output from the optimizer. These designs are then evaluated based on their respective objective function values.

$$x \equiv \left(\left\{ x_1^1 \right\} \left\{ x_2^1 \right\} \ldots, \left\{ x_{n_1}^1 \right\} \ldots, \left\{ x_1^m \right\} \left\{ x_2^m \right\} \ldots \left\{ x_{n_m}^m \right\} \right)$$

$$y \equiv \left(\left\{ y_1^1 \right\} \left\{ y_2^1 \right\} \ldots, \left\{ y_{n_1}^1 \right\} \ldots, \left\{ y_1^m \right\} \left\{ y_2^m \right\} \ldots \left\{ y_{n_m}^m \right\} \right)$$
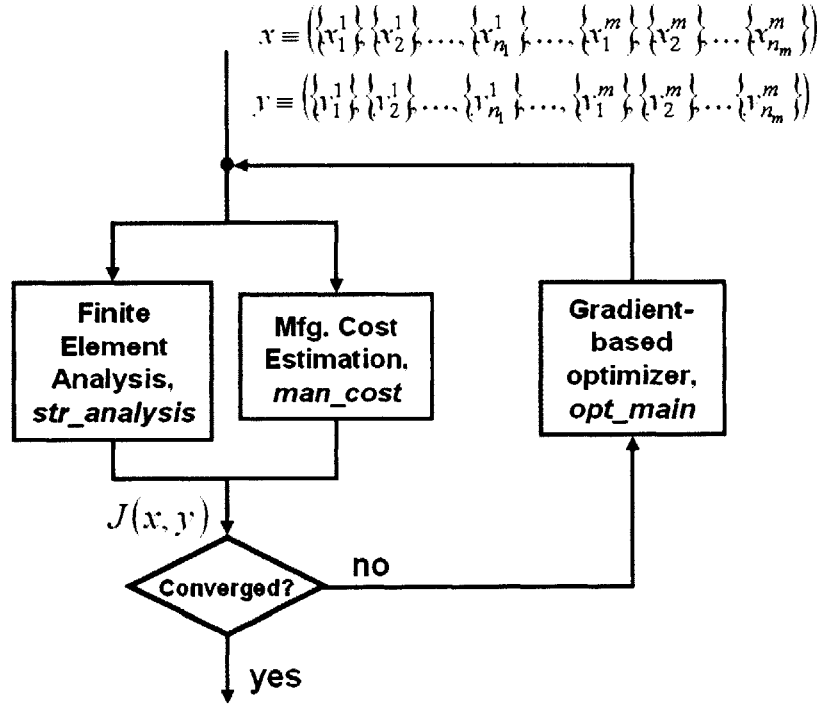
Figure 2-1: Shape optimization flow chart.

2.4.2 Gradient-based Shape Optimization

The optimization procedure used to optimize the shape of the cutting curves is performed using a gradient-based optimization algorithm. MATLAB function *fmincon*,

45

a sequential quadratic programming-based optimizer, is used. The relative ease with which *fmincon* was incorporated with the system model modules, also written in MATLAB, made the algorithm a suitable choice for this problem. In addition, a gradient-based optimization algorithm is selected because all design variables are continuous.

2.4.3 Manufacturing Cost Estimation: *man_cost*

This module is used to determine the manufacturing cost for performing abrasive waterjet manufacturing for structural components. The manufacturing process of abrasive waterjet cutting uses a powerful jet of a mixture of water and abrasive and a sophisticated control system combined with computer-aided machining (CAM) software. This provides for accurate movement of the cutting nozzle. The result is a machined part with tolerances ranging from ± 0.001 to ± 0.005 inches. It is possible for AWJ cutting machines to cut a wide range of materials including metals and plastics [97].

The inputs to the AWJ manufacturing cost estimation module include design variables and parameters such as material properties, material thickness, and abrasive waterjet settings. The output of this module is the AWJ manufacturing cost and time for the structural design.

Based on the material thickness and material properties, a maximum cutting speed is determined for the AWJ cutting machine. An assumption is made that the cutting speed of the waterjet cutter is constant throughout most of the cutting operation for a sufficiently large cutting path radius of curvature. In reality, the cutting speed of waterjet will slow if any sharp corners or curves with small arc radii lie along the cutting path. Equation 2.1 is used to determine the maximum linear cutting speed of the AWJ cutter, u_{max}. The overhead cost associated with using the AWJ cutting machine, OC, is shown in Equation 2.2. This cost factor is provided as an estimate of the manufacturing cost overhead for the MIT Department of Aeronautics

46

and Astronautics machine shop [87].

$$u_{max} = \left(\frac{f_a N_m P_w^{1.594} d_o^{1.374} M_a^{0.343}}{C q h d_m^{0.618}} \right)^{1.15} \tag{2.1}$$

$$OC = \$75/hr \tag{2.2}$$

In the above empirical equations, f_a is an abrasive factor, N_m is the machinability number of the material being machined, P_w is the water pressure, d_o is the orifice diameter, M_a is the abrasive flow rate, q is the user-specified cutting quality, h is the material thickness, d_m is the mixing tube diameter, and C is a system constant that varies depending on whether metric or Imperial units are used [96]. The AWJ settings used for this simulation are shown in Table 2.1.

AWJ Setting	Value
Abrasive factor, f_a	1
Machinability number, N_m	87.6
Water pressure, P_w (ksi)	40
Orifice diameter, d_o (in)	0.014
Abrasive flow rate, M_a (lb/min)	0.71
Cutting quality (1 = min, 5 = max), q	5
Mixing tube diameter, d_m (in)	0.030
Constant, C	163

Table 2.1: Abrasive waterjet machining settings used in cost model.

The cutting path in a typical abrasive waterjet manufacturing job is not linear. This issue requires a modification to the linear cutting speed estimation equation in order to estimate the cutting speed along cut curves with an arc section radius, u_{as}. This involves a modification to Equation 2.1 using Equation 2.3 to replace the quality factor, q. This modification takes into account the radius of curvature of the cut path, R. The resulting cutting speed estimation equation is Equation 2.4.

$$q = \frac{0.182h}{(R+E)^2 - R^2} \tag{2.3}$$

$$u_{max} = \left(\frac{f_a N_m P_w^{1.594} d_o^{1.374} M_a^{0.343} \left[(R+E)^2 - R^2 \right]}{0.182 C h^2 d_m^{0.618}} \right)^{1.15} \tag{2.4}$$

47
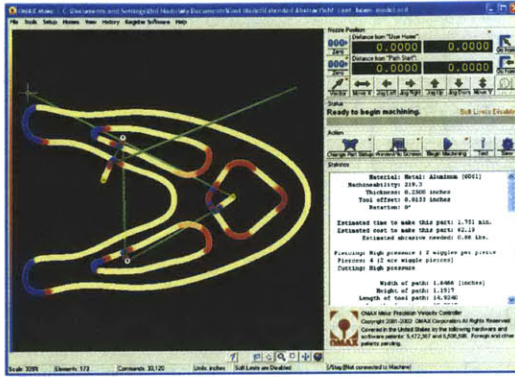
Figure 2-2: Omax output screenshot for short cantilevered beam example.
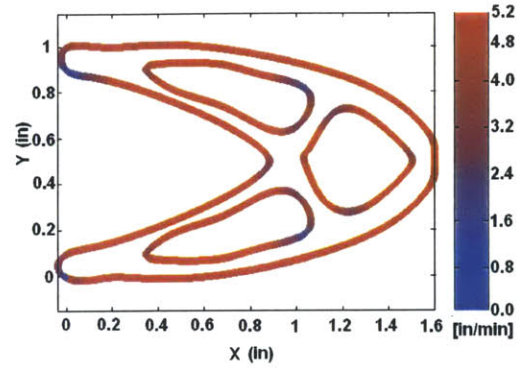
Figure 2-3: AWJ cost model output for short cantilevered beam example.

In the above equations, E is the error limit. In practice, the error limit is set by experience and judgment by the abrasive waterjet operator. For the purposes of this research, an error limit of 0.001 is used [61].

Total manufacturing cost is estimated using equation 2.5.

$$C_{man} = OC \left[\sum_{i=1}^{m} \left(\sum_{j=1}^{S_i} \frac{L_j}{u_{(i,j)}} \right) \right] \tag{2.5}$$

In Equation 2.5, L_j is the length of the jth step along the cutting curve, u is the AWJ cutting speed for the ith step along the jth curve, either arc section or maximum linear cutting speed, m is the maximum number of closed curves, and S_i is the total number of steps along the cutting curve for the ith curve.

In order to validate the manufacturing cost estimation model, results from the model are compared to Omax results for an identical manufacturing scenario. Omax contains an accurate manufacturing cost estimator and is a good benchmarking tool for this application. The short cantilevered beam, a commonly used structure to benchmark optimization methods, is used to validate the results of the manufacturing cost model. A screenshot of the Omax result is shown in Figure 2-2. Figure 2-3 is the output of the MATLAB AWJ cost estimation model. The darker the color of the cutting path, the slower the waterjet cutting speed.

The results of the software validation shown in Table 2.2 show the MATLAB

48

manufacturing cost estimation software accurately estimates manufacturing cost for abrasive waterjet cutting.

	Omax	Cost Model
Manufacturing Time (min)	1.69	1.71
Manufacturing Cost	$2.14	$2.11

Table 2.2: Manufacturing cost estimation module validation results.

2.4.4 Structural Analysis Module: *str_analysis*

Structural analysis for this analysis is performed using ANSYS finite element analysis software. This software is linked to MATLAB to provide the required connectivity for the optimization process. Required inputs to this module are the material properties, geometrical definitions for the structure, degree of freedom constraints for the structure, and load vectors applied to the structure. Outputs obtained from the module are the maximum stress and the structural volume. These outputs are used to evaluate the objective function and determine if the structural design satisfies the constraints.

2.5 Example 1: Generic Part Optimization

The first example presented is mass versus manufacturing cost optimization for a simple structural part.

2.5.1 Design Objectives

Using the weighted sum method, the two considered design objectives are combined into a single linear combination to create a single objective function to minimize. The first design objective is structural performance defined as mass. The second is manufacturing cost. This weighted-sum approach is used to explore the trade off

49

between these design objectives.

$$J(x_j^i, y_j^i) = \alpha M + (1 - \alpha)C_{man} \qquad (2.6)$$

The objective function used for these simulations is shown in Equation 2.6. In this equation, J is the objective function, M is the structural mass, C_{man} is the total manufacturing cost of the structural component, x_j^i and y_j^i are the design vectors composed of the X and Y-coordinates of the jth control point for the ith Non-uniform rational b-spline (NURBS) curve, respectively, and α is the weighting factor for the two objectives.

NURBS are used to describe the cut curves in the part. NURBS curves are chosen for their ability to control the shape of a curve on a local level by each of the defined control points, or knots. A complex shape can be represented with little data in the form of several of these control points. The NURBS formulation used is a proprietary ANSYS formulation. Equation 2.7 contains the generic NURBS formulation (see Figure 2-4) [88].

$$C(t) = \frac{\sum_{i=0}^{n} N_{(i,p)}(t)w_i \mathbf{P_i}}{\sum_{i=0}^{n} N_{(i,p)}(t)w_i} \qquad (2.7)$$
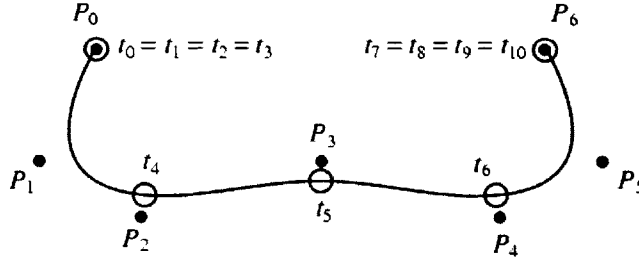
Figure 2-4: B-spline curve example [88].

In Equation 2.7, t is a knot vector composed of a non-decreasing sequency, $\mathbf{P_i}$ are the control points for a curve of order p, n is the total number of control points used to define the curve. $N_{(i,p)}$ are the B-spline basis functions for the NURBS curve for the ith control point and w_i is the weight of the ith control point.

50

2.5.2 Design Variables

The design variables for the simulation are the X and Y coordinates of the control points defining the curves along which the abrasive waterjet cuts are made. Therefore, two design variables are required for each control point to define cuts in the component being optimized. The total number of design variables depends on the number of cutting curves and the number of control points used for each curve.

$$X \equiv \left(\{x_1^1\}, \{x_2^1\}, \ldots, \{x_{n_1}^1\}, \ldots, \{x_1^m\}, \{x_2^m\}, \ldots, \{x_{n_m}^m\} \right) \tag{2.8}$$

$$Y \equiv \left(\{y_1^1\}, \{y_2^1\}, \ldots, \{y_{n_1}^1\}, \ldots, \{y_1^m\}, \{y_2^m\}, \ldots, \{y_{n_m}^m\} \right) \tag{2.9}$$

In Equations 2.8 and 2.9, n_i is the total number of control points for the ith curve and m is the total number of curves being optimized in the structure.

2.5.3 Design Constraints

The constraints imposed on this problem statement are side constraints of the design variables and maximum von Mises stress in the structure. These constraints are defined in the following equations.

$$\sigma_{max} \leq \sigma_c \tag{2.10}$$

$$x_{j,LB}^i \leq x_j^i \leq j, x_{UB}^i \tag{2.11}$$

$$y_{j,LB}^i \leq y_j^i \leq y_{j,UB}^i \tag{2.12}$$

In equations 2.10, 2.11, and 2.12, σ_{max} is the maximum von Mises stress in the structure and $x_{j,LB}^i$, $x_{j,UB}^i$, $y_{j,LB}^i$, and $y_{j,UB}^i$ are the lower (LB) and upper bound (UB) side constraints for the design vector variables controlling the jth control point for the ith NURBS curve. These side constraints are different for each design variable given the nature of the problems being optimized. Visualization of the design variable side constraints for the structural design is shown in Figure 2-5.

It can be seen in Figure 2-5 that the side constraints restrict the simulated abrasive
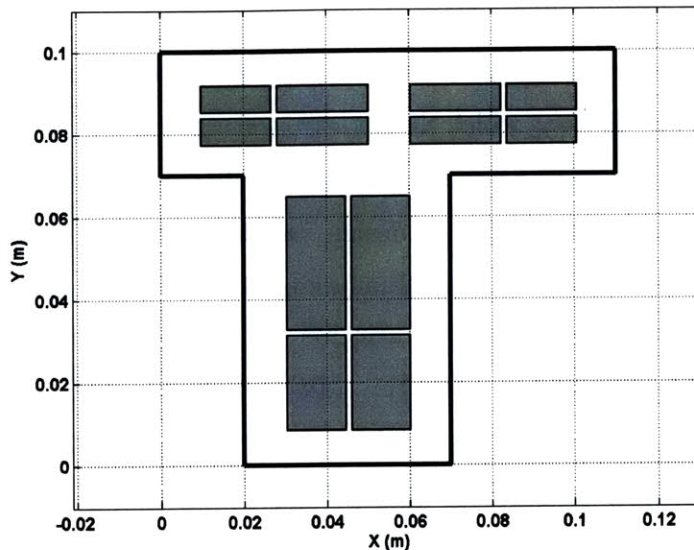
Figure 2-5: Side constraints of the control points for generic structural part optimization example.

waterjet cuts to be internal to the part. The side constraints for this example is restricted to the zones shown in order to prevent any of the resulting NURBS curves from intersecting each other for both examples or with the boundary of the part for the first example. If any of these intersections were to occur, the ANSYS [7] structural analysis module would not be able to generate a mesh of the part and compute a solution.

2.5.4 Simulation Routines

MATLAB modules were created to perform the structural optimization for manufacturing cost and structural performance for this example. These routines include a main software module, an AWJ manufacturing cost estimation module (see Section 2.4.3), and a structural analysis module (see Section 2.4.4). Important parameters and initialization techniques associated with each software module for this design example are presented in this section.

52

Main: *opt_main*

This routine is the main MATLAB module which calls all other routines. In this module, the initial structural design is defined, main parameters are defined, optimization routines are performed, and post-processing of results is handled.

Parameters

The important parameters set in this module are the geometry of the structural component, the number of initial designs to consider, objective function weighting factors, material properties of the truss structure elements, and abrasive waterjet settings. For this structural design example, the geometry defining the boundary of the part is defined. These properties are presented in Section 2.5.3. Three different initial designs were selected for the simulations. This is explained in more detail in the Initialization section. The material properties are defined in this module as well. The material selected is A36 Steel with a Young's modulus of 200 GPa, a Poisson's ratio of 0.26, and a yield strength of 250 MPa. The abrasive waterjet settings used are defined in Section 2.4.3.

In this example, objective function weighting factors of 0.2, 0.6, 0.65, 0.7, 0.75, 0.8, 0.85, 0.9, and 0.95 are used. The criteria used for selecting the weighting factors is explained in Section 2.5.5.

Initialization

This design optimization example is performed by starting the optimization algorithm at three different initial designs. Optimization is performed by first defining an initial structural solution guess. These three designs are selected to attempt to broadly search the design space with the goal of finding solutions close to the global optimum. The initial designs for the example, shown in Figure 2-6, include small, medium, and large holes cut in the blank metallic part.

The goal of starting the optimization with many different initial guesses is to attempt to find a near-global optimal solution. Since a gradient-based optimization method is used for the outer loop of this optimization framework, it has a tendency to get "trapped" at a local optimal solution. By starting the optimization routine

53
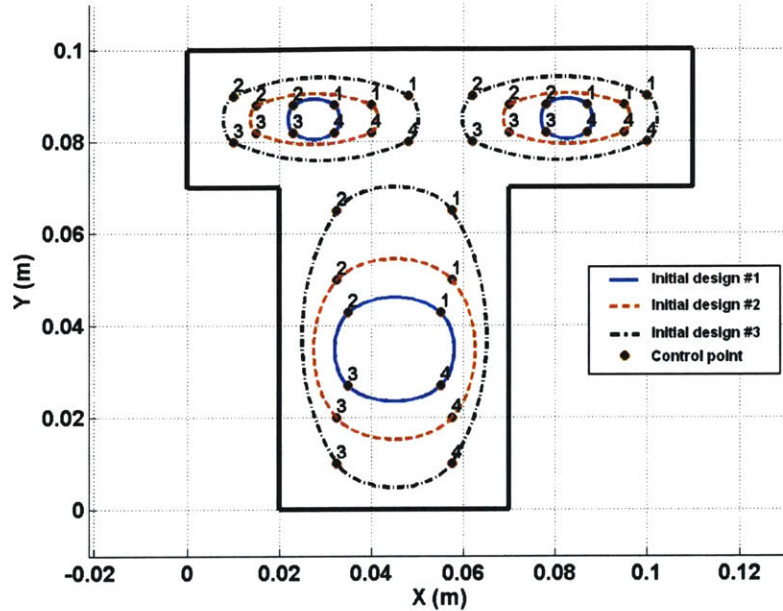
Figure 2-6: Initial designs for the generic structural part shape optimization example.

from several different locations in the design space, there is a greater potential for finding a near-optimal solution.

Optimization

Structural design optimization for this design example is performed using MAT-LAB function *fmincon*. Manufacturing cost, mass, and maximum stress results for the design specified by the optimization algorithm are determined by the appropriate MATLAB modules and the results are passed to *fmincon* for sensitivity analysis.

The resulting "optimal" solutions and objective functions are kept in memory for each iteration during the optimization process for post-processing usage.

Post-processing

The values of the objective functions for the "optimal" designs resulting from each initial design and weighting factor are compared and the "best" designs are used to create the Pareto frontier shown in Section 2.5.5.

In addition, the convergence behavior of the optimization framework can be analyzed by plotting the objective function results for each iteration during the optimization process. This information is presented in Section 2.5.5.

54

2.5.5 Results

Structural component shape optimization considering both performance and manufacturing cost is performed for a generic metallic structural part shown in Figure 2-7.

Simulation Parameters

The material thickness of the part is assumed to be 1 centimeter. The boundary conditions of the part are designed such that the part is fixed in all directions at the base as shown in Figure 2-7. The evenly-distributed pressure across the top of the part, also shown in Figure 2-7, is $3.7 \times 10^7 N/m^2$. A factor of safety of 1.5 is assumed for this example.
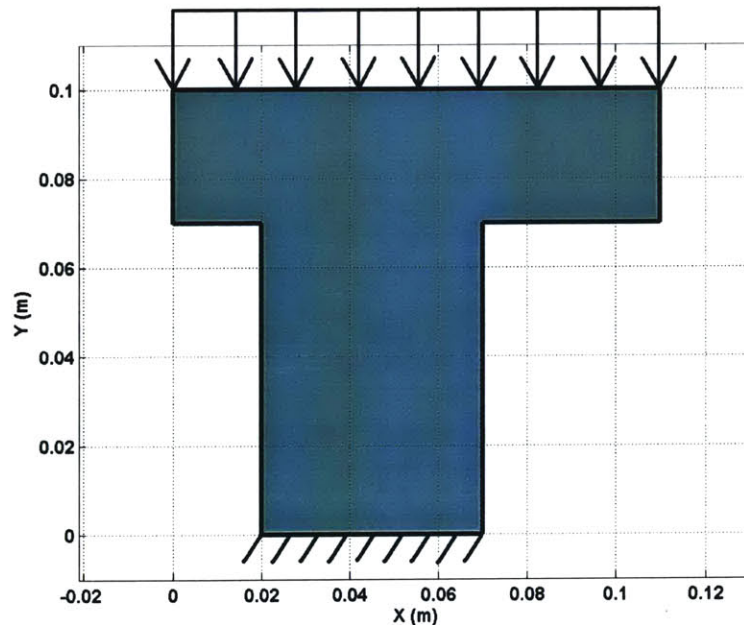
Figure 2-7: Generic structural part design including loading and boundary conditions.

Three holes are cut in the metallic part and the shapes of these holes are controlled by four control points each. These control points are illustrated in Figure 2-6. The cutting path created by the control points is determined using NURBS curves created in ANSYS using the *spline* command.

55

Objective Space Results

Pareto frontier results for shape optimization for this example are shown in Figure 2-8. The maximum stress constraint is active for all designs along the Pareto frontier except the results for weighting factors of 0.2 and 0.6.
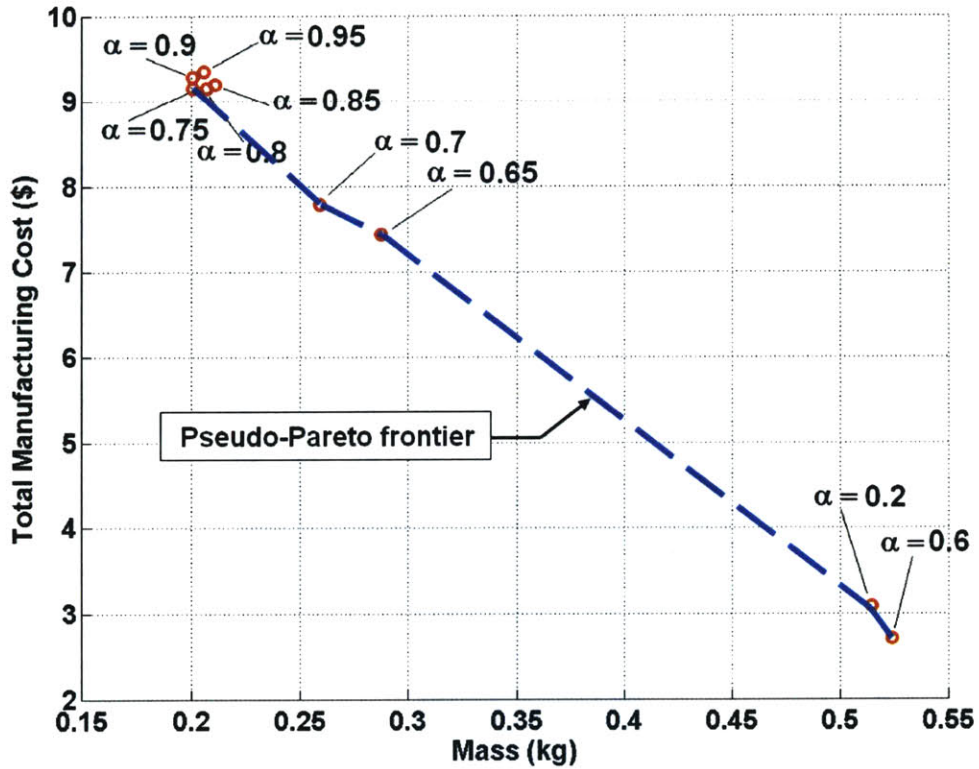
Figure 2-8: Objective space results for generic part optimization with objective function weighting factor, α, labeled for each design.

Although the Pareto frontier is not well-distributed, the trade off between mass and manufacturing cost can be seen. A pseudo-Pareto frontier is denoted by connecting all the non-dominated design solution points because the actual Pareto frontier is not known given the design solutions obtained.

Design Space Results

Selected structural designs from the set from Figure 2-8 are shown in Figure 2-9.

(a) Weighting factor of 0.6.   (b) Weighting factor of 0.7.   (c) Weighting factor of 0.9.
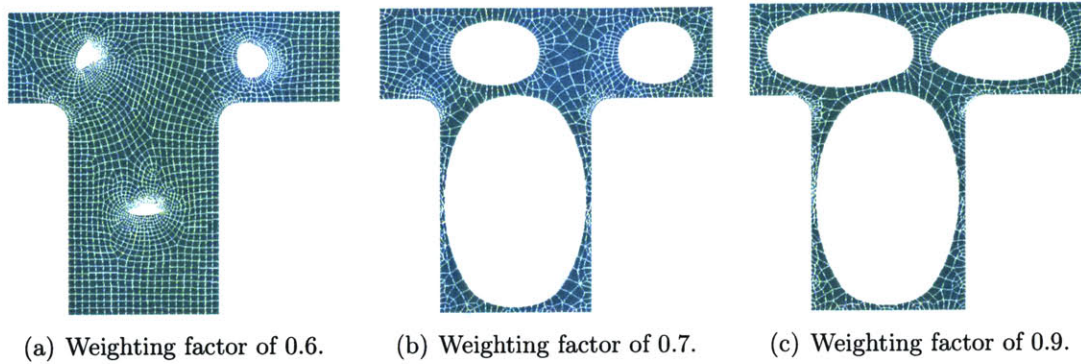
Figure 2-9: Structural design results for generic part example.

The structural design results demonstrate the trade off between cost and mass. When manufacturing cost is weighted more heavily, the cut-outs in the metallic part are small. However, when mass is weighted more heavily, the cut-outs in the part are significantly larger and one or more of the holes are at or near the side constraint boundaries. This means the optimization algorithm is attempting to remove material to minimize structural mass, as expected.

Objective Space Results Discussion

It is observed that the weighted sum design solutions are not in the correct order. The solution from the weighting factor of 0.2 should have lower cost and greater mass than the solution for the weighting factor of 0.6, yet this is not the case. There are two likely causes for this problem. First, it is possible that too few initial designs are investigated in order to find a near-global optimal design solution. The design solutions found are likely local optima and not global optimal solutions. However, a likely cause of this problem is that manufacturing cost is not only a function of cutting curve length but also the radius of curvature of the cutting path. As mentioned previously, in the manufacturing cost model, a specific cutting path radius of curvature limit exists at which cuts with radii greater than the limit are assumed to be at the maximum cutting speed. Below this radius of curvature limit, cutting speed is slower and not constant and therefore the cost per unit length of material increases.

An evenly distributed Pareto frontier is not found in this multiobjective opti-
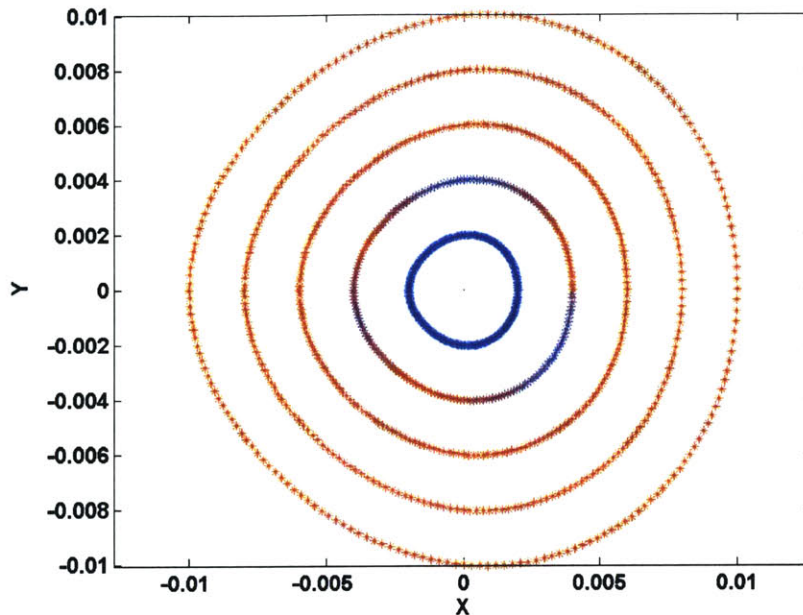
Figure 2-10: Cutting speeds for circular cuts of various radii. Dimensions are in meters.

mization. This phenomenon is likely caused by the fact that the objectives being minimized are highly nonlinear in terms of the weighting factor, α, and an even distribution of weighting factors is used. The use of the adaptive weighted-sum (AWS) method developed by de Weck and Kim [27] may alleviate this problem and will be implemented in future work. In order to attempt to overcome this difficulty, a select set of weighting factors is chosen to obtain a well-distributed Pareto frontier. As can be seen in Figure 2-8, even this set of weighting factors does not yield such a Pareto frontier.

Figures 2-10 and 2-11 illustrate this radius of curvature limit for manufacturing cost minimization. The example used to illustrate this phenomenon is a comparison of closed circular cuts with varying radii. Figure 2-10 is an example of the type of curves used to illustrate the minimum manufacturing cost radius of curvature. Solid red represents the maximum abrasive waterjet cutting speed and darker colors represent slower cutting speeds. Figure 2-11 shows the minimum manufacturing cost with respect to radius of curvature. A clear minimum manufacturing cost can be seen at
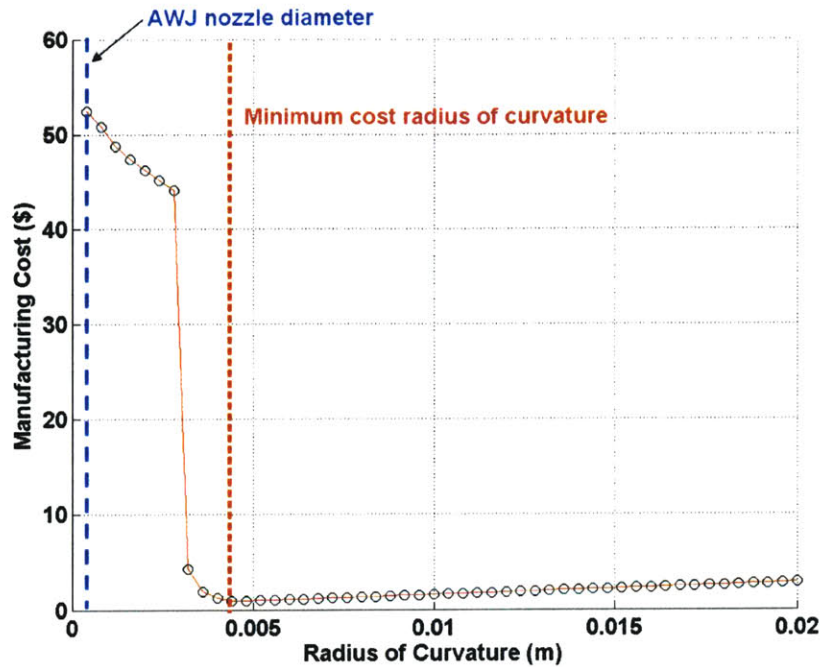
Figure 2-11: Manufacturing cost vs. radius of curvature for circular cuts.

the limit of the maximum linear cutting speed. This minimum was obtained from observations of the radius of curvature limit at which Omax software assumed the maximum linear waterjet cutting speed was used for various cutting qualities. Two important trends can be seen in Figure 2-11. First, when the radius of curvature is less than the minimum cost radius of curvature, cutting speed dominates the manufacturing cost. This results in a dramatic rise in manufacturing cost for small reductions in radius of curvature. For radii of curvature larger than the minimum cost radius, cost is dominated by cutting length. This leads to an increase in manufacturing cost with a linear relationship to radius of curvature.

The relative cutting speeds estimated by the AWJ cost model are shown in Figure 2-12. The same color scheme applies with respect to cutting speed. Most of the cuts made for the selected designs are at the maximum linear cutting speed. Only the design with a weighting factor of 0.6 has small portions of cuts in which the waterjet cutting speed is slower than the maximum linear speed.

59
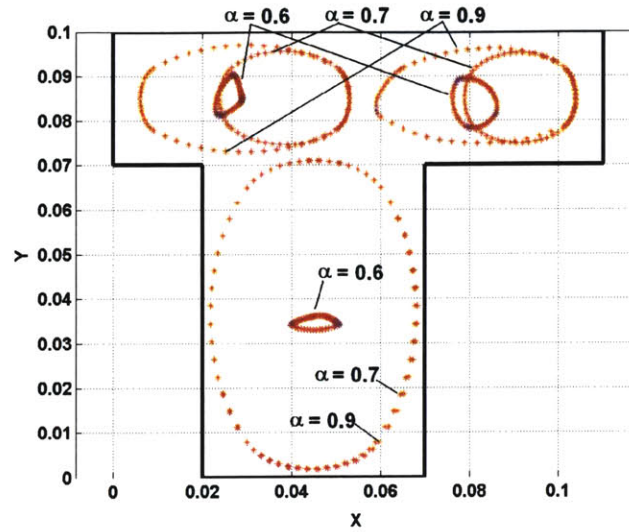
Figure 2-12: Cutting speeds for selected Pareto frontier structural designs. Each curve has an average cutting speed of 10.97 in/min.

Convergence Information

The convergence histories for the optimizations performed for each weighting factor are shown in Figure 2-13. The designs are feasible except where noted.

2.5.6 Cost Model Validation

In addition to the computer simulation to verify the cost model, the abrasive waterjet cutter was used to manufacture "optimal" design solutions obtained through the design process and verify the accuracy of the cost model. An example of one of these manufactured parts is shown in Figure 2-14.

Manufactured Part (Omax)	$2.91
Manufacturing Cost Model (MATLAB)	$2.96

Table 2.3: Further manufacturing cost estimation module validation results.

The model verification data is presented in Table 2.3. The error of the manufacturing cost estimation model is less than 2% for this example. This demonstrates the high accuracy of this cost model. However, this level of accuracy may not be good

60
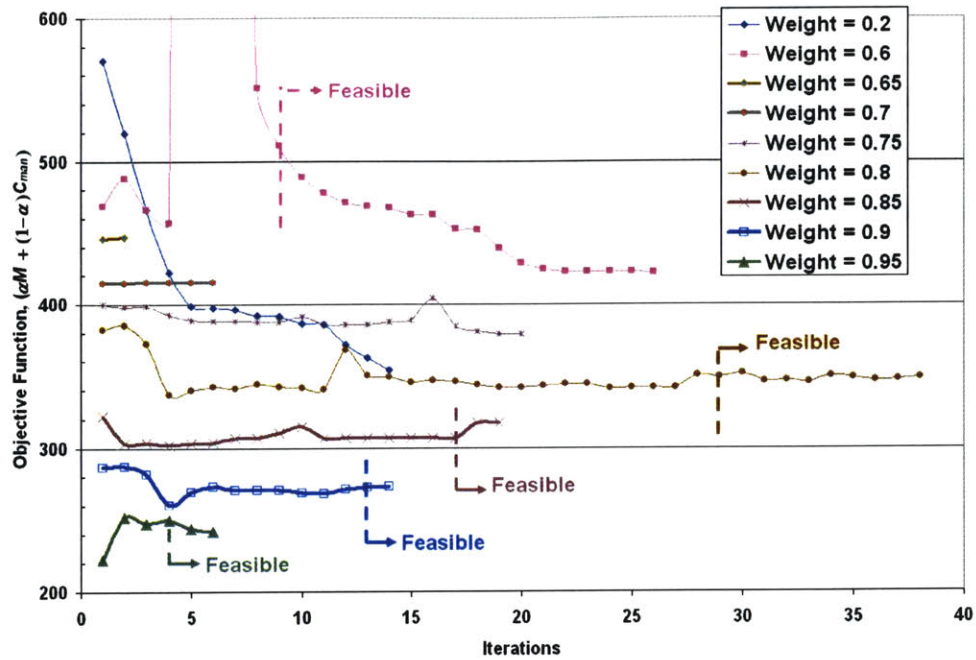
Figure 2-13: Convergence histories for the generic part structural optimization example.

enough due to the fact that a manufacturing cost savings of approximately 1.6% is observed when comparing the two anchor points of the Pareto frontier for the second design example. This issue will be investigated in future work.
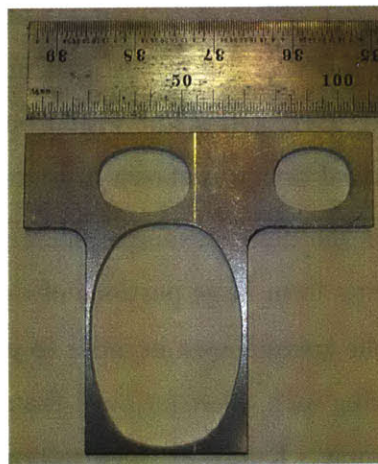
Figure 2-14: Generic part manufactured using AWJ. Structural design solution with a weighting factor of 0.7 is used.

2.6 Example 2: Bicycle Frame Optimization

This section includes the same optimization algorithm applied to a more complex structural component design example. This component is a two-dimensional bicycle frame-like structure.

2.6.1 Design Objectives

The design objectives for this example are the same as those for the generic part optimization example (see Equation 2.6).

2.6.2 Design Variables

The design variables for the simulation for this example are identical to those presented in Section 2.5.2.

2.6.3 Design Constraints

The constraints imposed on this problem statement are side constraints of the design variables and maximum von Mises stress in the structure. These constraints are defined in the Equations 2.10, 2.11, and 2.12. Visualization of the design variable side constraints for the structural design is shown in Figure 2-15.

The design constraints for the design example, shown in Figure 2-15, show the simulated abrasive waterjet cuts form large portions of the part boundary. The side constraints are restricted to the zones shown in order to prevent any of the resulting NURBS curves from intersecting each other for both examples or with the boundary of the part for the first example. If any of these intersections were to occur, the ANSYS [7] structural analysis module would not be able to generate a mesh of the part and compute a solution.
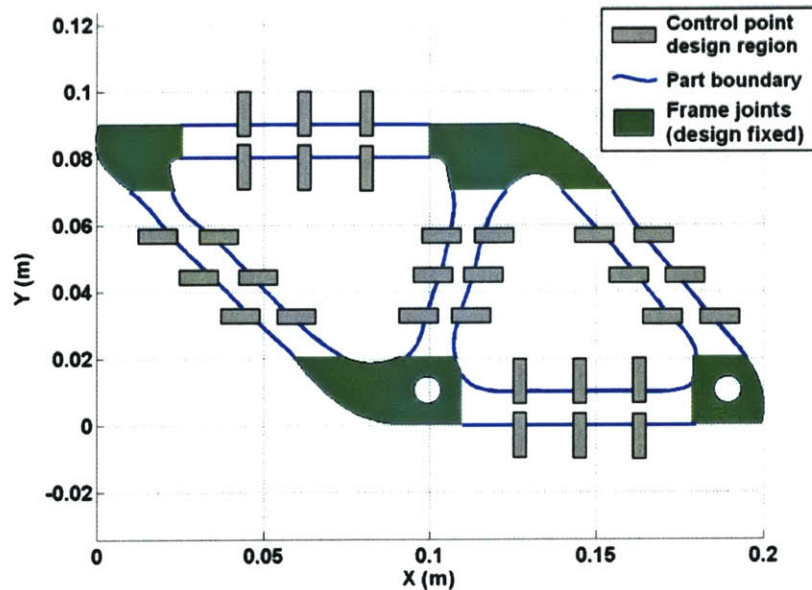
Figure 2-15: Side constraints of the control points for bicycle frame optimization example.

2.6.4 Simulation Routines

The same simulation routines presented for the generic part example are used for this design example. Differences in the design example problem setup are presented in this section.

Main: *opt_main*

This routine is the main MATLAB module which calls all other routines. In this module, the initial structural design is defined, main parameters are defined, optimization routines are performed, and post-processing of results is handled.

Parameters

For this design example, the boundaries of the portions of the structure not being optimized are defined. These properties are presented in Section 2.6.3. Three different initial designs were selected for the simulations. This is explained in more detail in the following Initialization section. The material properties and abrasive waterjet settings for this design example are the same as for the generic part design example.

63

For this example, an evenly distributed set of eleven weighting factors between 0 and 1 are used. The criteria used for selecting the weighting factors is explained in Section 2.6.5 for this example.

Initialization

Design optimization is performed by starting the optimization algorithm at three different initial designs. Optimization is performed by first defining an initial structural solution guess. These three designs are selected to attempt to broadly search the design space with the goal of finding solutions close to the global optimum.

For this example, the initial designs are shown in Figures 2-16, 2-17, and 2-18. The bicycle frame structures have thin, medium, and thick-sized structural members. A near-global optimum design is found by selecting the "best" design of the three solutions resulting from the three different initial designs. These "best" design solutions are used to create the Pareto frontier. ANSYS mesh results as well as the MATLAB control point locations are shown in Figures 2-16, 2-17, and 2-18 detailing the initial designs.
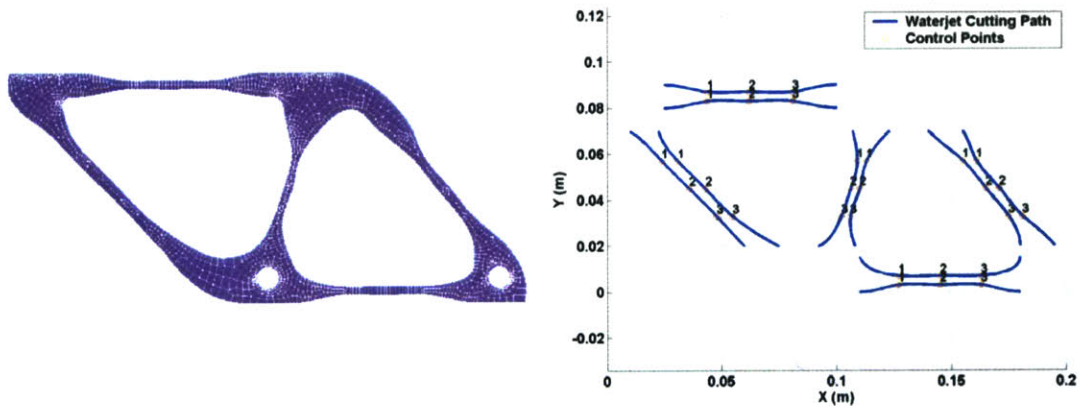
Figure 2-16: First initial design mesh and control points for bicycle frame structural optimization example.

Optimization

Structural design optimization for this example is performed in the same manner as previously explained for the generic part example.

Post-processing
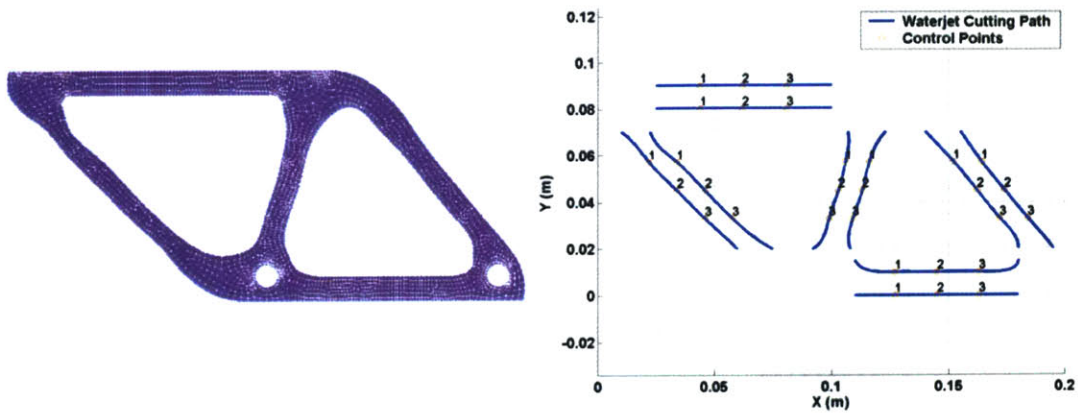
Figure 2-17: Second initial design mesh and control points for bicycle frame structural optimization example.
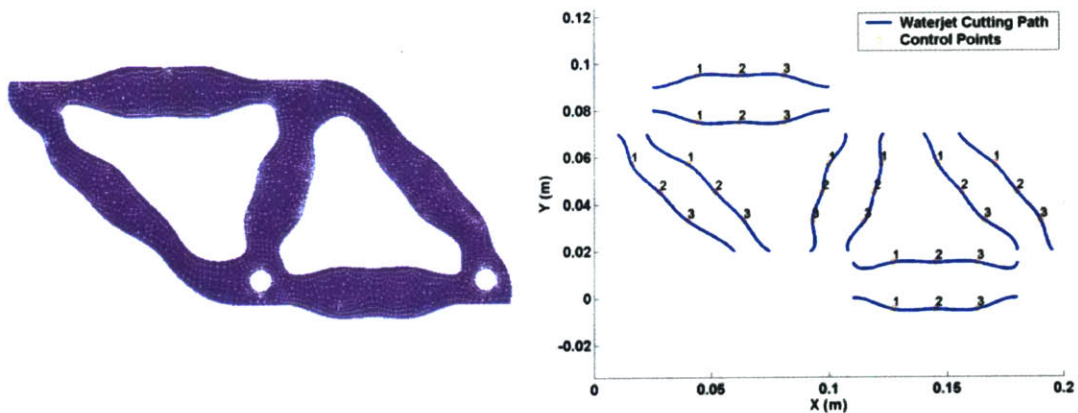
Figure 2-18: Third initial design mesh and control points for bicycle frame structural optimization example.

Structural design post-processing for this example is performed in the same manner as previously explained for the generic part example.

2.6.5 Results

Shape optimization considering both structural performance and manufacturing cost is performed for a bicycle frame-like part shown in Figure 2-19. This structure is roughly 20 by 10 centimeters in size.

Simulation Parameters

The material thickness of the part is set to 1 centimeter, the same thickness used for the generic part example. The part is fixed at two holes as shown in Figure 2-19. The loads applied to the structure are shown in the figure. A factor of safety of 1.5 is assumed for this example.
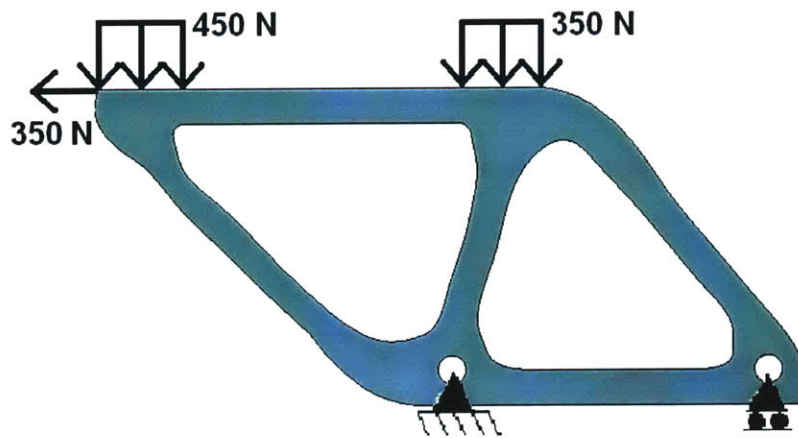
Figure 2-19: Structural part design with loading and boundary conditions shown.

Ten curves controlled by three control points each are used to determine the shape of the structure while the structural shape at the vertices of the structure remain unchanged. The relationship of the control points to the curves can be seen in the initial designs shown in Figures 2-16, 2-17, and 2-18. The cutting path created by the control points is determined using NURBS curves created in ANSYS.

Objective Space Results

The Pareto frontier shown in Figure 2-20 demonstrates the trade off between manufacturing cost and mass. The magnitude of improvement in manufacturing cost along the Pareto frontier is not large. For this example, a manufacturing cost savings of approximately 1.6% is observed when comparing the two anchor points of the Pareto frontier. However, a small improvement in manufacturing cost applied to a product being mass produced can result in a large cost savings for a manufacturer. In

addition, the observed tradeoff between cost and mass would be more significant if the shapes of the bicycle frame joints are included in the design space. Since large portions of the structure are fixed, the cost and mass trade off is restricted for this example.
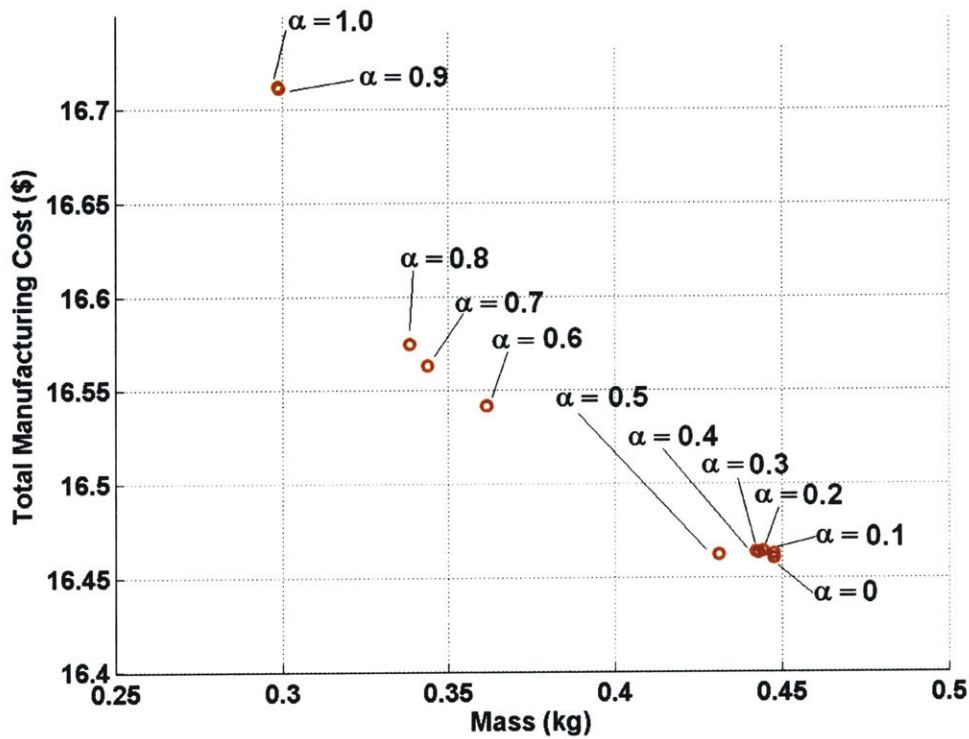
Figure 2-20: Pareto frontier for bicycle frame structural optimization with weighting factor, α, labeled for each design.

The maximum stress constraint is not active for any of the structural designs included in the Pareto frontier. This is a result of the side constraints being restrictive. Design freedom is limited by the side constraints in order to prevent part edge curves from intersecting each other, resulting in infeasible designs for which structural analysis cannot be performed.

Abrasive waterjet cutting speeds for all designs for this example are determined to be at the maximum linear cutting speed of the AWJ cutter for the selected example. This results in better objective space results than are obtained for the generic structural part example presented in Section 2.5.5.
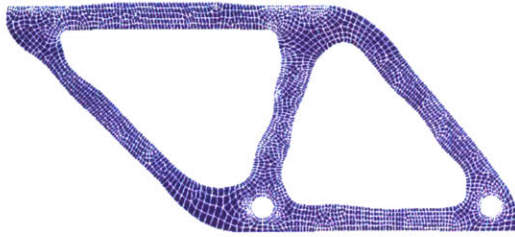
Figure 2-21: Structural design solution for weighting factor of 0.1.
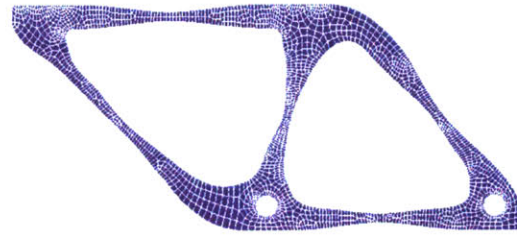
Figure 2-22: Structural design solution for weighting factor of 0.6.

Design Space Results

Selected structural designs from the Pareto set are shown in Figures 2-21 and 2-22. The trade off between objectives can be seen by comparing structural designs for these weighting factors. The design for which the weighting factor is 0.1 results in a structure with nearly straight edges for minimum manufacturing cost. However, the design for a weighting factor of 0.6 results in a design with narrow structural members in order to minimize structural mass. This results in low mass but higher manufacturing cost as a result.

2.7 Chapter 2 Summary

While the area of structural shape optimization is fairly mature, we introduce in this chapter the consideration of manufacturing cost in the optimization process. Although a two-dimensional manufacturing process, abrasive waterjet cutting, is selected for this research, other more complicated manufacturing processes can be used as well. Two examples are used to exemplify the application of this procedure for multiobjective structural optimization problems.

The trade off between structural performance and manufacturing cost is shown with Pareto frontiers for two example structural components. Mass is used as the metric for structural performance and maximum stress is the constraint.

Chapter 3

Multidisciplinary Structural Subsystem Topology Optimization for Reconfigurability

While the previous chapter focused on a single component, we now consider the interaction between multiple components. This chapter presents multidisciplinary structural optimization for a subsystem consisting of truss structural elements. The effect of designing for reconfigurability is observed for manufacturing cost. The optimization model, framework, theory, and results of this research are presented and discussed.

3.1 Introduction

Typically, structural design optimization is performed by only considering the structural performance of the design in the optimization process for a single load case. Conventional structural performance metrics are stress, mass, deformation, or natural frequencies. Another important aspect to be considered in structural optimization is loading condition variation. In this work, we propose a new design optimization framework that deals with structural subsystem optimization considering different loading conditions. It is assumed that these loading conditions are never applied

simultaneously to the structure. The goal is not to make the system insensitive, but to make it reconfigurable such that it can perform well when exposed to various loading conditions. While robust design is a passive response to different loading conditions, design for reconfigurability is an active response. The incorporation of this reconfigurability into structural design can lead to significant benefits such as reduced manufacturing cost.
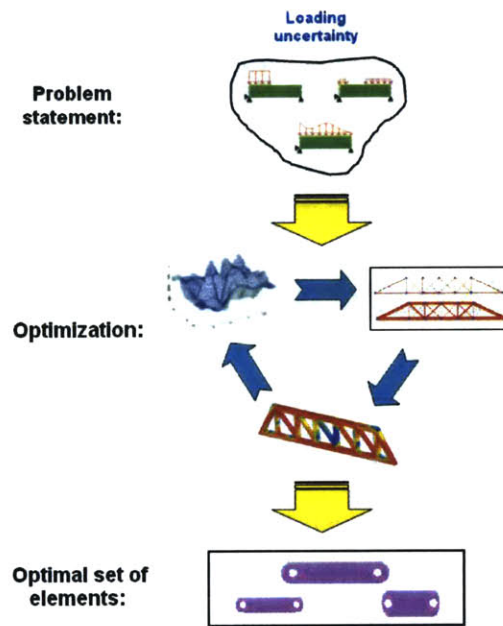
Figure 3-1: Optimization for reconfigurability procedure.

An overview depicting the procedure used to produce an optimal reconfigurable design introduced in this chapter is shown in Figure 3-1. This illustrative example is of a truss structure subject to various loading conditions. The solution to be obtained is not a single optimum solution, but an optimum set of optimum parts that can be reconfigured to form several different designs.

In this procedure, a reconfigurable two-dimensional truss structure is designed based on structural performance and the reconfigurability of the structure. The result of the optimization routine is an optimal set of optimal parts with a known assembly configuration based on the requirements defined in the problem statement.

70

The motivation for incorporating reconfigurability into structural design is to account for various loading conditions experienced in the application of a specific structural design. More specifically, in this work design reconfigurability allows for a structural design to accommodate loading variation.

Structural design optimization is typically done by considering one set of requirements to create a customized structural design. In this paper, this is referred to as "Method I" optimization. A second method of performing structural optimization is to consider several sets of requirements and design a structure which performs well for the set of requirements considered, a design envelope. In this chapter, this method of structural design optimization is referred to as "Method II" optimization. Structural design optimization for reconfigurability, in which a single set of components is designed to be reconfigured for various structural requirements, is referred to as "Method III" optimization. These structural design optimization methods are illustrated in Figure 3-2. In the figure, custom designs are created for each of the two considered load cases, an enveloping design is created for both load cases, and a set of structural components are created which can be reconfigured into feasible structural designs for each load case. The magnitudes of the cross-sectional areas of the truss structure elements are depicted as line thicknesses in Figure 3-2.

The goal is to design a set of parts that can be reconfigured to form various structural designs which accommodate different loading requirements. The set of optimum parts used to build these varying structural designs is obtained through design considering reconfigurability. In this design example, we consider an important metric to represent the performance of the structural design: manufacturing cost.

Manufacturing cost is chosen to be the metric for this design for flexibility example because the structural designs being optimized are assumed to be used in the private sector. The goal sought by the private sector is to improve profit margin. The consideration of reconfigurability in design allows for a reduction in costs. This reduction in costs is made possible because the manufacturer can mass produce one set of components which satisfy many customer requirements rather than manufacturing a custom-designed structure for each set of requirements. This ability to manufacture
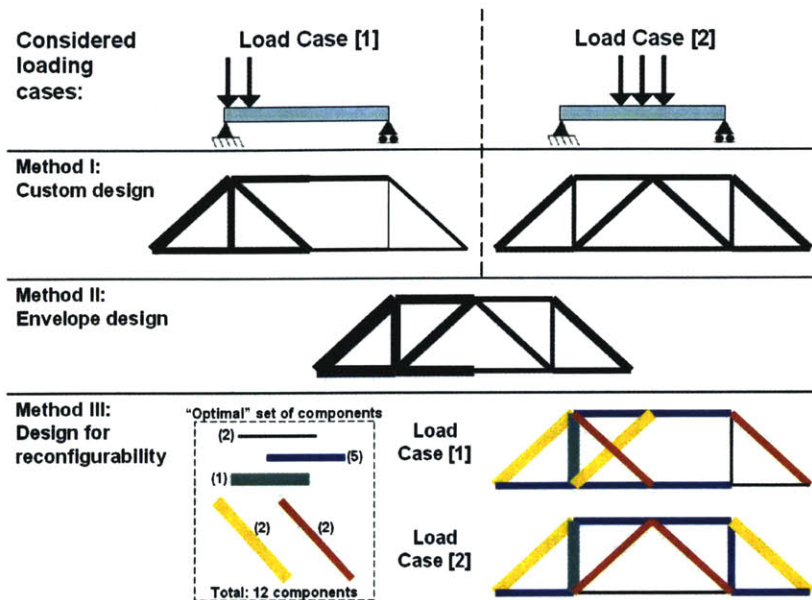
Figure 3-2: Three structural design optimization methods considering different loading conditions.

few custom designs and satisfy many requirements allows a manufacturer to reduce costs. This can be achieved in one way through reducing inventories. If a company sold a more capable product, it could keep fewer numbers of products in stock since they will satisfy a larger customer base. This in turn improves the profit margin of the manufacturer and is integral to the health of a private business. Design for reconfigurability can help private industry reduce costs by reducing manufacturing costs for a structure by designing a reconfigurable structure that can handle various loading conditions.

Penalties such as the labor cost of reconfiguring the structure and mass penalties result from the incorporation of reconfigurability into the design process.

A more general definition for structural design reconfigurability presented is one in which a reconfigurable structure is composed of modules that are interchangeable and can be configured to create various structural designs. Structural reconfigurability is the ability of the structure to be modified in order to respond to different loading conditions. In the case of structural subsystem elements composed of truss elements

considered in this chapter, a module is an element of the set of structural elements. Reconfiguration is performed by substituting truss structure elements of the same length.

An example of structural reconfigurability comes from the Swiss Army. Many armies, including the Swiss Army, use a modular, reconfigurable bridge called the Medium Girder Bridge [8] for supporting military transport. This bridge can be assembled quickly for various spans and loading conditions resulting from vehicles such as jeeps or tanks. A picture of this bridge design is shown in Figure 3-3.

Figure 3-3: The Medium Girder Bridge being used by the Swiss Army [2].

3.2 Literature Survey

The goal of structural topology optimization is to determine an optimal layout in order to minimize an objective function of a structure while satisfying given constraints.

Pantelides and Ganzerli [63] performed truss structure design optimization for uncertain loading conditions. Loading uncertainties of magnitude and direction were considered and optimization objectives of structural volume and displacement were minimized.

One major component of flexible design, modularity, has been studied as a component of structural design. This work has been performed Cetin, Saitou, Nishigaki, Nishiwaki, Amago, and Kikuchi [19]. In their research, Cetin *et. al.* performed a two-step optimization process in which an optimal structural topology design was decomposed into optimal modular components. Structural strength, assemblability, and modularity were considered in the decomposition optimization problem.

While research has been done on structural topology optimization as well as topics such as modularity, no research has been done on structural topology optimization considering design reconfigurability.

The goal of this design example is to investigate the manufacturing cost benefits resulting from the incorporation of reconfigurability into structural subsystem design by studying the effects of design reconfigurability on two dimensional truss structure designs.

3.3 Structural Optimization Model

This section presents the structural optimization model used for this research. Design assumptions, variables, objectives, and constraints are presented.

3.3.1 Modeling Assumptions

Several assumptions are made in the models for simplification. These are:

- The truss elements are made of rod elements. These elements only take axial load and do not take moments.

- All truss structure joints are assumed to be pin joints unless otherwise specified.

- A factor of safety of 1.5 is assumed for the example presented.

- The maximum linear cutting speed is assumed for all manufacturing operations.

The models developed for this research are used to investigate the manufacturing cost benefit by designing a structure for reconfigurability. This is done in a multi-

74

disciplinary optimization framework. The assumptions mentioned here allow for an exploration of the design space within a reasonable amount of time. More advanced models could be developed such as considering the truss elements to be beams and designing the cross-sectional geometries of the beams.

3.3.2 Design Objectives

A single design objective is minimized in this optimization model. The design objective is manufacturing cost of the abrasive cutting process. The objective function to be minimized is shown in Equation 3.1. This same objective function is used for "Method I," "Method II," and "Method III" simulations.

$$f(X) = C_{man} \tag{3.1}$$

In the above equation, C_{man} is the total estimated manufacturing cost of the structure and X is a design vector composed of the cross-sectional areas of the truss structure elements. The design variables are defined in Section 3.3.3.

3.3.3 Design Variables

The design variables for the simulation are the cross-sectional areas of each of the truss structure elements. Therefore, there is one design variable for each truss element in the structure.

$$X \equiv (\{x^{(1)}\}, \{x^{(2)}\}, \ldots, \{x^{(m)}\}) \tag{3.2}$$

In Equation 3.2, x^j is a vector of cross-sectional areas of jth length and m is the total number of unique truss element lengths in the structure.

3.3.4 Design Constraints

The constraints imposed on this problem statement are side constraints of the design variables, maximum von Mises stress, and maximum nodal deflection. The stress and deflection constraints depend not only on the cross-sectional areas of the truss

75

elements but also the truss structure configuration. These constraints are defined in the following equations.

$$\delta^{[n_{max}]}(X,Y) \leq \delta_c \tag{3.3}$$

$$\sigma^{[n_{max}]}(X,Y) \leq \sigma_c \tag{3.4}$$

where

$$\delta^{[n_{max}]}(X,Y) = max[\delta^{[1]}(X,Y) \cdots \delta^{[n_{lc}]}(X,Y)] \tag{3.5}$$

$$x_{LB} \leq x_i \leq x_{UB} \quad (i = 1,\ldots,n) \tag{3.6}$$

In the above equations, $\sigma^{[i]}$ is the vector of element stresses in the truss structure exposed to the ith loading condition, $\delta^{[i]}$ is the maximum vertical nodal deflection in the truss structure while exposed to the ith loading condition, n_{lc} is the total number of loading cases considered, n_{max} is the loading case in which the maximum vertical nodal deflection constraint is maximum, and n is the total number of truss elements being optimized in the truss structure. In addition, x_{LB} and x_{UB} are the lower and upper side constraints for the design vector variables, respectively.

3.4 Optimization Framework

This section presents the optimization framework used to obtain an "optimal" reconfigurable design for the design requirements. The gradient-based optimization algorithm and random search technique used in this framework are discussed. Details of the software modules used in the simulation are presented.

3.4.1 Framework Flow Chart

The optimal reconfigurable structural design for the given range of design requirements driven by various loading conditions is determined using an optimization approach shown in Figure 3-4. The outer loop optimizes the cross-sectional areas of the structural elements. An inner loop for each considered loading condition performs a random search reconfiguration of the structural elements to find a feasible configura-

tion. Random search was selected rather than optimization because the configuration is independent of the objective function. The constraint values from the inner loop are passed as constraints to the outer loop to act as penalty functions if no feasible configuration can be found given the set of structural elements from the outer loop.
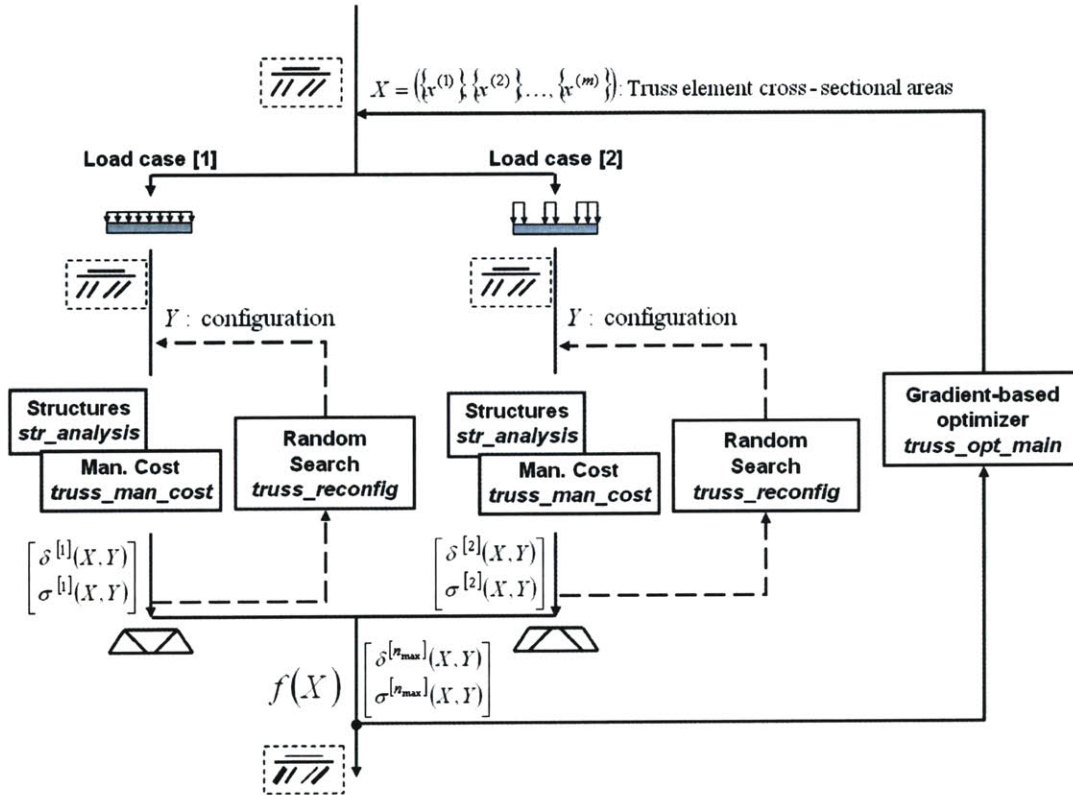
Figure 3-4: Method III optimization flow chart.

3.4.2 Outer Loop: Gradient-based Size Optimization

The outer loop of the optimization procedure, used to optimize the cross-sectional areas of the set of truss structure elements, is performed using a gradient-based optimization algorithm. MATLAB function *fmincon*, a sequential quadratic programming-based optimizer, is used. The relative ease with which *fmincon* was incorporated with the system model modules, also written in MATLAB, made the algorithm a suitable choice for this problem. A second reason for the selection of a gradient-based opti-

mization algorithm for the outer loop was the fact that all outer loop design variables are continuous.

3.4.3 Inner Loop: Reconfiguration by Random Search

The inner loops of Method III optimization perform a random search for a feasible structural configuration. One inner loop is required for each loading condition considered. The goal is to find a structural configuration which satisfies the design constraints. This procedure is illustrated in Figure 3-5. The random search is performed by perturbing the structural design and performing structural analysis of the perturbed design to check if it satisfies the stress and deflection constraints. Each perturbation in the random search interchanges one pair of truss elements of the same length at a time in the design vector. Optimization is not necessary in the inner loop because the structural configuration is independent of the objective function. Random search may be less efficient than an optimization algorithm and the incorporation of such an algorithm will be done in future work.

3.4.4 Simulation Routines

Several MATLAB routines were created to work together to perform the structural optimization for manufacturing cost for a two-dimensional reconfigurable truss structure. These routines include a main software module, a truss manufacturing cost estimation module, a truss reconfiguration module, and a structural analysis module. Important parameters and initialization techniques associated with each software module along with additional software details are included in this section.

Main: *truss_opt_main*

This routine was the main MATLAB module which called all other routines. In this module, the truss structure is defined, main parameters are defined, optimization routines are performed, and post-processing of results is handled.

Parameters

78
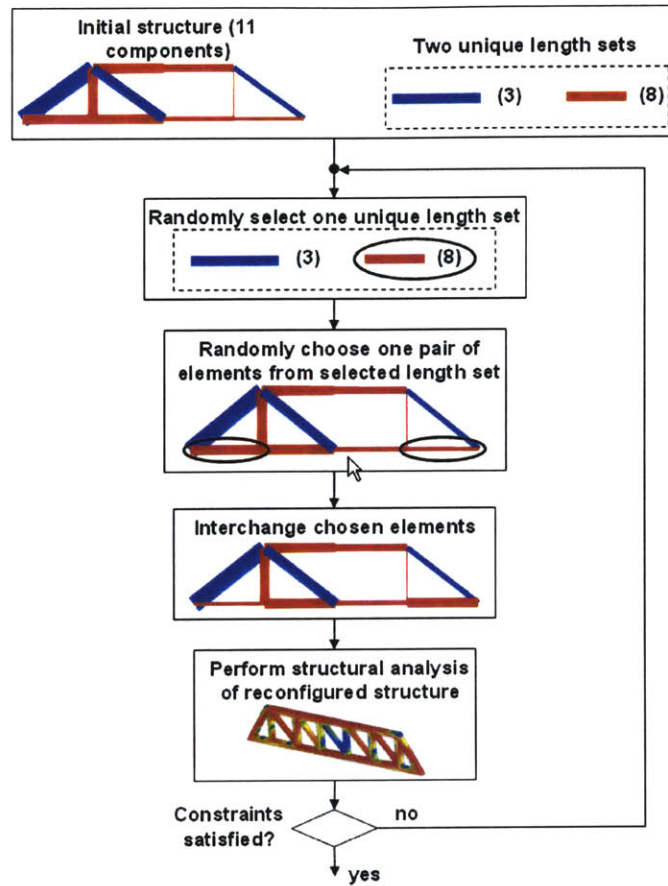
Figure 3-5: Method III inner loop reconfiguration procedure, *truss_reconfig* algorithm.

The major parameters set in this module are those defining the geometry of the truss structure, the number of loading cases to consider, the number of initial designs to consider, material properties of the truss structure elements, and abrasive waterjet settings. The geometrical properties of span, height, vertical element spacing, and end section width for the truss structure are specified in this module. These properties along with the required abrasive waterjet settings are presented in Section 3.5.1. The number of initial designs to consider depends on whether "Method I," "Method II," or "Method III" optimization is being performed. The material properties are defined in this module as well. For this design example, the material selected is A36 Steel with a Young's modulus of 200 GPa, a Poisson's ratio of 0.26, and a yield strength of 250 MPa.

79

In addition, the design variable scaling factor is set. A scaling factor, f_s, of 10^{-2} (see Equation 3.7) is used to adjust the order of magnitude of the design variables as they are passed between internal *fmincon* modules. These scaled design variables, X^*, are used to make the order of magnitude of the condition number of the optimization Hessian matrix, $H(x)$, a reasonable order of magnitude (e.g. between 10^{-1} and 10). The resulting scaled Hessian matrix is shown in Equation 3.8.

$$f_s \cdot X = X^* \tag{3.7}$$

$$H(X^*) \equiv \nabla^2(X^*) = \begin{bmatrix} \frac{\partial^2 J}{\partial x_1^{*2}} & & & \\ & \frac{\partial^2 J}{\partial x_2^{*2}} & & \\ & & \ddots & \\ & & & \frac{\partial^2 J}{\partial x_m^{*2}} \end{bmatrix} \tag{3.8}$$

Initialization

"Method I" and "Method II" optimizations are performed by first defining a set of initial structural solution guesses. These guesses are truss structures with all adjacent nodes connected by truss elements with identical cross-sectional areas. A visualization of a set of initial guesses used for these optimization methods is shown in Figure 3-6. A wide range of cross-sectional areas is used to attempt to sample a large portion of the design space.

The goal of starting the optimization with many different initial guesses is to attempt to find a near-global optimal solution. Since a gradient-based optimization method is used for the outer loop of this optimization framework, it has a tendency to get "trapped" at a local optimal solution. By starting the optimization routine from several different locations in the design space, there is a greater potential for finding a near-optimal solution.

"Method III" optimization is performed by defining the initial structural guess as the best design from the "Method II" optimization resulting design solutions. This was found to be the best way to get "Method III" to converge to a good solution in a reasonable amount of time. If the algorithm is started in an infeasible region, the
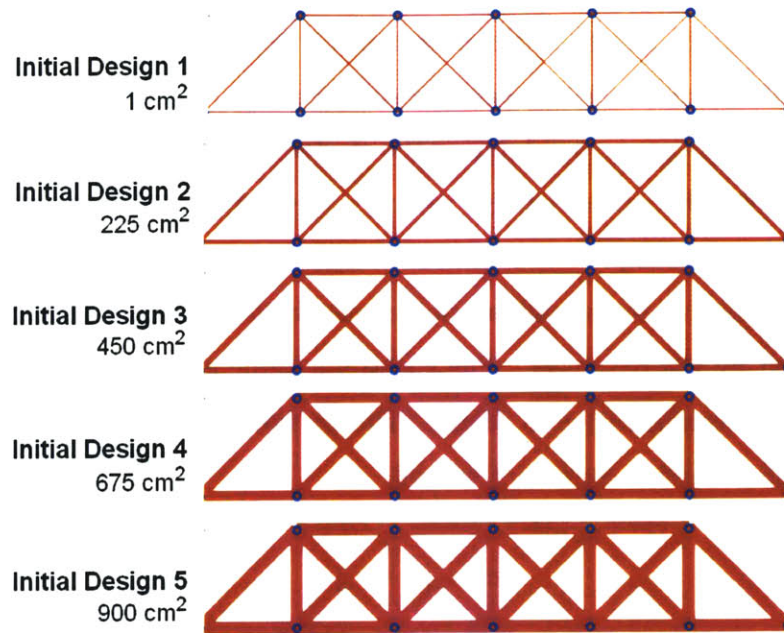
Figure 3-6: Example "Method I" and "Method II" initial designs.

random reconfiguration inner loop runs to the maximum number of iterations and slows the algorithm considerably. The slow speed of this algorithm can potentially be mitigated by:

- Increasing the number of structural configuration perturbations between each constraint evaluation.

- Use a heuristic-based optimization algorithm such as Simulated Annealing to broadly search the design space to find any potential feasible configurations.

Optimization

Outer loop optimization is performed by the MATLAB function *fmincon* combined with the objective function module, *truss_objective*, and a module which evaluates the maximum stress nonlinear constraint. The *truss_objective* module, defining the inner loop of the optimization framework, is used not only to determine the objective function for the outer loop optimizer but also to call the MATLAB reconfiguration module, *truss_reconfig*, for the truss structure. Structural designs sent from *fmincon*

81

to *truss_objective* to be evaluated are passed to *truss_reconfig* to perform random search reconfiguration of truss structure elements with the structure exposed to each loading case. If no truss structure configuration which satisfies the maximum stress and deflection constraints is found during the random search reconfiguration process, the resulting violated stress constraint vector, σ_p, is output to the stress constraint evaluation module (see Equation 3.9). This violated constraint is output to provide feedback that a feasible truss configuration cannot be found based upon the element designs selected by the optimizer. The constraint value acts as a penalty function when no feasible configuration is found. Future work will incorporate a penalty function for the deflection constraint as well.

$$\sigma_p = |\sigma - \sigma_c| \qquad (3.9)$$

The objective function is not modified by the inner loop because manufacturing cost is independent of structural configuration in this design example.

The resulting "optimal" solution is kept in memory for comparison with the "Method I" and "Method II" solutions. In addition, the objective functions from each iteration of the optimization algorithm are stored in memory for post-processing.

Post-processing

The optimal objective functions for the "Method I," "Method II," and "Method III" solutions are compared to evaluate the benefits of the incorporation of reconfigurability in structural design. These results can be seen in Section 3.5.3. Also, design space results are presented in Section 3.5.2.

The convergence behavior of the optimization framework can be analyzed by plotting the objective function results for each iteration of the optimization algorithm. This information is presented in Section 3.5.4.

Reconfiguration: *truss_reconfig*

This module performs reconfiguration of truss structure elements and evaluates the design constraints for each reconfigured (perturbed) truss configuration. The frame-

work for this module is presented in Section 3.4.3. In addition, this module stores in memory the designs which are output to *fmincon* following the iterative reconfiguration process.

A critical parameter for this software module is the maximum number of perturbations allowed to search for a feasible structural configuration. This setting, *rfgsteps*, is critical because it is one of the driving factors for whether or not a feasible configuration will be found for the proposed set of structural elements input from the outer loop optimizer. The significant computational time to perform all possible random reconfigurations requires that only a portion of the total possible configurations be attempted in order to obtain results in a reasonable amount of time. For example, for the "Method III" truss structure design solution (see Figure 3-13), there are roughly $15! \cdot 10!$ possible configurations. This is derived from estimating the number of permutations of the two equal length sets of fifteen and ten available truss structure locations for short and long lengths, respectively. The equation used to determine the number of permutations is shown in Equation 3.10. However, a setting of 2000 is used for *rfgsteps* for the optimization. Due to the computational time constraint, a small portion of the possible configurations is examined.

$$_nP_k \equiv \frac{n!}{(n-k)!} \tag{3.10}$$

where $_nP_k$ is the number of permutations of a subset of k elements from a set of n elements.

Manufacturing Cost Estimation: *truss_man_cost*

This module is used to determine the manufacturing cost of the parts that compose the truss structure. The manufacturing method used to estimate manufacturing cost for the bridge structural components is abrasive water jet (AWJ) cutting. This cost estimation module is similar to the cost estimation module used for the optimization examples presented in Chapter 2.

The inputs to this manufacturing cost estimation module include the design vector

83

variables and parameters such as element lengths, material properties, and material thickness. The output of this module is the total manufacturing cost of the set of bridge structural elements. Important parameters to this module include abrasive waterjet settings, which are presented later in this section.

To determine manufacturing cost for each truss structure element, each truss element is assumed to be a rectangular bar similar to that pictured in Figure 3-7. This is different from what was done in Section 2.4.3 for the previous optimization example. With the material thickness, h, set as a parameter, the machining operation is two-dimensional and lends itself to abrasive waterjet machining. Based on the material thickness and material properties, a maximum cutting speed is determined for the AWJ cutter. An important assumption made in this module is that the cutting speed of the waterjet cutter is constant throughout the cutting operation. Although the cutting speed of waterjet will slow at sharp corners or curves with small arc radii lie in the cutting path, this is ignored for this example. L_i is the length of element i, w_i is the width of element i, h is the user-defined material thickness, and x_i is the cross-sectional area of element i.
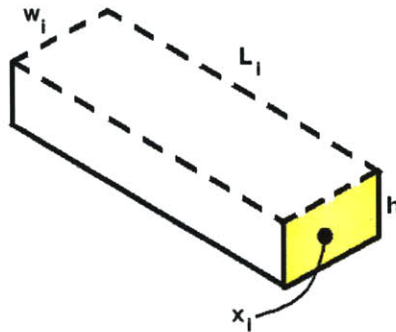
Figure 3-7: Example truss structure element to be machined using AWJ cutting (dashed line denotes cutting path).

The important factors used in determining the manufacturing cost are the cutting length, P_i, the maximum linear cutting speed, u_{max}, the overhead cost associated with using the AWJ cutting machine, OC, and the cross-sectional areas of each element, x_i. The equations for the cut length, cut speed, and overhead cost are detailed in

Equations 3.11, 2.1, and 2.2.

$$P_i = 2L_i + 2w_i \tag{3.11}$$

Total manufacturing cost is estimated using Equation 3.12.

$$C_{man} = \sum_{i=1}^{n} \left(\frac{P_i}{u_{max}} * OC \right) \tag{3.12}$$

In order to validate this module, a simple truss structure is created and manufacturing cost results from the cost estimation module are compared to hand calculations. The truss structure used to perform this validation is shown in Figure 3-8. The numbers near the elements are the labels of those elements.
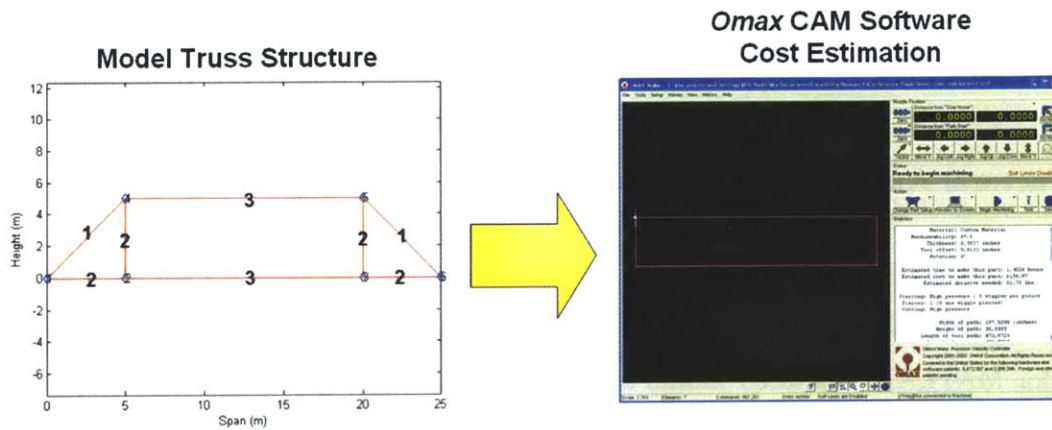
Figure 3-8: Manufacturing cost validation procedure.

To estimate the manufacturing cost for the structure in Figure 3-8, the cross-sectional areas for all of the truss structure elements are assumed to be 100 cm^2, the material thickness is assumed to be 1 cm, and the structure material is selected to be A36 steel. Using these inputs, the manufacturing cost of each element is estimated using the manufacturing cost estimation module and compared to the corresponding manufacturing cost using Omax AWJ computer-aided manufacturing software [6, 5]. These results are in Table 3.1.

The manufacturing cost estimates from the cost estimation model overestimate the cost by approximately 25% compared to the Omax CAM waterjet manufacturing

85

Element Design	Omax Manufacturing Cost ($)	Cost Model Manufacturing Cost ($)	% Error
1	146.31	182.88	25.0
2	108.87	135.97	24.9
3	289.74	362.59	25.1
Totals	544.92	681.44	25.1

Table 3.1: Manufacturing cost estimation module verification results.

cost estimation results. This is due to the fact that the cost model is based on a theoretical maximum linear cutting speed while the Omax CAM software allows for increased cutting speed. Although the discrepancy in the cost estimation is somewhat large, the difference is consistent and should not negatively affect the results of this chapter because we are mainly interested in a relative cost comparison.

Structural Analysis: *str_analysis*

Structural analysis for this structural design optimization example is performed using the Integrated Modeling of Optical Systems (IMOS) finite element analysis toolkit [4] for MATLAB. Required inputs to this module are the geometrical definitions of the truss structure, truss element interconnectivity between nodes, degree of freedom constraints of the nodes, and load vectors applied to the structure. Outputs obtained from the module are the nodal deflections and truss element stresses of the structure while experiencing a specified loading condition. These outputs are used to determine if the structural design satisfies the constraints given in Equations 3.3 and 3.4.

3.5 Truss Optimization Results

The concept of structural design optimization for reconfigurability is applied to a two-dimensional truss structure. "Method I," "Method II," and "Method III" design optimization results for the same truss structure are presented in this section.

86

3.5.1 Simulation Parameters

The important parameters specified for this simulation are the structure geometry, material properties, AWJ settings, loading conditions, degree of freedom constraints, and design variable side constraints.

The geometry, degree of freedom constraints, and loading directions for loading cases [1] and [2] are defined in Figure 3-9. Two different loading conditions are considered for this design optimization example. The load magnitudes of both load cases are 6200 kN each. This load is applied to two nodes depicted in Figure 3-9 for each load case. All nodes are free in the XY plane except for the constrained nodes depicted in the figure to create a simply-supported structure.
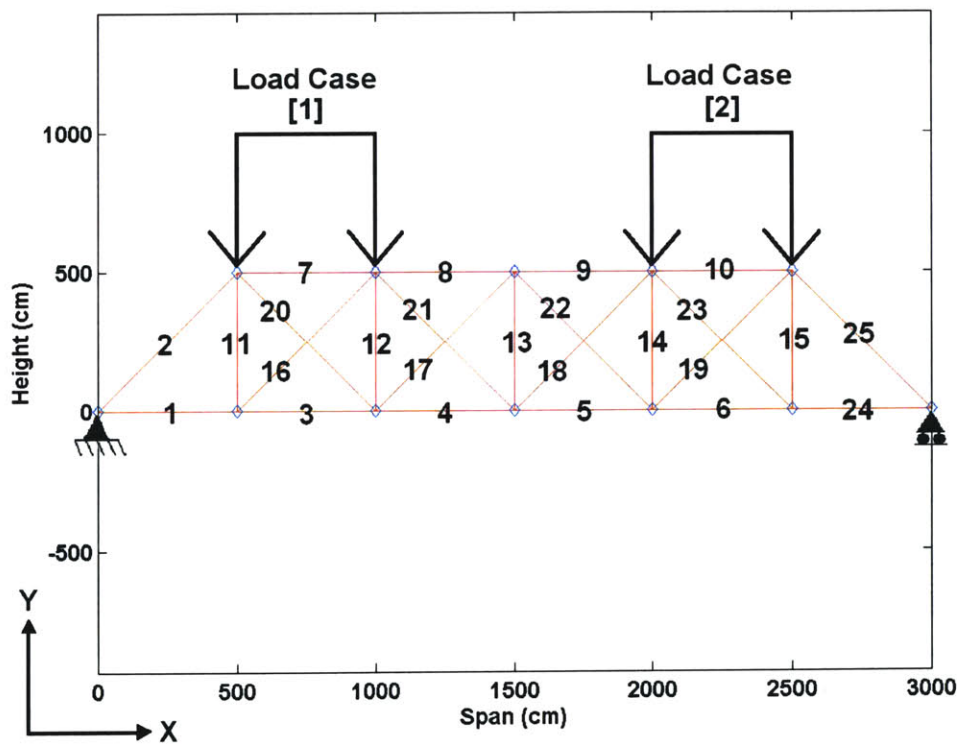
Figure 3-9: Simply-supported truss structure layout with labeled truss elements and considered loading conditions.

The material selected for this example is A36 Steel with a Young's modulus of 200 GPa, a Poisson's ratio of 0.26, and a yield strength of 250 MPa.

Side constraints defining the maximum and minimum cross-sectional areas of each truss element are 1100 and 0.001 cm^2, respectively. The nonzero lower bound was selected to allow the optimizer to remove truss elements by reducing the cross-sectional areas to values approaching, but not necessarily equal to zero. The upper bound is an arbitrarily chosen number used to help obtain reasonable cost results given the preselected material thickness.

3.5.2   Design Space Results

The design solutions obtained from optimization simulations are presented in this section.

Method I Optimization: Custom Design

Optimizing the structure for each load case results in unique structural designs for each load case considered. The two resulting custom designs for this example are shown in Figures 3-10 and 3-11. The magnitudes of the cross-sectional areas of each truss structure element are depicted as the thickness of the lines in the following figures.

The Method I structural design results for each loading case differ significantly. The "optimal" cross-sectional areas of each structure are different due to the different loading conditions. The truss elements with thicker cross-sectional areas are concentrated near the highly loaded portion of the structure, as expected. This allows the stress constraint to be met while minimizing manufacturing cost, a function of cross-sectional area.

Method II Optimization: Design for Requirements Envelope

Designing a structure that can accommodate all load cases is a different strategy for structural design than "Method I." If all load cases are considered simultaneously during structural design optimization, an "optimal" structure which can accommodate all considered loading cases while satisfying constraints is obtained. The resulting
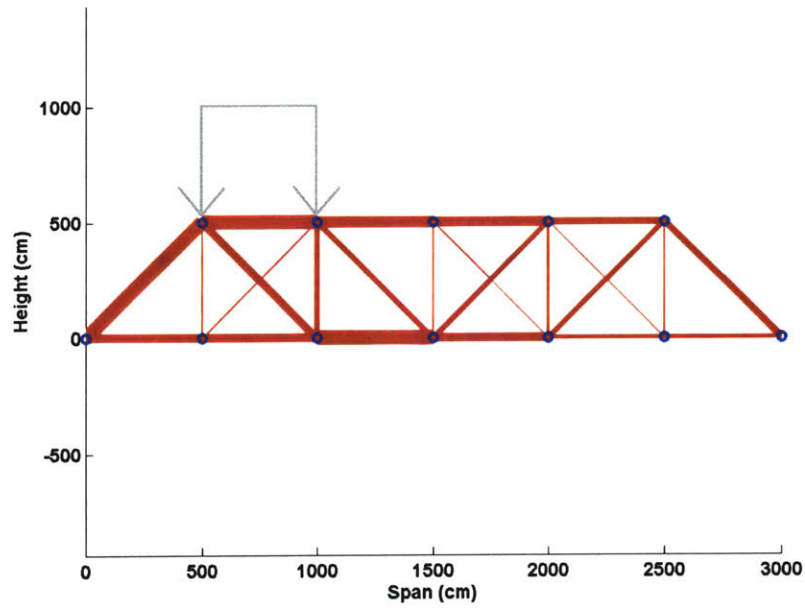
Figure 3-10: Method I structural design solution for load case [1] with loading displayed (see Table 3.2 for dimensions).
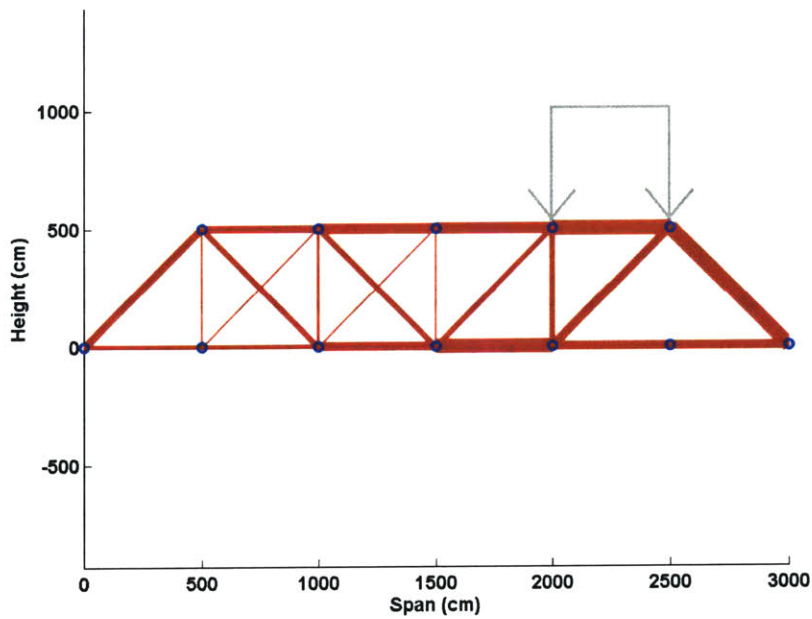
Figure 3-11: Method I structural design solution for load case [2] with loading displayed (see Table 3.2 for dimensions).

structure for this design optimization approach is shown in Figure 3-12.
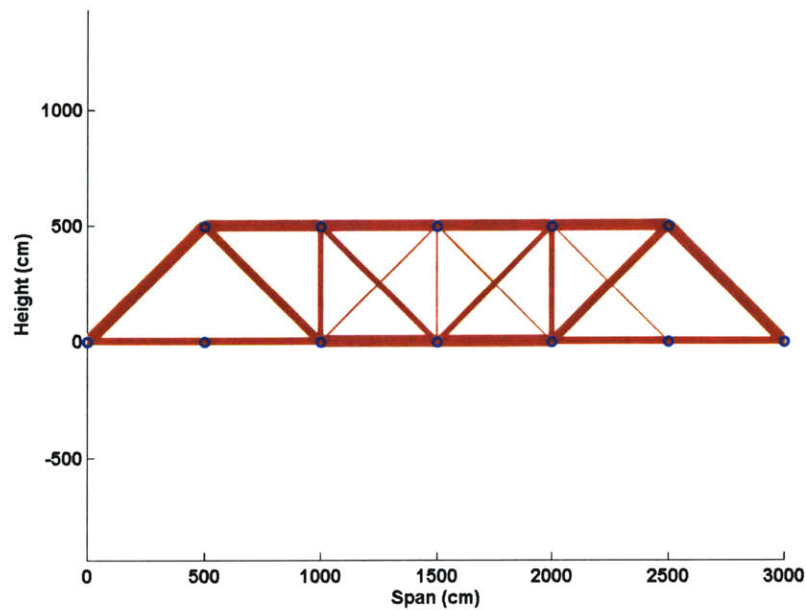
Figure 3-12: Method II structural design solution (see Table 3.2 for dimensions).

The structural design solution resulting from "Method II" optimization in which all loading cases are considered at-once is nearly symmetric. This is due to the fact that the two load cases considered are mirror images of each other. The slight asymmetry in the structural design is due to the non-symmetric boundary conditions imposed by simply-supporting the structure. This structural design is inefficient because it must accommodate all loading cases and the assumption is made that both load cases will - in reality - not be applied simultaneously. The above structural design, therefore, is "over-designed." If it is simply exposed to one of the considered loading conditions, the structure is more massive than required. Mass and manufacturing cost penalties result from the structure being "over-designed."

Method III Optimization: Design for Reconfigurability

A structure designed for reconfigurability can provide benefits of a custom design while also accommodate all loading cases considered. The resulting structural design is a single set of structural elements which can be reconfigured to accommodate each

90

loading case. The results from structural design for reconfigurability for this design example are shown in Figures 3-13 and 3-14. This optimization was performed using the optimization method presented in Figure 3-4.

The best results were obtained by using the Method II structural design result as the initial design topology for Method III structural design optimization. This initial design choice was made in order to start in the feasible region of the design space for Method III optimization. This was found to reduce computation time since less time is spent randomly searching the design space for feasible configurations in the inner random reconfiguration loop of the "Method III" optimization approach. This random search time would take significant time if feasible configurations could be found from an infeasible set of truss elements.
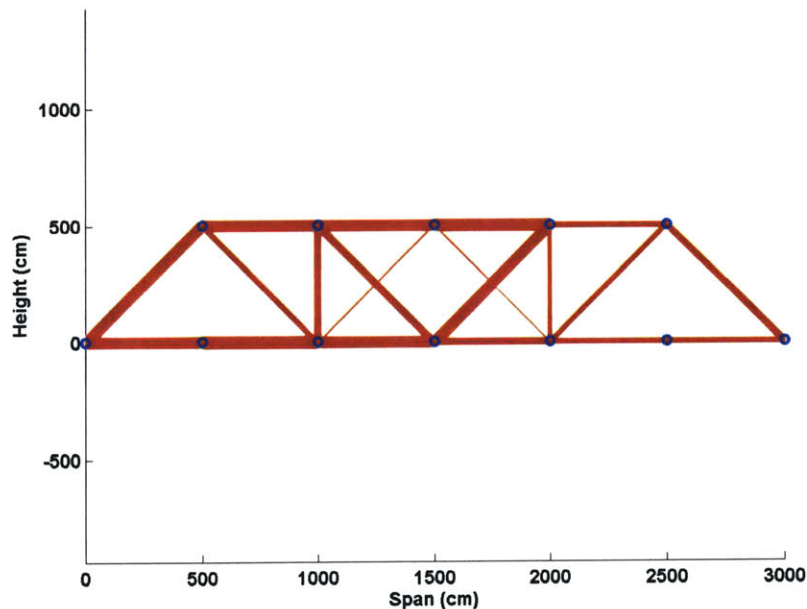
Figure 3-13: Method III structural design solution for load case [1] (see Table 3.2 for dimensions).

Rather than designing a custom structure for each possible load case or designing one structure to perform adequately for all considered load cases, a single set of components is designed which can be reconfigured to form structures which can perform well for all considered load cases. This is structural design for reconfigurability.

91
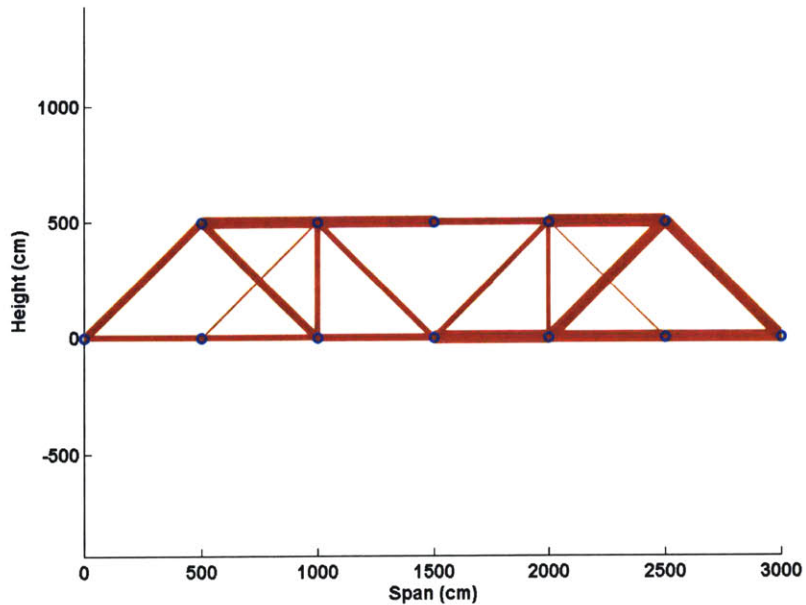
Figure 3-14: Method III structural design solution for load case [2] (see Table 3.2 for dimensions).

Design Space Results Discussion

The design solutions obtained by the optimization algorithm follow the expected design trends. The optimizer produced results in which the placement of the truss elements of larger and smaller cross-sectional areas is reasonable. The cross-sectional areas of the truss structural elements for the Method I, II, and III configurations are shown in Table 3.2. A dash in the table represents no truss element is present at that location.

From Table 3.2, the mass penalty incurred in the "Method III" design can be seen. Comparing "Method I" to "Method III" solutions for load case [1], structural elements 1, 3, 12, 14, 17, 18, and 24 are significantly larger in cross-sectional area for the reconfigurable, "Method III" structural design. Many of these members are on the left-hand side of the structure near the nodes experiencing the greatest loading. Making the same comparison for load case [2], structural elements 1, 6, 7, 12, 15, 19, 20, 22, 23, and 24 are significantly larger in cross-sectional area for the reconfigurable, "Method III" structural design. Many of these structural elements are near the right-

92

Element Number (see Figure 3-9) for labels	Method I Load Case [1], 24 elements	Method I Load Case [2], 22 elements	Method II, 22 elements	Method III Load Case [1], 20 elements	Method III Load Case [2], 20 elements
1	641	263	510	836	403
2	1081	446	859	821	507
3	638	323	509	895	375
4	1044	568	856	857	479
5	574	1046	856	479	895
6	323	637	511	375	836
7	1031	469	862	869	783
8	788	726	818	783	857
9	740	778	818	924	508
10	471	1047	863	429	924
11	6	57	-	-	-
12	361	149	340	508	429
13	48	48	1	-	-
14	151	371	339	246	246
15	55	-	-	-	-
16	8	104	-	-	78
17	-	81	38	78	-
18	356	439	421	817	333
19	338	618	561	333	817
20	614	337	563	426	455
21	428	364	421	507	426
22	81	-	37	98	-
23	104	-	1	-	98
24	264	643	510	403	869
25	442	1070	857	455	821
Mfg. cost	$5701.56	$5700.92	$5920.21	$5826.67	$5826.67

Table 3.2: Structural element cross-sectional areas (cm^2) and corresponding manufacturing cost estimates for Method I, II, and III solutions.

hand of the truss near the load case [2] loaded nodes. Overall, the reconfigurable design set of structural elements is more massive than the custom-designed structures.

The "Method II" structural design, designed to accommodate all considered loading conditions, is more massive than all other designs. This is a result of the "Method II" design having structural elements sized to the worst-case considered loading condition. The philosophy of designing for a requirements envelope allows the "Method II" design to accommodate all considered loading conditions. While the "Method II"

structure can handle all loading conditions, a mass penalty is incurred for designing a single structure to accommodate a requirements envelope composed of multiple loading conditions.

3.5.3 Objective Space Results

A comparison of the manufacturing cost objectives for the resulting configurations is presented in Figures 3-15 and 3-16. Figure 3-15 compares the manufacturing cost for Methods I, II, and III with only one of the two considered loading requirements. Figure 3-16 compares the manufacturing cost for the three design optimization methods for both loading condition requirements.
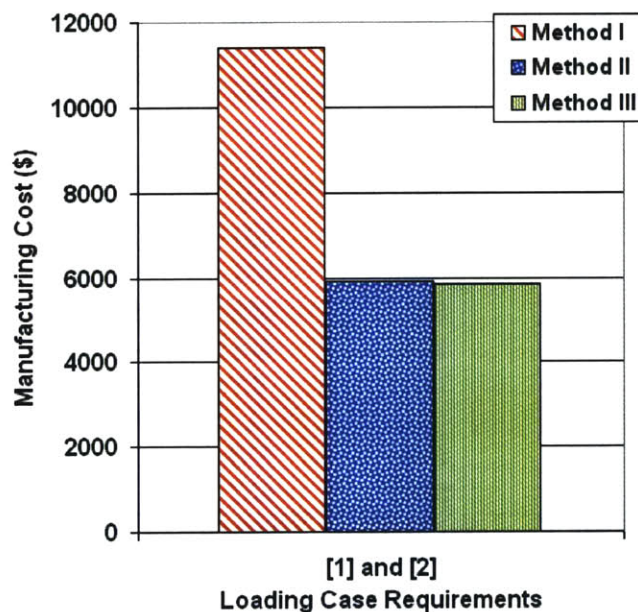
Figure 3-15: Method I, II, and III manufacturing cost comparison with one loading requirement.

From Figure 3-15, it is clear that for one specific loading requirement, the custom designed structure provided from Method I results in the structure with lowest manufacturing cost. However, the reconfigurable structure has the second-lowest manufacturing cost of the three and is 1.6% less expensive than the Method II design solution. Compared to the custom, Method I designs, the reconfigurable structure
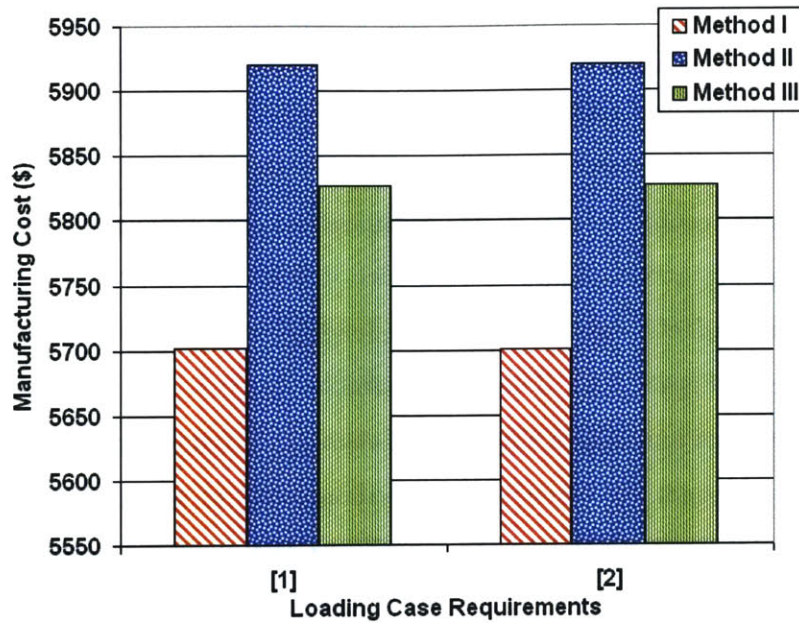
Figure 3-16: Method I, II, and III manufacturing cost comparison with both loading requirements.

is 2.2% more expensive. This manufacturing cost penalty is due to the fact that for Method III design, only one set of design elements is being used to accommodate several different structural design requirements. The reconfigurable design, as a result, must balance the requirements of all loading cases considered. This restriction of the number of unique design elements reduces the feasible design space for "Method III" design. On the other hand, the design space for "Method I" design is much larger because "Method I" designs are completely customized for each design requirement.

The result of designing for reconfigurability is a set of structural design elements which, when properly reconfigured, form structures for each loading condition that perform better than the "Method II" structure. The results are reasonable because it is not possible for a reconfigurable set of structural elements to be less massive and therefore less expensive to manufacture than a custom-designed structure. Although reconfiguration allows for good performance, the reconfigurable structural design must also balance the requirements of each load case considered. Therefore, because the reconfigurable set of structural elements must accommodate all load cases considered,

the performance of the reconfigurable structural design is limited by this worst case loading condition. A mass penalty is the result. This mass penalty translates directly into a manufacturing cost penalty.

Although it appears from Figure 3-15 that "Method I" structural optimization produces the best results, "Method III" optimization does have an advantage. This benefit of designing a reconfigurable structure is seen in Figure 3-16. This graph compares the manufacturing cost with both loading requirements rather than only one as assumed in Figure 3-15. The reconfigurable structure can accommodate both loading requirements and only a single set of elements is required. The benefit of the reconfigurable structure will increase as the orthogonality of the considered load cases is increased. Additional benefits of the reconfigurable structure design not shown in these results figures are advantages due to learning curve manufacturing, assembly, and testing cost savings due to commonality of parts among design configurations.

The "Method II" structural design, while inefficiently designed for each independent loading condition, can accommodate both loading conditions and only needs to be manufactured once. The custom-designed "Method I" structural designs both need to be manufactured in order to satisfy the requirements. This requires the manufacturing cost for both Method I structures to be summed together for comparison to the other two structural design approaches. In this case, the "Method III" solution is the most economical. However, the results shown are specific to the number and types of load cases considered in this chapter.

3.5.4 Convergence

The convergence history of the three structural design optimization approaches is shown in Figure 3-17.

Starting from a feasible design by using the "Method II" solution, the "Method III" optimization improves steadily and less dramatically than the Method I and II optimization trials. This is due to the fact that the Method I and II optimizations did not use feasible initial designs. The optimization algorithms used for Methods I and II are robust enough to find feasible, optimal solutions given infeasible initial
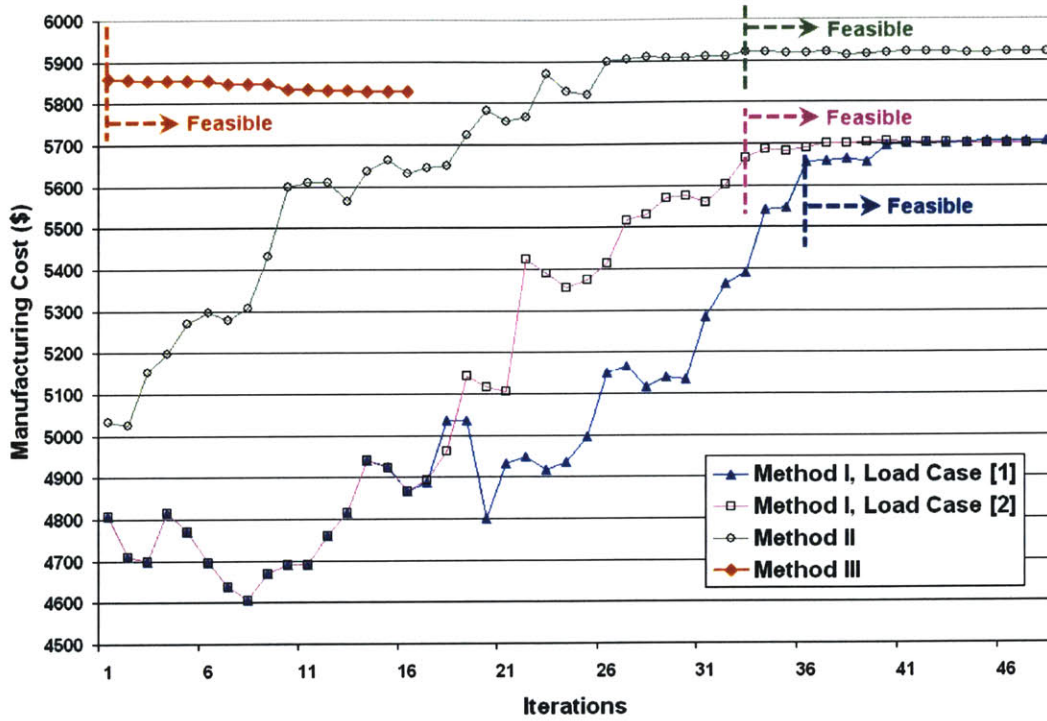
Figure 3-17: Method I, II, and III optimization convergence histories.

designs.

3.5.5 Computational Effort

The number of function evaluations and total CPU time required to converge to an "optimal" feasible solution are shown in Table 3.3. The results vary significantly between the Method I, II, and III optimizations. The large increase in CPU time for Method III optimization results from the time required to randomly reconfigure the set of structural elements in the inner loop to find feasible design configurations. The decrease in the number of function evaluations is a result of the increased CPU time required to perform the random search in the inner loop.

Optimization Method	Function Evaluations	CPU Time (min)
Method I, Load Case [1]	1378	0.4
Method I, Load Case [2]	1349	0.4
Method II	1370	0.7
Method III	702	71.1

Table 3.3: Number of function evaluations and CPU time required for Method I, II, and III optimization convergence.

3.6 Chapter 3 Summary

An optimization method using an inner loop performing random search structural reconfiguration was used for structural design optimization for reconfigurability. Reconfigurability was incorporated into the design process by the "Method III" optimization process. Manufacturing cost benefits were realized due to the embedment of reconfigurability into the structural design optimization process. For the case with two load cases, the manufacturing cost of the reconfigurable structural design is not only less than the structure designed for a requirements envelope, it is cheaper than the custom design structures due to the fact that each set of design requirements can be satisfied with the single reconfigurable set of components rather than two sets of custom-designed structural elements.

The disadvantages of the incorporation of reconfigurability were shown. A mass penalty is incurred by designing reconfigurability into a structure. This mass penalty results in increased manufacturing costs compared to the costs of a custom design. In order to meet the minimum structural performance requirements, a reconfigurable structure may be "over designed" for several of the possible loading scenarios for which it was designed. Designing reconfigurability into a structure reduces manufacturing cost while incurring a relatively small mass penalty in the structural design. A second penalty to consider is the labor cost of reconfiguring the structure. If the structure is significantly complex in design, this may be an important factor to consider.

In addition to the benefits of incorporating reconfigurability into structural design discussed in this paper, other benefits are possible from this design methodology. For

example, reconfigurable design could save money for a manufacturer as these reconfigurable component sets are mass produced. Rather than manufacturing many different sets of custom parts for each set of design requirements, one set of components can be manufactured to accommodate all of these considered design requirements. Manufacturing cost savings from learning curve effects can result. In addition, non-recurring engineering cost reductions could result from having fewer structures to design and test. As an increasing number of different customer requirements is considered in the design of the reconfigurable set of structural elements, the cost benefits compared to designing custom structures will increase. A third benefit of designing for reconfigurability is a cost benefit from inventory. A manufacturer will no longer need to maintain an extensive inventory of each custom design. Instead, a smaller inventory of reconfigurable structural element sets can be maintained which can accommodate all customer requirements as effectively.

The work presented in this chapter is at an intermediate stage and the benefits of designing for reconfigurability will be studied in more detail in future work. Although the structural design optimization example presented in this chapter considered two loading cases, this optimization method can be used for more complex structures with as many load cases as is needed for the particular application. A major limitation to the number of load cases considered, however, is the computation time required to perform the optimization.

Chapter 4

The Truncated Octahedron: A New Concept for Modular, Reconfigurable Spacecraft Design

This chapter presents a new structural design concept for spacecraft. The benefits and penalties of using the truncated octahedron as a modular building block for spacecraft design are shown.

Modular space exploration systems have been built in the past and they exist today. Most of these systems, starting with Apollo and Soyuz, assign high level functions to various physical spacecraft modules and assemble these in a linear stack. The predominant building block for such systems is the cylinder. Unfortunately, this configuration is inflexible and does not promote reuse of modules over a broad range of missions. We argue that future space exploration systems should be reconfigurable and therefore require additional docking ports, reconfiguration options and improved structural and volumetric efficiency. A survey of the modular spacecraft literature and analysis reveal that the truncated octahedron emerges as the most promising polyhedron-based spacecraft geometry for future application to space exploration. This argument is supported by comparison of various spacecraft geometries with four metrics: volumetric efficiency, launch stowage and packing efficiency, reconfigurability, and stability. In addition, extensible spacecraft design is enabled by this design

concept. This is shown in a preliminary design of manned exploration vehicles based on the truncated octahedron concept in which a mass penalty in designing a modular version of a Mars transfer and surface habitat vehicle compared to a "point design," linear stack concept, was found to be approximately 25%.

4.1 Introduction

The traditional paradigm in modular, manned spacecraft design has been to create a linearly stacked sequence of modules, which are either launched together on a single, heavy-lift launch vehicle or launched separately on smaller launchers with subsequent assembly in LEO. Typically each of the modules is assigned a different high level function, and the modules carry out their function in one or more of the primary mission phases. Figure 4-1 shows an example of an extensible space transportation system based on this linear stacking paradigm [72]. This is similar to the Apollo/Soyuz design philosophy, but adds the aspect of extensibility of the modular stack for more and more ambitious missions. For missions to and from the International Space Station (ISS), one can envision a command module (CM) for housing crew, life support systems, attitude control systems as well as communications gear and other electronics. The nose of the CM is equipped with a docking port for human access. The service module (SM) provides consumables for the crew, stores propellant and contains the main engine(s). This stack can be extended by an orbital (maneuvering) module (OM) for extended operations in LEO. For more challenging missions with higher ΔVs an extended service module (ESM) could be substituted. Finally, one may want the ability to add a transfer module (TM) for planetary transfer operations to the moon or to Mars. As Figure 4-1 shows, each module is based on a cylindrical structure, each featuring two manned, or unmanned docking interfaces front and aft. While this scheme is simple, it has two major drawbacks:

1. The number of possible configurations of a linear stack of N modules is small, $N!$ at best, but is likely to be much smaller due to docking/interface restrictions.

102
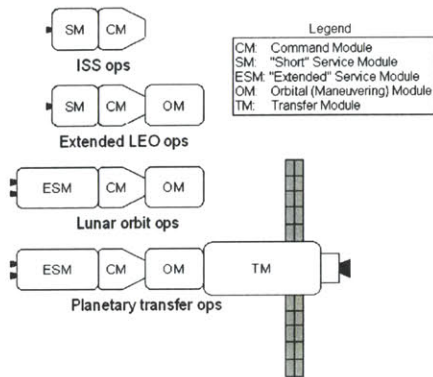
Figure 4-1: Linear stack, modular architecture.
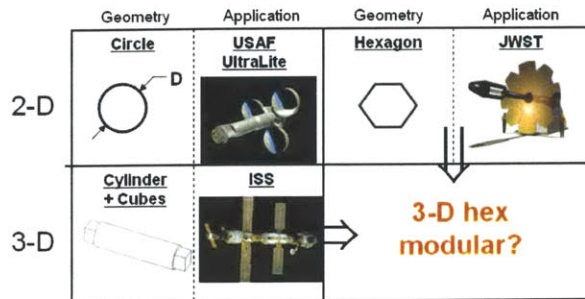
Figure 4-2: Extensibility of two and three-dimensional space structures.

2. The stack cannot be grown arbitrarily large, because the inertia matrix of the entire assembly becomes increasingly ill-conditioned with each additional module. Pencil-like structures are difficult to control in space (see Explorer I experience [54]).

This chapter explores non-linear stacking sequences for modular, manned spacecraft. This requires considering alternate geometrical building blocks. After briefly reviewing the literature on modular spacecraft (Section 4.2), the truncated octahedron is proposed as an interesting alternative building block (Section 4.5). After discussing the construction of this particular convex polyhedron, the ability of multiple truncated octahedra to form various linear and non-linear stacks is shown. In order to compare modular spacecraft building blocks, four metrics are developed:

1. Volume/Surface ratio as a measure of volumetric efficiency (Section 4.6.2)

2. Close-packing and launch stowage packing efficiencies (Section 4.6.2)

3. Reconfigurability coefficient, i.e. number of possible configurations over number of modules, N (Section 4.6.2)

4. Spacecraft stability (see Section 4.9)

Another way to frame this chapter is by considering current modular space systems in two and three dimensions. Two-dimensional modules are increasingly attractive

103

for antennas, solar arrays and optical mirrors (Figure 4-2, upper row). While sparse, circular apertures have been proposed, it can safely be said that hexagonal panels are finding increasing use because of their close-packing properties (small or no gaps when assembled side-by-side) as well as their advantageous surface area-to-circumference ratio. In three-dimensional space structures we have mainly relied on a combination of cylindrical elements, with cube-based connecting nodes (ISS) (see Figure 4-2 lower left). One may wonder if there exists a hexagon-based three-dimensional geometry that may serve as building block for efficient manned (or unmanned) spacecraft modules.

4.2 Close-Packing Spacecraft Design Literature Review

As early as 1985, engineers had begun to recognize the limitations of the cylinder as the shape of basic spacecraft modules. Frisina points out the need for close-packable modules that maintain modularity without creating the voids associated with cylinders when stacked together [39]. In 1994, Frisina proposed the isosceles tetrahedron as the basic unit from which to construct modules that do not create voids when stacked together. Triangular beams constitute the basic tetrahedral grid on which engineers can attach triangular faces, permitting reconfigurability [40].

Though such a technique would be practical for construction of large enclosed spaces, such as a space hangar, it would be infeasible for the creation of modules. Certain essential subsystems, like avionics, propulsion and life support, must be connected in fixed topologies. Modularizing a spacecraft arbitrarily may break these critical connections.

Some space designers recognize the need to reduce the cost of design by introducing common components to families of space missions similar in design requirements. Five proposed platform designs, including two from the 1980's, extol the virtues of common hardware components and interfaces. These are proposed by Parkinson [65],

104

Mikulas and Dorsey [57], Whelan, et. al. [89], Miller [58], and Smithies et al. [76], with an emphasis on extensibility and cost reduction. Daniels and Saavedra of EER Systems offer a modular platform for launch vehicles [25]. The explosion of space platform literature following the appearance of modularity literature indicates cross-fertilization of ideas occurred.

In addition, the literature from the past two decades points to a realization of the need for standardized spacecraft interfaces. Baily, et al. [14], Harwood and Ridenoure [43], and Abbott of Ontario Engineering International [9] offer different proposals for standardized interfaces.

The movement toward modular thinking in spacecraft design is largely motivated by cost. At the end of the Cold War, cost, rather than performance, became the dominant priority in program budgets [33]. Changes in foreign policy could no longer justify the tremendous costs associated with space transport and space activity could continue only by adopting the "commercial attitude" of cost reduction [66]. The cost of on-orbit assembly, an enabling technology for modular spacecraft design, has been modeled by Morgenthaler [59].

The benefits and penalties associated with modularity are covered in the following section.

4.3 Modularity Literature Review

Although the idea and design practice of modularity has existed for a long time, formal treatment of modularity has begun only in the past two decades [15]. This section defines modularity and discusses the benefits and penalties of modular design.

4.3.1 Definition of Modularity

In addition to the modularity definition in Section 1.2.1, modularity has been defined in other ways in literature. Ulrich and Tung [83] primarily define modularity as depending on two design characteristics. First, similarity between the physical and functional architecture of the design. Second, minimization of incidental interactions

105

between physical components. Using this definition, ideal modularity consists of a one-to-one correspondence between each design function and a single physical component. Huang and Kusiak define modularity as the use of common units to create product variants [47]. This is done by designing independent, standardized, or interchangeable units to satisfy a variety of functions. In broad terms, Mikkola defines modularity as an approach for organizing complex products and processes efficiently by decomposing tasks into simpler activities so they can be managed independently [56]. Enright, Jilla, and Miller define modularity as the standardization of interfaces between design elements and the reuse of functional units [33].

4.3.2 Types of Modularity

There are five different ways modularity can be used in current industrial practice. These five modularity types are: component-swapping modularity, component-sharing modularity, fabricate-to-fit modularity, bus modularity, and sectional modularity (see Figure 4-3) [83, 47].
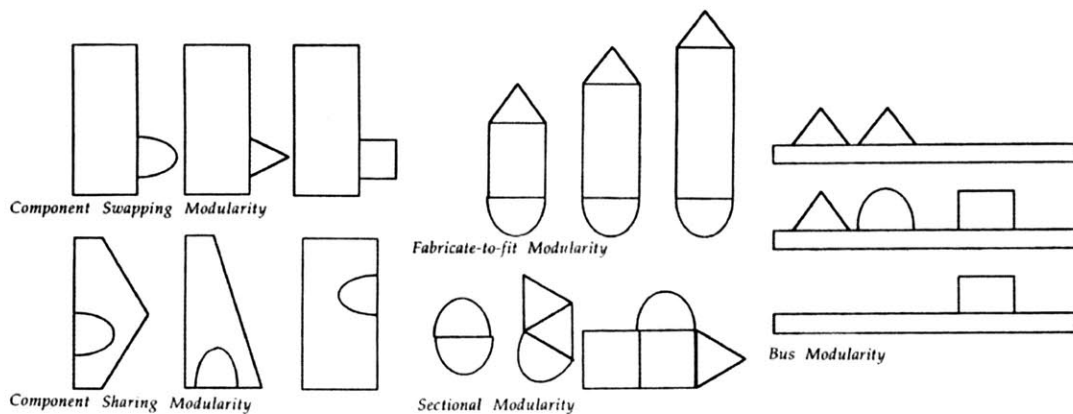
Figure 4-3: Types of modularity [83].

Component-Swapping Modularity

Component-swapping modularity occurs when two or more alternative components can be paired with the same modular components creating different product variants

106

belonging to the same product family. Examples of this from the automotive industry are the availability of different types of car stereos, windshield glass types, and wheel types for the same automobile model [83].

Component-Sharing Modularity

Component-sharing modularity is the complementary case to component-swapping modularity in which various modular components sharing the same basic components create different product variants from different product families. An example of this is the use of the same brake pads in several different product families of automobiles.

Fabricate-to-Fit Modularity

Fabricate-to-fit modularity is the use of one or more standard components with one or more infinitely variable-size additional components. Usually the variation is associated with the modification of physical dimensions (e.g. cut to length). An example of this type of modularity is a cable assembly in which two standard connectors can be used with an arbitrary length of cable.

Bus Modularity

Bus modularity is used when a module with two or more interfaces can be matched with any number of the components selected from a set of basic components. The product interfaces will accept any choice from the component set in any combination. Examples of bus modularity can be found in electrical or electronic systems with busses such as computers. Bus modularity allows for variation in number and location of the components in the system.

Sectional Modularity

Sectional modularity allows a collection of components chosen from a set of component types to be configured in an arbitrary way as long as the components are connected at their interfaces. An example of sectional modularity is found in piping systems in which elbows, tees, caps, and many others are components.

4.3.3 Benefits of Modularity

While there are many benefits provided by incorporating modularity into structural design, most benefits are related to reducing costs. Development costs and production costs are the two main costs to be reduced through the use of modularity.

Modularity benefits which reduce development cost are listed below [83, 33, 91].

- **Decoupling of tasks:** This requires definition of interfaces. Decoupling results in reduced task complexity and the ability to complete tasks in parallel. Also, a component's interactions become largely confined to it's defined interface, further simplifying the connectivity of a complex system.

- **Product variety:** A large variety of end products can be constructed from a much smaller set of different components. Product variety is the ability to use one of several alternative component options to implement a functional element of a design. A major benefit from product variety is the ability to capture a wider segment of the market without the high development costs of creating integral product variations.

- **Order leadtime:** Modularity allows order leadtime to be shorter for made-to-order products. If standardized products are combined with custom components, development can focus only on the components that are customized and simply inventory the bulk of the standard product.

Modularity benefits which reduce production cost are listed below [83, 33, 91].

- **Component economies of scale:** Modularity allows the same component to be used in many product variants and product lines. This allows development resources and capital expenses to be amortized across a large number of units and the exploitation of higher-volume, more-efficient production technology in component manufacturing. Units produced in mass quantities can result in manufacturing learning curve cost reductions.

- **Integration, assembly, verification, and testing:** Modular components correspond to particular functional elements and therefore the function of the

component is well defined and a functional test should be possible. The interface of the component being tested may be relatively easily simulated. Learning curve cost savings can be made possible by assembly-line construction and automated test facilities.

- **Design and production focus:** Modularity allows the division of a product into independent components. This allows design and production activities to be specialized and focused.

- **Product maintenance:** Modular design allows for the replacement of a faulty component in a product rather than attempt to diagnose and repair the component. This can potentially improve the speed and reduce the cost of repairing a product.

Additional modularity benefits relating to upgradability and consumption of components are listed below [83, 91].

- **Product change:** Modularity benefits the ease with which a product can be changed. If desired rates of change of components of a product are different, modularity accommodates this by allowing for components to be replaced at different rates. The entire product can be upgraded or changed without disrupting the overall product design.

- **Differential consumption:** Similar to product change, specific components which are consumed faster than the rest of the product are appropriate for modular design. Modularity can simplify and standardize replacement of such components. The batteries in a compact disc player are an example of this.

4.3.4 Penalties of Modularity

There are several disadvantages of designing for modularity. A list of many of these disadvantages is shown below [83, 33].

- **Obsolescence:** Modular hardware may become obsolete before development costs can be recouped. Also, interface standards may suffer from obsolescence. The pace of technological progress may outstrip that of hardware.

- **Servicability:** For spacecraft, there is little opportunity for servicing of hardware. The ability to replace components or reconfigure spacecraft is not as attractive unless there is a viable "in-space" servicing option. Such an option does not currently exist but is in development in the Orbital Express program by DARPA [74].

- **Performance compromise:** A modular design is one that is not optimized for performance. Penalties such as mass, volume, duplication of subsystems, and complexity of required interfaces between modules are not incurred for custom, optimized products. Interface hardware is non-productive weight because it does not add functionality to the product other than enabling modularity. The more modular a product, the less "optimal" the product. However, "optimality" over the entire lifecycle may favor modular systems.

- **Lack of diversity:** Although modularity can save money by amortizing costs across many different product lines, the failure of one product due to a common module may hold up the production of many other products. Until the origin of the failure can be determined, any products using similar hardware will be delayed. This risk of downtime is usually used to justify hardware diversity.

- **Excess capability:** If a module is used across multiple product lines, it will be designed to handle the worst-case design inputs. This module will therefore have excess capability for many products in which it is used. This is another cause of the sub-optimality of modular design.

4.4 Examples of Modular Space Systems

Many modular space systems have been designed and some have been built. Examples of modular space systems are the ISS, NASA's Orbital Aggregation and Space In-

frastructure Systems (OASIS) concept [90], and the NASA Design Reference Mission (DRM) concept [3]. These space systems exhibit modularity by designing distinct modules which each have unique functionality. For example, long duration habitation modules have unique designs while orbit transfer propulsion stages are standard designs. Separate modules such as these are utilized in an architecture to perform the desired space mission. The remainder of this chapter presents the truncated octahedron and how it can be used as a building block for modular spacecraft design.

4.5 The Truncated Octahedron Concept

4.5.1 Properties and Construction of the Truncated Octahedron

The truncated octahedron is a fourteen-sided polyhedron composed of six square faces and eight hexagonal faces. All edges of the truncated octahedron have equal length. A truncated octahedron can be created by joining two square pyramids together at their bases to form an octahedron and then cutting all six corners to remove one-third of the edge length from each vertex. The resulting truncated octahedron has edges that are all one third the length of the "parent" octahedron. The relationship between the edge length of an octahedron and a truncated octahedron is shown in Equation 4.1.

$$b = \frac{a}{3} \tag{4.1}$$

4.5.2 Truncated Octahedron Insphere

In order to estimate an internal usable volume of a truncated octahedron-shaped spacecraft, the equation defining a completely inscribed sphere in the truncated octahedron was determined. This "hex" insphere, tangent to the hexagonal faces of the polyhedron, is defined in Equation 4.2. Since there are both hexagonal and square
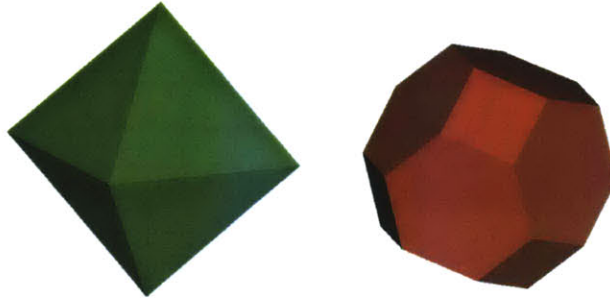
Figure 4-4: Left: equilateral octahedron with edge length a. Right: regular truncated octahedron with edge length b.

faces in a truncated octahedron, there is also an insphere related to the square faces. This inscribed sphere is not as useful, however, because parts of this sphere are external to the polyhedron. The equation defining the "square" insphere is Equation 4.3. These inspheres are shown in Figure 4-5.

$$D_{hex} = \sqrt{6}b \tag{4.2}$$

$$D_{sq} = 2\sqrt{2}b \tag{4.3}$$

In Equations 4.2 and 4.3, D_{hex} is the diameter of the "hex" insphere, D_{sq} is the diameter of the "square" insphere, and b is the edge length of the truncated octahedron.
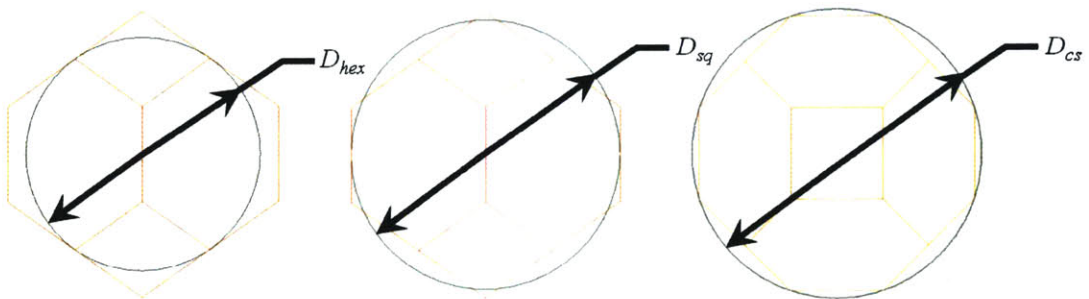
Figure 4-5: Hexagonal insphere (left), square insphere (center), and circumsphere (right) diameters.

4.5.3 Truncated Octahedron Circumsphere

A useful dimension for determining the envelope of the truncated octahedron is the circumspherical diameter, D_{cs}. For example, this dimension is used to size modules which fit inside a specific launch fairing. The circumsphere is a sphere in which the truncated octahedron is inscribed (see Figure 4-5).

$$D_{cs} = \sqrt{10}b \tag{4.4}$$

4.5.4 Analogs in Nature

Close approximations to hexagonal partitioning as well as truncated octahedron partitioning can be found in nature. Sandpipers in the tundra, terns on the barrier islands off North Carolina, and bottom-living African cichlid fish in a breeding tank all exhibit hexagonal partitioning [84]. The most famous case in nature of hexagonal partitioning are honeycombs and larval cells of bees and wasps, shown in Figure 4-6. Close approximations of truncated octahedra can be made by compressing a container filled with lead shot until the shot deforms enough to squeeze out all air in the container [84]. In addition, the thin-walled cells that fill the middles of the stems of many herbaceous plants approach the ideal truncated octahedron shape with about fourteen faces on each [84].

Figure 4-6: Bee with honeycomb [42].

4.5.5 Multi-Octahedron Configurations

The truncated octahedron allows for the creation of different structural design configurations. Three basic configurations possible with this modular building block are the linear stack, ring, and "sphere." These concepts are shown in Figure 4-8. The ability of the truncated octahedron module to attach at a square face, hexagonal face, or a combination of faces results in a large, but finite number of unique configurations if more modules are added to the structural system.

The linear stack concept is useful for a small number of modules launched in a single launch vehicle since the payload fairing is a cylindrical shape. The ring design may be useful for a spinning transfer habitat to provide artificial gravity for the astronauts. The spherical structure concept is useful for improving spacecraft stability, compacting structure for protection by a heat shield during atmospheric entry, and for radiation protection. Plume impingement during aerocapture or atmospheric entry can be reduced using this concept.
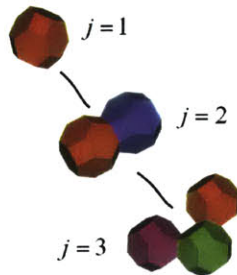
Figure 4-7: Modular structural designs with increasing numbers of design elements, j.
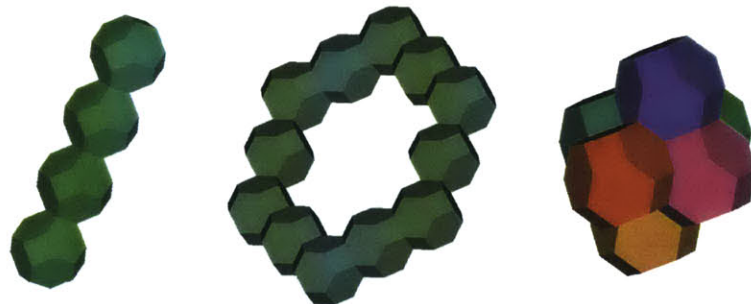
Figure 4-8: Linear stack, ring, and "sphere" truncated octahedron configuration concepts.

4.6 Comparison of Building Block Geometries

4.6.1 Mathematical Tiling Theory

The notional utility of the truncated octahedron concept can be formalized via the theory of combinatorial tiling. This concept can be applied to close-packing polyhedra, that is, solid shapes capable of completely filling three-dimensional space.

A surprising result in combinatorial tiling theory [30] shows that the number of *face-k-transitive* tilings is finite: in fact, there exist only 88 such tilings, falling into seven topological equivalence classes. These classes are defined by the following symmetries: tetrahedron, cube, octahedron, rhombic dodecahedron, special rhombohedron, and covered rhombohedron.

Strong candidates for modular spacecraft geometry may be derived from the maximally symmetric elements of these classes: less symmetric elements are likely to exhibit poorer surface area-to-volume ratios and weaker reconfigurability with no gains in packing efficiency. Though general proofs have yet to be constructed, empirical analysis of the metrics in Section 4.6.2 shows the truncated octahedron to be among the most favorable among these possibilities.

4.6.2 Metrics: Volumetric and Launch Efficiencies and Reconfigurability

For analysis in space systems we will develop a set of, perhaps simpler, metrics which measure a set of desirable properties of individual spacecraft modules and their combinations:

1. **Reconfigurability Coefficient**: Design reconfigurability is defined as the number of non-redundant design configurations, i, divided by the total number of design elements, j.

2. **Volume/Surface Area**: V/A, this ratio is a measure of the volumetric efficiency of a module. One of the goals of space system design is to maximize

$$\mu_1 = \frac{1}{1} = 1$$

$$\mu_2 = \frac{1}{2} = 0.5$$

$$\mu_3 = \frac{2}{3} = 0.67$$

$$\mu_4 = \frac{6}{4} = 1.5$$

$$\mu_1 = \frac{1}{1} = 1$$

$$\mu_2 = \frac{2}{2} = 1$$

$$\mu_3 = \frac{6}{3} = 2$$

(a) Cube. (b) Truncated octahedron.
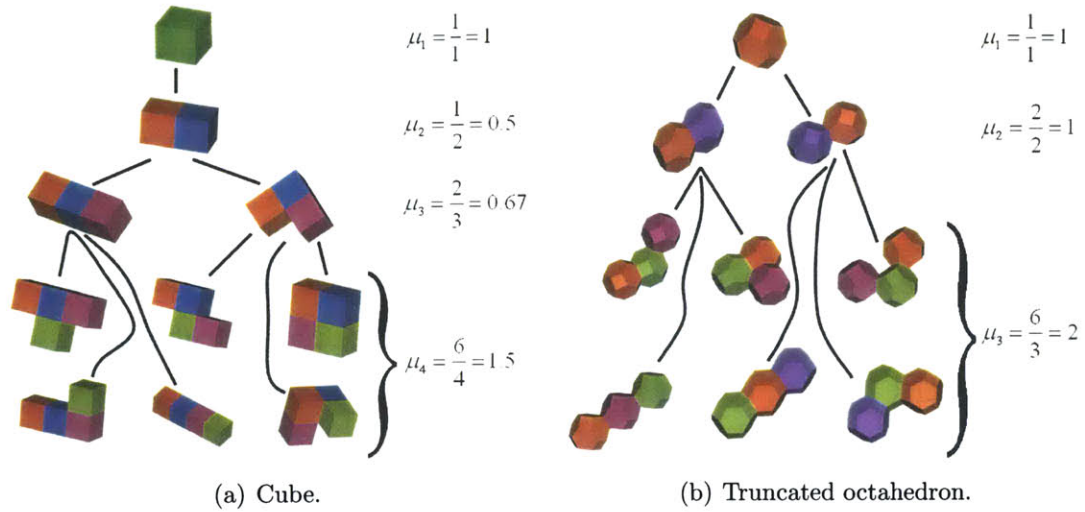
Figure 4-9: Design reconfigurability trees for the cube and truncated octahedron.

the amount of usable volume (e.g. for crew habitation, equipment installation or storage of consumables), while minimizing the mass needed to contain the volume. This metric applies to a single module.

3. **Packing Efficiency**: This is the ratio of filled volume over the total enveloping volume of a set of modules that are closely packed. We distinguish between close-packing efficiency (deployed on orbit) and launch stowage efficiency (inside a launch vehicle fairing).

4.6.3   Design Reconfigurability

For the purposes of this study, design reconfigurability of a modular spacecraft structural design is defined as the number of non-redundant design configurations divided by the total number of unique design elements used. The equation defining this metric, μ, is shown in Equation 4.5. In the equation, i is the total number of possible non-redundant design configurations given a number of design elements, j. In this case, design elements are considered to be identically-sized truncated octahedron modules.

$$\mu_j = \frac{i}{j}, \ where \ j = 1, 2, \ldots, \infty \tag{4.5}$$

116

It is assumed that each face of the truncated octahedron can mate with an identical face of another truncated octahedron. The two mating faces must be oriented such that the edges are aligned. As more design elements are added, the complexity of the design increases significantly. Non-redundant configurations are unique designs which are created by using j design elements. Both square and hexagonal faces are considered for docking. In addition, configurations are restricted to those which preserve the close-packing property of the truncated octahedron. This restricts the angle at which each module is oriented with respect to the corresponding mate. An illustration of how the number of unique configurations depends on the number of design elements is shown in Figure 4-9 for the truncated octahedron and cube. All faces of the cube are assumed to be able to mate with all faces of other cubes because all faces are of equal dimensions.

The design reconfigurability of the truncated octahedron and the cube are compared in Figure 4-10. The truncated octahedron exhibits a greater design reconfigurability than the cube as more elements are added to the structural design configuration. The dashed line is included in the figure for the truncated octahedron design reconfigurability for greater than three design elements because this performance for the truncated octahedron has yet to be computed. However, the trends shown in the figure are indicative of the design flexibility performance of the truncated octahedron for greater numbers of design elements. It is likely the truncated octahedron will continue to outperform the cube for even greater numbers of design elements.

4.6.4 Volume-to-Surface Area Ratio

For a pressurized volume spacecraft structure, the volume-to-surface area ratio is an important factor to consider. Ideally, a spherical structure would be used for a pressurized volume since it would result in evenly-distributed loading throughout the pressurized surface of the structure.

In reality, many pressurized volumes sent into space are not spherically-shaped. Fuel tanks generally are spherically-shaped, but crewed vehicles are usually cylindrical, cone-shaped, or have a custom shape. This is the case because of the interface
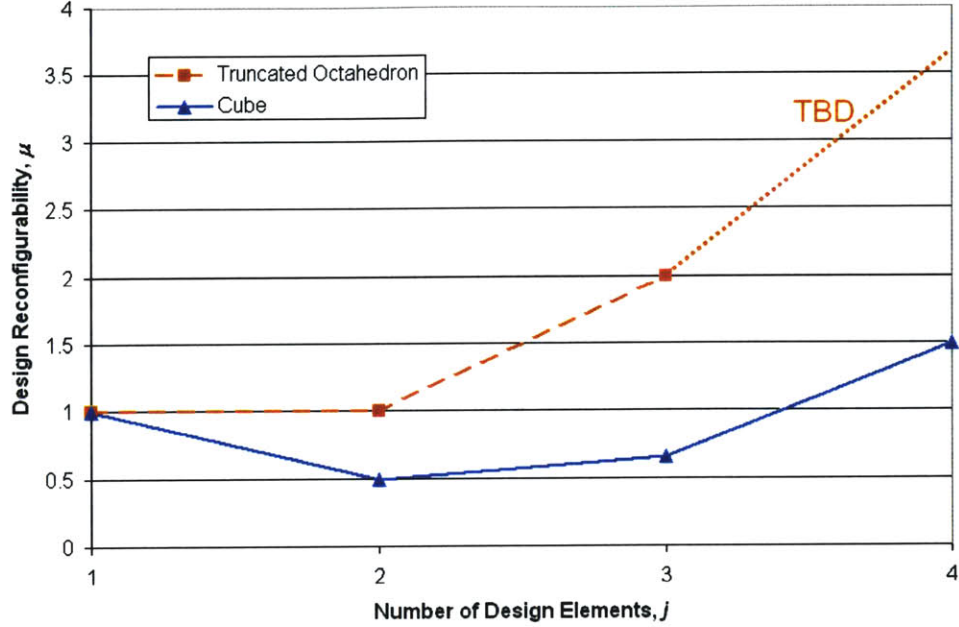
Figure 4-10: Design reconfigurability comparison of the truncated octahedron and cube.

requirements of these space structures. Fuel tanks do not require interfaces beyond simple structural mounting and pipes to transport fuel, oxidizer, and pressurant. Crewed pressurized structures, on the other hand, require large, flat interfaces for people and cargo to pass through. This large, flat interface requirement makes a spherical design for crewed space vehicles less practical. Cylindrical structures with interfaces on each end are usually the design of choice. The ISS is composed of many cylindrical, pressurized volume structures, for example. The truncated octahedron, in fact, has faces that can accommodate these interface requirements while maintaining a more favorable volume-to-surface area ratio.

The volume-to-surface area ratio of the truncated octahedron is compared to that of a sphere, cube, and cylinder. The results of this comparison are shown in Figure 4-11. It is assumed that each three-dimensional shape contains a unit volume. The truncated octahedron has the highest volume-to-surface area ratio of the non-spherical shapes considered. This is because the truncated octahedron more closely resembles a sphere than the other non spherical modules. The truncated octahedron's volume-

118

to-surface area ratio performance is 91% as good as the sphere, 4% better than the cylinder at its most favorable aspect ratio, and 13% better than the cube.
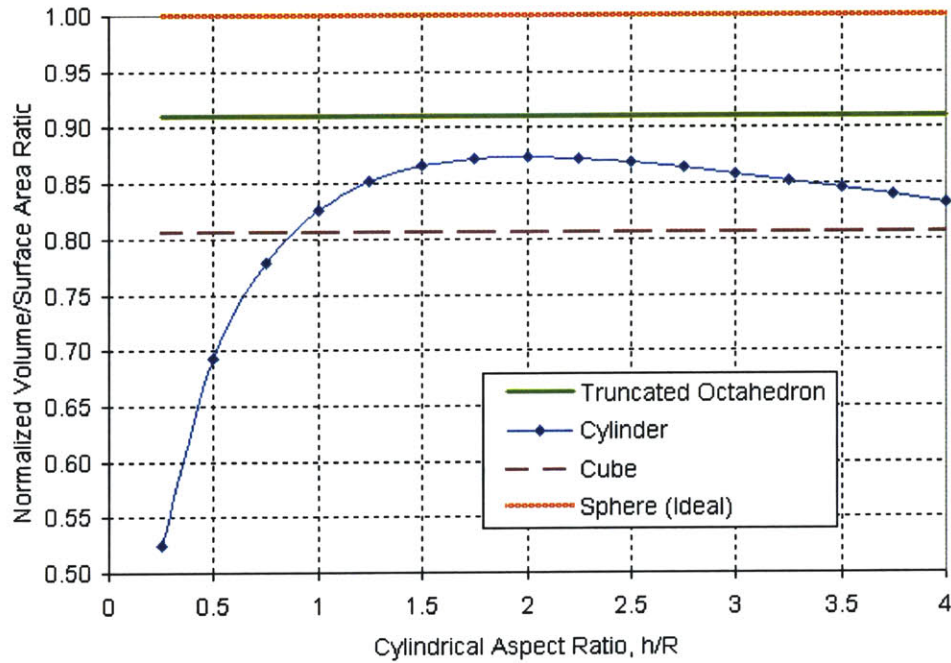
Figure 4-11: Volume-to-surface area ratio comparison of the sphere, truncated octahedron, cylinder, and cube.

4.6.5 Packing Efficiency

The packing efficiency of a structural modular building block is important for the stowed and deployed configurations of a space structure. The stowed configuration is defined as the structure as configured in the launch vehicle fairing. The deployed configuration is the final, assembled structure in space.

The ability of the truncated octahedron to pack together without voids results in perfect deployed packing efficiency. However, the stowed packing efficiency is somewhat inefficient due to the inability of large truncated octahedron modules to pack densely inside a cylindrical payload fairing. The cylinder may achieve close to 100% stowed packing efficiency compared to almost 50% for the truncated octahedron

Launch Fairing	D_{cs}	No. of Modules	Stowed Efficiency
Delta IV, 4-m	3.75	2	46%
Delta IV, 5-m, sht.	4.57	2	48%
Delta IV, 5-m, lng.	4.57	3	48%
Atlas V, 5-m, sht.	4.57	1	27%
Atlas V, 5-m, med.	4.57	2	42%

Table 4.1: Truncated octahedron stowed packing efficiency results.

(see Table 4.1). However, whether or not launch stowage efficiency is acceptable depends on whether the mass limit or the volume limit is the active constraint. For LOX (high density) modules expect the former, for LH_2 (low density) modules expect the latter.

An important constraint which prevents better stowed efficiency results is the requirement that the circumspherical diameter, D_{cs}, be the value of the maximum usable launch fairing. This allows for the use of modules of such size for crewed missions. The smaller the module size, the more efficiently the fairing volume can be filled, but such small module sizes would not be useful for manned spacecraft. Examples of stowed packing configurations for the truncated octahedron are shown in Figure 4-12. The deployed packing efficiency of the truncated octahedron is 100% compared to 100% for the cube, 91% for the cylinder, and 78% for the sphere.
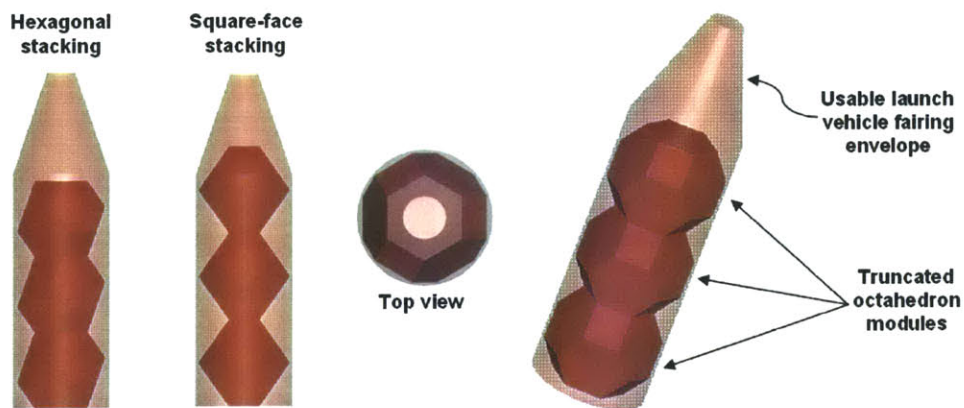
Figure 4-12: Stowed packing visualizations of truncated octahedron for the Delta IV, 5-meter, long fairing.

4.7 Design Application: NASA CER Vehicle Modularization

The space exploration initiative set forth by the current US administration calls for the manned exploration of the Moon, Mars, and beyond. The initiative requires an affordable exploration system design to ensure program sustainability [17]. This section presents a methodology for incorporating modularity into spacecraft structural design to help achieve sustainable, affordable space exploration. In addition, the modularization presented in this section is used to demonstrate the use of the truncated octahedron as a structural building block for space applications.

4.7.1 Transportation Architecture

A Mars and Moon mission exploration architecture developed by the MIT Fall 2004 16.981 Advanced Special Projects class working on the NASA Concept Evaluation and Refinement study for President Bush's space exploration initiative is used for motivation for this design example [45, 68]. The vehicle to be modularized to investigate the benefits of the truncated octahedron is the Transfer and Surface Habitat (TSH) defined in Figure 4-13 [45, 68, 3].
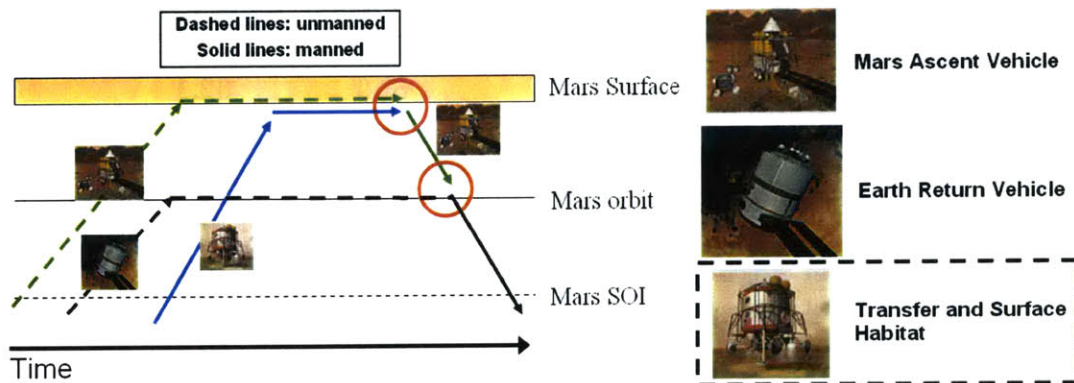
Figure 4-13: Example Mars mission architecture.

The Mars architecture selected for this analysis is similar to NASA's Mars Design

Reference Mission [3]. This architecture includes three vehicles: the Mars Ascent Vehicle (MAV), Earth Return Vehicle (ERV), and TSH. The MAV and ERV are prepositioned at Mars and it is verified that they are functioning properly before the crew travels to Mars. The crew of six travels to Mars in the TSH, lands, lives for 500 days on the surface, enters the MAV, launches into LMO, transfers to the ERV, travels back to Earth, and lands on Earth in the Earth Entry Module. It is assumed that each vehicle uses aerocapture at Mars instead of a propulsive orbit insertion. Mission architecture trajectory information is shown in Table 4.2 [45]. TMI and TEI stand for trans-Mars injection and trans-Earth injection, respectively.

Trajectory	Fuel/Oxidizer	ΔV (m/s)	Transfer Time (days)
TMI	LH_2/LOX	3600	260
TEI	LCH_4/LOX	2115	260

Table 4.2: Mars mission architecture trajectory details.

4.7.2 "Point Design" Analysis

Based on calculations performed by the MIT 16.981 class [45, 68], detailed mass breakdowns for the vehicles used in this architecture were calculated. These masses are included in Table 4.3 [45].

Component	MAV (mT)	ERV (mT)	TSH (mT)
Earth Entry Module	-	12.0	-
Habitat	3.6	52.9	**62.1**
TEI stage dry	-	8.0	-
TEI stage prop	-	53.1	-
Mars ascent stage dry	1.4	-	-
Mars ascent stage prop	9.0	-	-
Mars descent stage dry	1.4	-	**6.3**
Mars descent stage prop	2.7	-	**12.1**
Heat shield	3.6	25.2	**16.1**
TMI stage dry	5.1	35.2	**22.5**
TMI stage prop	33.8	234.9	**150.0**
Total mass	60.7	421.3	**269.0**

Table 4.3: Mars mission architecture vehicle mass breakdowns.

Design Constraints

The design constraints considered for modularization of the Transfer and Surface Habitat are imposed by the launch vehicle. For this analysis, an upgraded Delta IV Heavy launch vehicle is assumed to be the only launch vehicle system used. Based on information from Boeing about upgradability of the Delta IV [80], a Delta IV with a 6.5 meter diameter fairing and a payload capability of 40,000 kg to LEO is assumed. The assumed upgraded Delta IV Heavy launch fairing dimensions can be seen in Figure 4-14 [80, 48].

Assumptions

In order to compare the modular version of the TSH, a non-modular version must be designed. This "point design" of the TSH is assumed to be composed of cylindrical, linearly-stacked components. These components are the following: the descent module (DM), the transfer and surface habitat module, and the TMI orbit transfer module. The cylindrical dimensions of the habitat and propulsion modules are limited by the launch vehicle constraints as defined in Section 4.7.2.

Figure 4-14: Upgraded Delta IV Heavy launch vehicle fairing (dimensions in meters).

Transfer and Surface Habitat Module Design

The high-level design of the habitat in the TSH was performed by estimating the mass and volume. The pressurized volume required for this module is determined from the number of crew and the manned duration of the habitat. The pressurized volume required per crew member is assumed to be 19 m^3 [92]. The manned duration of this habitat is approximately 760 days.

Once the volume required per crew member, $V_{habitable}$, is known, the total pressur-

ized volume, $V_{pressurized}$, is calculated using Equation 4.6 [92]. The number of crew, N_{crew}, is six for this mission. The pressurized volume required for this habitat is 342 m^3.

$$V_{pressurized} = 3V_{habitable}N_{crew} \tag{4.6}$$

The total mass of the habitat is determined using Equation 4.7, an equation based on historical data for human spacecraft modules which has been modified for mission durations greater than 200 days [67, 45].

$$m_{hab} = 592 \left(N_{crew}\Delta t_{man}V_{pressurized}\right)^{0.346} + N_{crew}f_{ECLS}\dot{m}_{cons}\left(\Delta t_{man} - 200\right) \tag{4.7}$$

In Equation 4.7, Δt_{man} is the duration the habitat is crewed in days, f_{ECLS} is the environmental control and life support system (ECLS) recovery factor, set to a value of 0.68 [55], and $\dot{m}_{cons}$ is the mass flow rate of consumption of consumables per crew member in kilograms per day, set to a value of 9.5 based on Apollo mission data [55]. The resulting habitat mass is determined to be 62,070 kg.

Orbit Transfer Module Design

The Orbit Transfer Module (OTM), a large, single-stage propulsion module used to provide the ΔV for the TMI leg of the Mars mission, consists of large propellant tanks and an engine. Given the payload being transported to Mars, the rocket equation, shown in Equation 4.8, is used to size the OTM. The specific impulse, I_{sp}, and mass ratio of the LOX/LH_2 propellant are 450 seconds and 6:1, respectively [36]. The payload for the OTM, m_{pl}, consists of Mars landing stage, habitat, and aerocapture heat shield with a combined mass of 96,564 kg. The propulsion system mass fractions used for propellant tanks and engines are 0.113 and 0.037, respectively [45]. The detailed initial and final mass breakdowns are shown in Equations 4.9 and 4.10, respectively. The OTM propulsion system masses were calculated using the equations mentioned previously. Propellant masses are shown in Table 4.4. In addition, a dry

mass of 22,500 kg is determined using an assumed dry mass fraction of 15%.

$$\Delta V = I_{sp} g_0 ln \left(\frac{m_0}{m_f} \right) \tag{4.8}$$

$$m_0 = m_{pl} + m_{prop} + m_{tank} + m_{eng} \tag{4.9}$$

$$m_f = m_{pl} + m_{tank} + m_{eng} \tag{4.10}$$

Prop	Mass (kg)	Density (kg/m^3)	Vol. (m^3)
LH_2	21,430	70.8	302.7
LO_X	128,570	1141	112.7

Table 4.4: OTM propellant mass breakdown.

In Equations 4.8, 4.9, and 4.10, m_0 is initial mass, m_f is final mass, m_{prop} is propellant mass, m_{tank} is propellant tank mass, and m_{eng} is engine mass.

Heat Shield Mass Estimation

The mass of the heat shield, m_{hs}, required for aerocapture of the habitat and descent module of the TSH is estimated using Equation 4.11. The factor of 20% used in this equation is selected to roughly approximate the mass of the heat shield. While this factor does not produce an accurate heat shield mass, it adequately represents the heat shield for the purposes of this analysis.

$$m_{hs} = 0.2 \, (protected \, mass) \tag{4.11}$$

Design Solution

Using the masses and volumes for the "point design" TSH vehicle, shown in Figure 4-15, a CAD model is created with the calculated volumes and mass properties of the landing stage, habitat, OTM, and heat shield. Solar cell arrays are included in the CAD model for illustrative purposes but are not used for mass properties analysis.
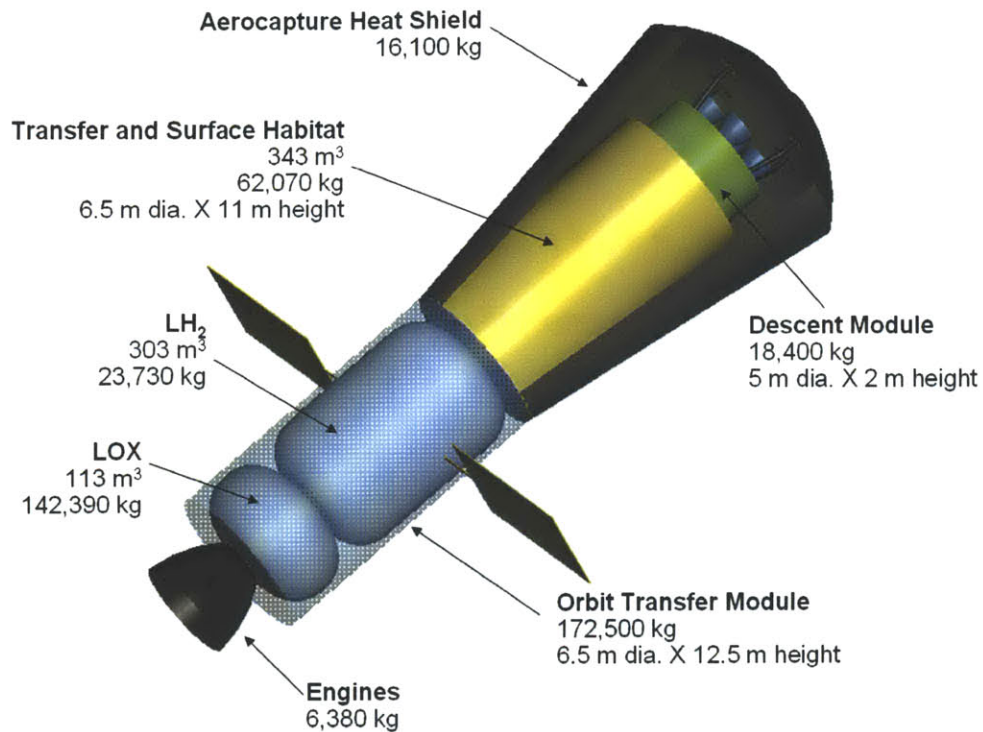
Figure 4-15: Linear stack "point design" vehicle (heat shield partially removed for habitat and descent module viewing).

4.7.3   Vehicle Modularization

In order to incorporate modularity using the truncated octahedron concept for TSH design, three parts of the vehicle are selected for modularization: the habitat, fuel tank, and oxidizer tank. Truncated octahedron-shaped modules are used to create the required structures for each of the selected components.

Modularization Assumptions

A set of assumptions is used to perform the modularization of the Transfer and Surface Habitat vehicle. First, the hexagonal insphere (see Section 4.5.2 for definition) is used to determine the estimated internal pressurized volume of a truncated octahedron module. Second, the circumsphere diameter of the module is the benchmark for determining the size of the module. This sphere is useful for determining the envelope of the module for stowage in a launch vehicle fairing. Third, a structural modularity

126

factor, f_{mod}, of 10% is assumed. This modularity factor is included to account for the overall structural mass increase from the additional structure required to enclose smaller volumes than the one-module "point design." Finally, a docking hardware penalty, m_{dock}, of 400 kg per module is assumed. This mass penalty accounts for standardized docking hardware between modules and extra hardware required for the facilitation of electronic, thermal, environmental, and propellant transport between modules.

Design Objectives

Two design objectives, J_1 and J_2, are used to determine the "optimal" modular quanta for vehicle components. J_1 and J_2 are the number of launches required to put the complete vehicle in LEO, $N_{launches}$, and the total initial mass in LEO (IMLEO), m_{IMLEO}, respectively. These objectives are both functions of three variables, the truncated octahedron module circumsphere diameter, D_{mod}, a propulsion system scaling factor, $f_{propscale}$, and an oxidizer tank fill factor, f_{oxfill}. These objective functions are shown in Equations 4.12 and 4.13.

$$J_1 \left(D_{mod}, f_{propscale}, f_{oxfill} \right) = N_{launches} \tag{4.12}$$

$$J_2 \left(D_{mod}, f_{propscale}, f_{oxfill} \right) = m_{IMLEO} \tag{4.13}$$

Design Variables

Three design variables are used to search the modular quanta design space. These design variables are a propulsion system scaling factor, $f_{propscale}$, an oxidizer tank fill factor, f_{oxfill}, and the truncated octahedron circumsphere module diameter, D_{mod}. The propulsion system scaling factor is a design variable because it needs to be adjusted in order for the ΔV constraint to be satisfied depending on the modular quanta selected. The oxidizer tank fill factor is used to allow for the feasibility of large propulsion tank sizes while still satisfying the launch vehicle payload mass constraint by only partially filling the oxidizer tanks. This allows for the possibility of

127

investigating larger modular sizes even though liquid oxygen, a very dense liquid, is one of the propellants. D_{mod} is used to determine the "optimal" truncated octahedron module size to select for the modular spacecraft design.

Design Constraints

The primary constraints for the modularization of the TSH vehicle are the launch vehicle constraints detailed in Section 4.7.2 and the ΔV requirement of 3,600 m/s for the TMI burn in the Mars architecture (see Table 4.2). In addition, all modules used for the spacecraft design must have the same circumsphere diameter. This allows habitat, fuel tank, and oxidizer tank modules to all fit together properly to take advantage of the packing efficiency and manufacturing cost benefits of the truncated octahedron modular design. The upper bound for the module diameter is the launch vehicle fairing diameter. The lower bound of 4.4 meters for the module diameter is selected to be a reasonable number based on the internal dimensions necessary for useful manned spacecraft design. These constraints are shown in Equations 4.14, 4.15, 4.16, 4.17, 4.18, and 4.19.

$$\Delta V_{sys} \geq 3600 m/s \tag{4.14}$$

$$m_{habmod}, m_{oxmod}, m_{fuelmod} \leq 40,000 kg \tag{4.15}$$

$$D_{mod} = D_{habmod} = D_{oxmod} = D_{fuelmod} \tag{4.16}$$

$$4.4m \leq D_{mod} \leq 6.5m \tag{4.17}$$

$$0 \leq f_{propscale} \leq 1 \tag{4.18}$$

$$0 < f_{oxfill} \leq 1 \tag{4.19}$$

In the design constraint equations, ΔV_{sys} is the velocity change imparted on the spacecraft for the TMI mission segment. The mass of each habitat, oxidizer tank, and fuel tank module is denoted by m_{habmod}, m_{oxmod}, and $m_{fuelmod}$, respectively. The circumsphere diameter of each habitat, oxidizer tank, and fuel tank module is denoted

by D_{habmod}, D_{oxmod}, and $D_{fuelmod}$, respectively.

Module Sizing Procedure

A flow chart of the procedure used to create modular designs is shown in Figure 4-16. First, the masses and volumes of the components of the system to be modularized are specified (see Figure 4-15 for these values). Second, the propellant volume to be used is scaled by the $f_{propscale}$ design variable to allow for ΔV feasibility. This scaling factor allows for a more simplified set of calculations by eliminating the need to iterate propulsion system wet and dry masses to "optimally" size the modules while satisfying the ΔV constraint. Third, the components to be modularized are subdivided into design interpolation points (see Subdivision of Modules section). Fourth, the fill fraction of the oxidizer tanks is specified which determines the number of oxidizer tanks required. Fifth, the constrained design space is explored for the range of module sizes considered. The total IMLEO and number of launches of each feasible design is calculated and feasible results are output and recorded for analysis.
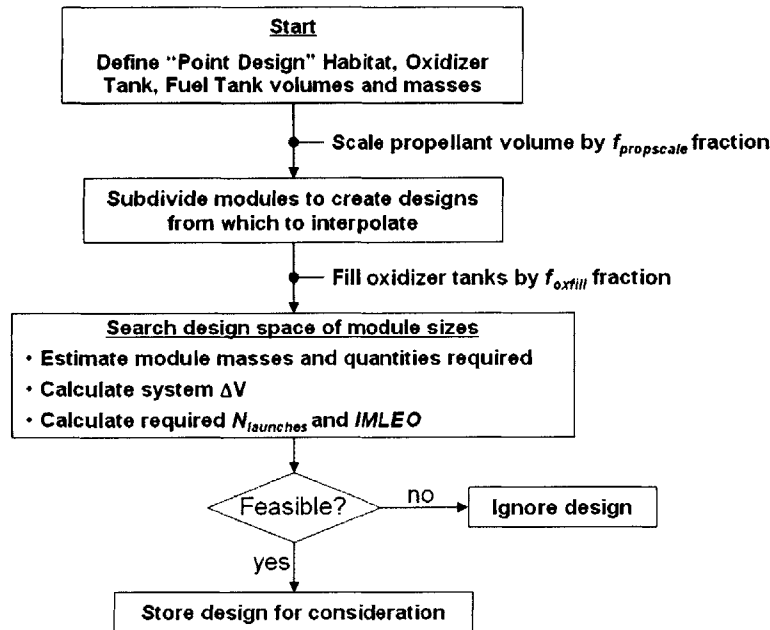
Figure 4-16: Modular sizing process flow chart.

N_{mod}	D_{mod} (m)	V_{Imod} (m^3)	M_{Imod} (kg)
1	11.21	342	62,070
2	8.9	172	32,211
3	7.77	114	21,607
4	7.06	86	16,305
5	6.56	69	13,124
6	6.17	57	11,004
$\vdots$	$\vdots$	$\vdots$	$\vdots$

Table 4.5: Subdivision of the habitat portion of Transfer and Surface Habitat vehicle.

Subdivision of Modules

To obtain masses of modules of various sizes, module design interpolation points are required. This is done by subdividing the original "point design" volumes into smaller pieces, providing design reference points for which the module sizes being investigated use as interpolation reference points for the mass calculations of each habitat, fuel tank, and oxidizer tank module. An example of the modularization of the habitat component is shown in Table 4.5.

In order to calculate the mass of a 6.2 meter diameter habitat module, for example, the design is scaled from the closest interpolation design that is smaller than or equal to the design being investigated in size (6.17 meters). The volume ratio of the design being considered versus the interpolation point is used to size the structural mass of the 6.2 meter habitat module (see Table 4.5 for reference. Equation 4.20 is used to calculate the mass of the mass of the interpolation point module design m_{Imod} and Equation 4.21 is used to estimate the total mass of the vehicle component being investigated, m_{mod} (e.g. habitat, oxidizer, fuel).

$$m_{Imod} = \left(\frac{m_{lin}}{N_{mod}} \right) + f_{mod} \left(\frac{m_{linstr}}{N_{mod}} \right) + m_{dock} \tag{4.20}$$

$$m_{mod} = N_{mod} \left[m_{Imod} + \frac{m_{Istr}}{N_{mod}} \left(\frac{V_{mod}}{V_{Imod}} - 1 \right) \right] \tag{4.21}$$

In Equation 4.20, m_{lin} is the total mass of the linear design component being modularized and m_{linstr} is the dry mass of the component.

130

	Habitat	Oxidizer	Fuel
N_{mod}	12	5	14
m_{Imod} (kg)	5,718	36,589	2,554
m_{Istr} (kg)	15,518	18,163	3,027
V_{mod} (m^3)	28.6	28.6	28.6
V_{Imod} (m^3)	28.6	28.3	27.1
m_{mod} (kg)	68,616	183,169	35,930

Table 4.6: Example of calculation of tank module masses for D_{mod} of 4.9 meters, $f_{propscale}$ of 0.25, and f_{oxfill} of 1.0.

In Equation 4.21, m_{mod} is the total mass of a set of modules being investigated (i.e. habitat, oxidizer, fuel), N_{mod} is the number of modules required for the component, m_{Istr} is the structural mass of the interpolation point module design, V_{mod} is the volume of the module being investigated, and V_{Imod} is the volume of the interpolation point module design. An example of how m_{mod} is calculated for a given module diameter is shown in Table 4.6.

Calculation of Required Number of Launches

The number of upgraded Delta IV Heavy launches required to put the entire TSH vehicle in LEO is calculated using the mass, size, and quantity of modules required. A set of rules is used to determine the launch manifests. First, only modules of the same type are launched together. Second, modules are packed "in-line" in the fairing. Third, a 14.25 meter limit for module stacking height in launch vehicle fairing is imposed (see Figure 4-17). This height limit is the maximum height a quantity of three 4.75 meter diameter modules can be stacked within the fairing envelope. A maximum quantity of two modules of diameter from 4.75 to 6.5 meters can be stowed in the fairing as well.

Using the launch vehicle fairing constraints described above, the launch vehicle payload constraint, and the quantities and masses of modules to be launched, the total number of launches required can be calculated. Equations 4.22, 4.23, 4.24, and

131
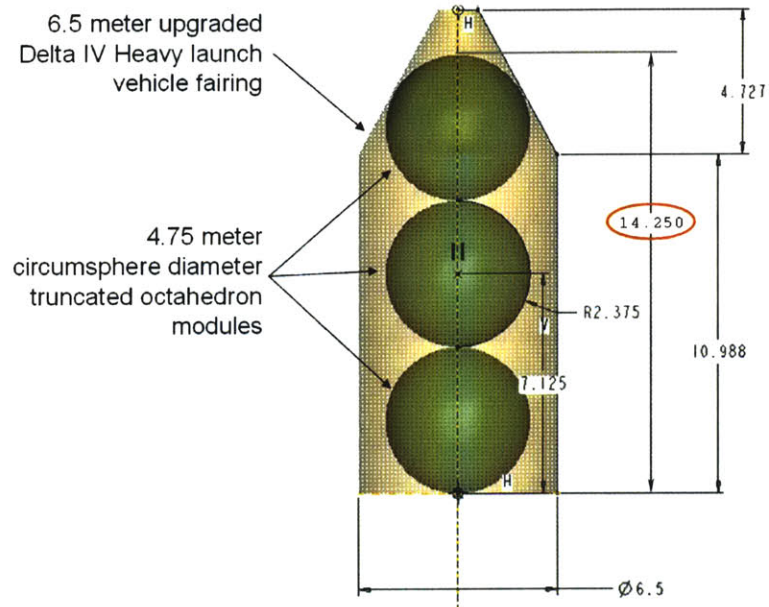
Figure 4-17: Upgraded Delta IV Heavy fairing loaded with truncated octahedron modules. 14.25 meter module stacking height limit shown [80, 48]. All dimensions are in meters.

4.25 are used to perform this calculation.

$$N_{LVdim} = \left\lfloor \frac{H_{limit}}{D_{mod}} \right\rfloor \tag{4.22}$$

$$N_{LVmass} = \left\lfloor \frac{m_{limit}}{m_{mod}} \right\rfloor \tag{4.23}$$

$$N_{LVmod} = \min\left(N_{LVdim}, N_{LVmass}\right) \tag{4.24}$$

$$N_{LV} = \sum_{i=1}^{3} \left\lceil \frac{N_{mod}}{N_{LVmod}} \right\rceil_i \tag{4.25}$$

In the equations used to calculate the number of required launches, N_{LVdim} is the number of modules the launch vehicle can transport to LEO based only on dimension constraints, N_{LVmass} is the number of modules the launch vehicle can transport to LEO based only on mass constraints, H_{limit} is the launch fairing height limit, m_{limit} is the mass limit of the launch vehicle, m_{mod} is the mass of a module, N_{LVmod} is the number of modules the launch vehicle can transport to LEO, and N_{LV} is the total

132

number of launches required for the vehicle. In Equation 4.25, the range of i is 1 to 3 because there are three types of modules considered in this modularization analysis.

Modularization Results

After searching the modularization design space using a spreadsheet, objective function results are obtained. These results are shown in Figure 4-18. The non dominated designs are connected by the dashed line to denote a possible Pareto front. In general, f_{oxfill} is increasing for designs as the total IMLEO mass decreases. Also, $f_{propscale}$ increases as IMLEO mass and number of launches increase.

The "optimal" modular design selected based on the objective space search is the truncated octahedron with a circumsphere diameter of 4.9 meters with the propellant volume increased by 25% and the oxidizer thanks filled to capacity. This design was selected because it nearly has the minimal number of launches required and the design has the minimum IMLEO mass.
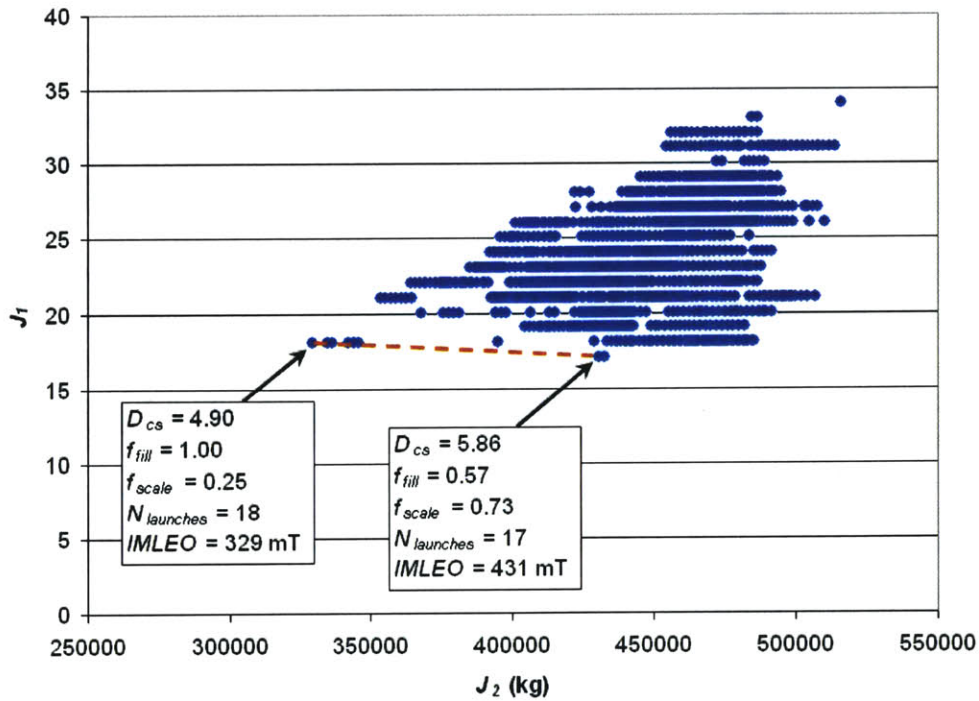
Figure 4-18: Modularization objective space results with non-dominated designs labeled.

133

The "optimal" modular design is composed of twelve habitat modules, five oxidizer tanks, and fourteen fuel tanks. The interpolation point designs used are shown in Figure 4-19. In this figure, the interpolation points used for this design are labeled and the corresponding number of modules is shown.

An additional feasibility check was performed to ensure the "optimal" modular vehicle design will have the ΔV necessary to successfully perform the Mars exploration mission. The results for this check are shown in Figure 4-20. A large range of module sizes are infeasible due to their violation of the launch vehicle payload mass constraint. The maximum size was constrained to be the size at which the heaviest module is at the payload mass limit.
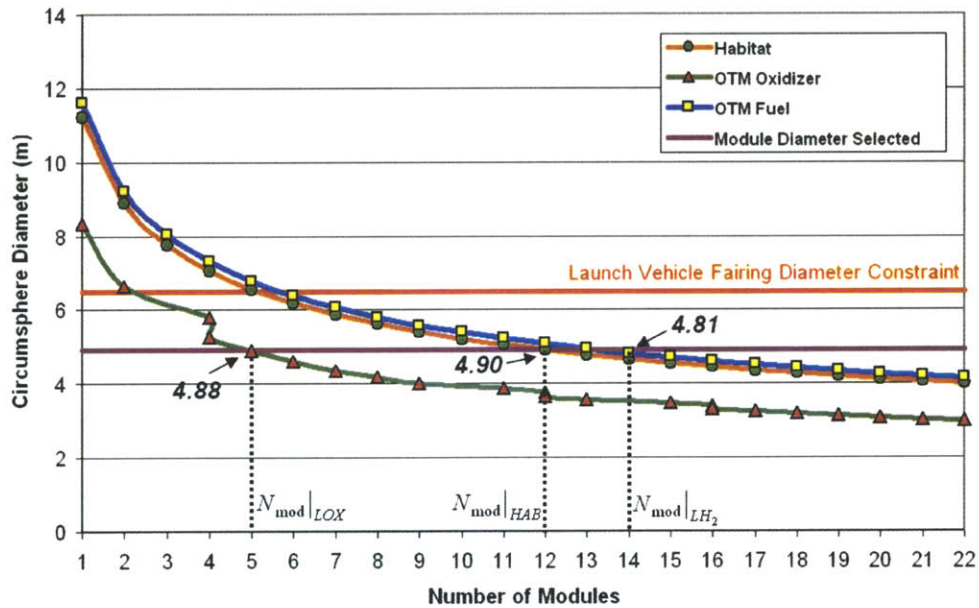
Figure 4-19: Modularization design interpolation points with "optimal" design interpolation points and constraints shown.

Modular Design Solution

The resulting modular design solution is shown in Figure 4-21. Using a D_{cs} value of 4.9 from the analysis performed in the previous sections, a spacecraft was designed with identically-sized habitat, fuel tanks, and oxidizer tank diameters. In Table 4.7,

134
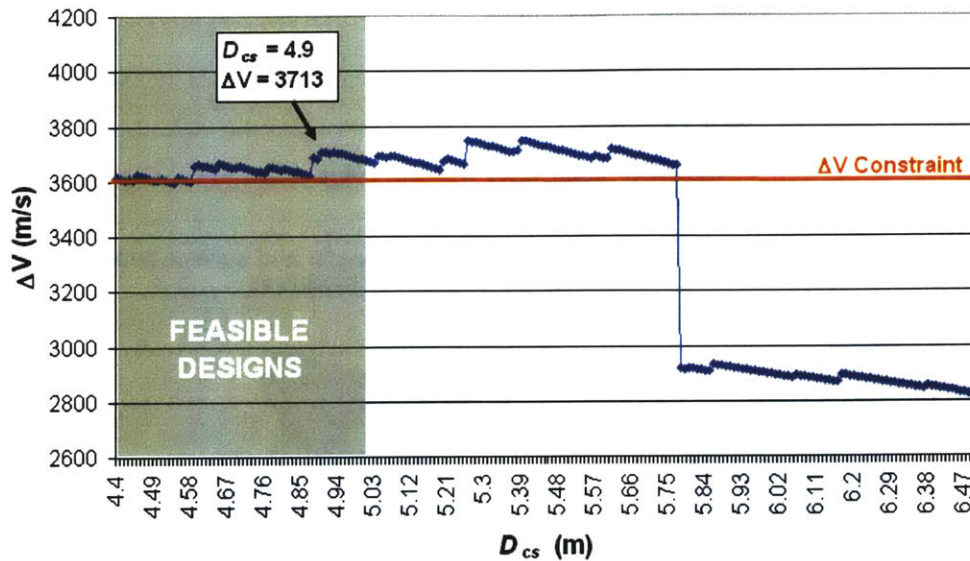
Figure 4-20: Modular spacecraft ΔV results for module sizes with "optimal" modular design variable settings.

the modular and linear design masses are compared.

Component	N_{mod}	m_{mod} (kg)	Module Mass, $\frac{m_{mod}}{N_{mod}}$ (kg)	Linear Design Mass (kg)	Modular Design Volume (m^3)	Point Design Volume (m^3)
Habitat	12	68,422	5702	62,100	343	343
LO_X prop.	5	162,000	32,400	128,570	143	113
LH_2 prop.	14	31,500	2,250	21,430	401	303
LO_X dry	5	22,000	4,400	18,160	N/A	N/A
LH_2 dry	14	8,820	630	3,030	N/A	N/A
Heat shield	1	16,094	16,094	16,100	N/A	N/A
Lander	1	18,400	18,400	18,400	N/A	N/A
Engines	4	7,720	1,930	5,550	N/A	N/A

Table 4.7: Comparison of modular and optimal Transfer and Surface Habitat vehicle component masses.

From the exploded spacecraft view in Figure 4-21, the interconnectivity between spacecraft modules can be visualized. The habitat is formed into a pyramid-like structure and the oxidizer tanks are assembled into a shape that fits into the center of a ring-like structure of fuel modules. The engines are assembled to the spacecraft to both fuel and oxidizer tanks at each of the four locations. The Mars descent propul-

135
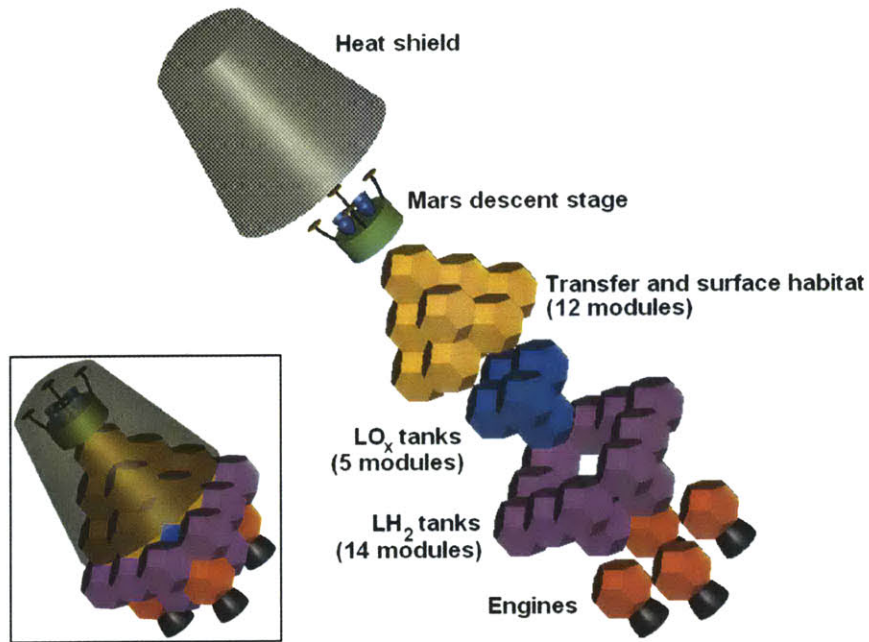
Figure 4-21: Exploded and unexploded views of modular TSH vehicle design (heat shield translucent for viewing of hidden components). Solar panels not included in figure.

sion stage is stacked on top of the habitat and a heat shield is used to protect the descent stage and habitat for aerocapture at Mars. Detailed structural interconnections between modules, the descent propulsion stage, and the heat shield are beyond the scope of this analysis and therefore have been omitted from the design presented.

Sensitivity Analysis

Sensitivity analysis was performed for modularization mass penalty design parameters. These design parameters are the docking hardware penalty, m_{dock}, and the structural modularity penalty, f_{mod} (see Section 4.7.3). The sensitivity of each objective with respect to two design parameters is investigated. The Jacobian matrix, shown in Equation 4.26, is determined for the two objective, two parameter sensitivity analysis. For the calculation of the partial derivatives, various step sizes were investigated to determine if the derivative is dependent on the step size. Step sizes of 25, 50, and 100 kilograms for m_{dock} and 0.0125, 0.025, and 0.05 for f_{mod} are in-

vestigated. Based on this investigation, it is determined that the derivatives are not dependent on step size.

$$\nabla J(\mathbf{x}^0) = \begin{bmatrix} \frac{\partial J_1}{\partial m_{dock}} & \frac{\partial J_2}{\partial m_{dock}} \\ \frac{\partial J_1}{\partial f_{mod}} & \frac{\partial J_2}{\partial f_{mod}} \end{bmatrix}_{\mathbf{x}^0} = \begin{bmatrix} 31 & 0 \\ 36708 & 0 \end{bmatrix} \tag{4.26}$$

In Equation 4.26, $\mathbf{x}^0$ is the "optimal" design vector used for this analysis.

To obtain more useful sensitivity results, the terms in the Jacobian are normalized. The normalization factors used are an approximate method to normalize the Jacobian terms. The origin of the normalization factor is shown in Equation 4.27 with more detail in Equation 4.28.

$$\frac{\Delta J/J}{\Delta p_i/p_i} \simeq \frac{p_{i,0}}{J(\mathbf{x}^0)} \cdot \nabla J(\mathbf{x}^0) \tag{4.27}$$

$$\frac{p_{i,0}}{J(\mathbf{x}^0)} = \begin{bmatrix} \frac{\partial m_{dock}(\mathbf{x}^0)}{\partial J_1(\mathbf{x}^0)} & \frac{\partial m_{dock}(\mathbf{x}^0)}{\partial J_2(\mathbf{x}^0)} \\ \frac{\partial f_{mod}(\mathbf{x}^0)}{\partial J_1(\mathbf{x}^0)} & \frac{\partial f_{mod}(\mathbf{x}^0)}{\partial J_2(\mathbf{x}^0)} \end{bmatrix} \tag{4.28}$$

In Equation 4.27, $p_{i,0}$ is the ith design parameter (for $i = 1, 2$) at the "optimal" design point, $\mathbf{x}^0$. From this equation, the normalized sensitivities of the two objectives with respect to each design parameter are determined. These results are shown in Table 4.8.

Design Parameter	J_1 Norm. Sensitivity	J_2 Norm. Sensitivity
m_{dock}	0.038	0.000
f_{mod}	0.011	0.000

Table 4.8: Sensitivity analysis results for modularization mass penalty design parameters.

The sensitivity analysis results show the J_1 objective, total IMLEO, is sensitive to both design parameters with J_1 being being roughly three times more sensitive to a change in m_{dock} than to f_{mod}. The practical meaning of these normalized sensitivity values is that a 100% increase in the value of m_{dock}, for example, will result in an increase in J_1 of 3.8%, or approximately 12,500 kg. The J_2 design objective, number of launches required, is not sensitive at all to either of the design parameters. The relatively small effect of the paramter settings on the design objectives reduces the

137

importance of how closely these parameter settings match to realistic mass penalties associated with modularization.

4.8 Lunar Variant Analysis and Design

In this section, a transfer and surface habitat vehicle is designed for a Moon mission based on the Mars mission architecture in Section 4.7.1. This lunar transfer and surface habitat is built using components of the TSH used for the Mars mission. This design approach is called "Mars-back."

4.8.1 "Mars-Back" Design

A major benefit of modular spacecraft design is the ability to design extensibility into a space exploration system. Extensible design can improve the affordability for a system to explore the Moon and Mars, ultimately enhancing the sustainability of the program. Extensibility is incorporated into such an exploration system using a "Mars-back" vehicle design approach. A "Mars-back" approach means the exploration system hardware is designed for Mars missions with the ability of the same or similar hardware to be used in advance during Moon missions. This has the effect of eliminating the cost of developing a suite of Moon-specific hardware as well as Mars-specific hardware and instead develop one set of dual use hardware. In addition, since this hardware design is composed of identical building block structures, the cost of integration, assembly, and testing of the hardware will be reduced due to learning curve cost savings and the ability to streamline and automate the process.

4.8.2 Lunar Variant Architecture

In this section, hardware from the transfer and surface habitat vehicle designed in Section 4.7 will be used to create a vehicle for a Moon mission. The Moon mission used is called a "lunar variant" since the vehicles used are variants of those used for Mars missions. The lunar variant architecture selected for this analysis, similar to

138

work done by the MIT Fall 2004 16.981 Advanced Special Projects class, is shown in Figure 4-22 [45, 68, 3]. The vehicle selected for "Mars-back" design is the transfer and surface habitat (TSH) vehicle, with similar functionality to the TSH vehicle used in the Mars architecture. Relevant lunar variant TSH vehicle information for this architecture is shown in Table 4.9 [35, 10].

Mission Phase	$\Delta V(m/s)$	Duration (days)
TMI	3,150	3.5
LOI	850	0.5
Descent	2,083	0.5
Surface ops	N/A	180
Total	6,083	184.5

Table 4.9: ΔV and duration information for lunar variant architecture.
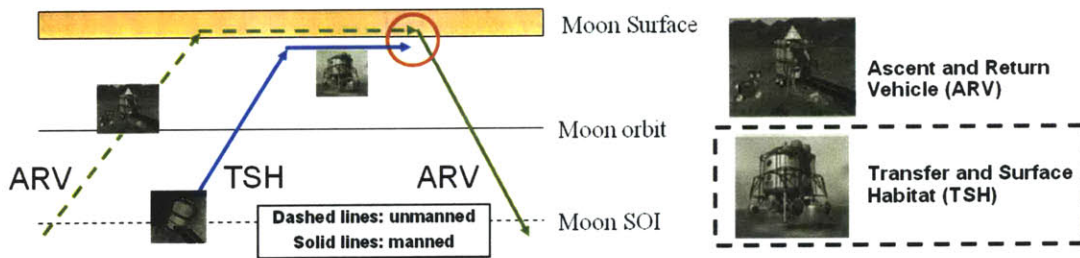
Figure 4-22: Example lunar variant architecture.

4.8.3 Analysis Assumptions

Several assumptions have been made to perform this analysis. First, the total ΔV needed to be performed by the TSH propulsion system is assumed to be the sum of the ΔVs needed for all three burns (see Table 4.9). Second, the propellants selected for the engine are the same as in the Mars mission spacecraft design example. Third, the fuel and oxidizer tanks are allowed to be partially filled with propellant. In addition, a crew of four is assumed to be flying on this lunar exploration mission as opposed to a crew size of six for the Mars mission described earlier in this chapter. Finally, a volume of 19 m^3 is assumed again for each crew member for the lunar variant TSH vehicle.

4.8.4 Habitat Mass Estimation

The first step to estimate the total lunar variant TSH habitat mass, m_{habLV}, is to determine the dry mass of each habitat module, $m_{hab_{mod}}^{dry}$. This mass is determined using the Mars mission TSH habitat design according to the "Mars-back" design approach. This mass estimate was obtained by subtracting the total consumables required for the Mars TSH habitat, m_{hab}^{cons}, from the total TSH habitat mass, m_{hab}. The remaining mass is then divided by the total number of Mars TSH habitat modules, $N_{mod_{hab}}$, to obtain the result. This is shown in Equations 4.29 and 4.30. In addition, Equation 4.29 is used with lunar mission parameters to determine the total consumables required for the lunar mission habitat, m_{habLV}^{cons}.

$$m_{cons_{hab}} = N_{crew} f_{ECLS} \dot{m}_{cons} \left(\Delta t_{man} \right) \tag{4.29}$$

$$m_{hab_{mod}}^{dry} = \frac{m_{hab} - m_{hab}^{cons}}{N_{mod_{hab}}} \tag{4.30}$$

In Equation 4.29, a variant of Equation 4.7 is used and again the required consumables mass flow rate, $\dot{m}_{cons}$, is assumed to be $9.5 kg/crew/day$ [55, 45].

Next, the required habitat volume for the lunar variant habitat, V_{habLV}, is determined using Equation 4.6 for lunar mission parameters. The number of lunar mission habitat modules, $N_{mod_{habLV}}$, is determined using Equation 4.31 by comparing V_{habLV} to the Mars mission required habitat volume, V_{hab}. Due to the volume-per-crew constraint, the crew size drives habitat volume rather than the mission duration.

Finally, Equation 4.32 is used to determine the total lunar variant habitat mass. Results for this analysis are shown in Table 4.10.

$$N_{mod_{habLV}} = \left\lceil N_{mod_{hab}} \left(\frac{V_{habLV}}{V_{hab}} \right) \right\rceil \tag{4.31}$$

$$m_{habLV} = m_{habLV}^{cons} + N_{mod_{habLV}} m_{hab_{mod}}^{dry} \tag{4.32}$$

Parameter	Description	Mars Mission	Lunar Variant
V_{hab}	Total habitat volume (m^3)	343	228
$N_{mod_{hab}}$	No. habitat modules	12	8
$m_{hab_{mod}}^{dry}$	Dry mass per module (kg)	3,239	3,239
$m_{hab}^{cons}/N_{mod_{hab}}$	Consumables mass per module (kg)	2,463	596
$m_{mod_{hab}}$	Total mass per module (kg)	5,702	3,835
m_{hab}	Total habitat mass (kg)	68,422	30,679

Table 4.10: Mass calculation results for lunar variant habitat.

4.8.5 Propulsion System Sizing

For the lunar variant TSH mission, oxidizer and fuel tanks sized according to the Mars TSH mission are used. The propulsion system is sized in order to satisfy the ΔV requirement of 6,083 m/s. The rocket equation (see Equation 4.8) is used to perform this analysis. Maintaining the required oxidizer/fuel mass ratio, the mass of oxidizer is used as a variable to size the overall propulsion system to search for feasible designs. The number of fuel and oxidizer tanks is determined such that there are enough to contain all fuel and oxidizer required. Equations 4.33, 4.34, and 4.35 are used to perform this analysis.

$$N_{mod_{LOX}} = \left\lceil \frac{V_{LOX}}{V_{mod}} \right\rceil \tag{4.33}$$

$$N_{mod_{LH_2}} = \left\lceil \frac{V_{LH_2}}{V_{mod}} \right\rceil \tag{4.34}$$

$$\Delta V = g_0 I_{sp} \ln \left(\frac{m_{habLV} + N_{mod_{LOX}} m_{LOX}^{dry} + N_{mod_{LH_2}} m_{LH_2}^{dry} + m_{LOX}^{prop} + m_{LH_2}^{prop}}{m_{habLV} + N_{mod_{LOX}} m_{LOX}^{dry} + N_{mod_{LH_2}} m_{LH_2}^{dry}} \right) \tag{4.35}$$

$N_{mod_{LOX}}$ and $N_{mod_{LH_2}}$ are the number of oxidizer and fuel modules required, respectively. V_{LOX} and V_{LH_2} are the total required volumes of oxidizer and fuel, respectively. m_{LOX}^{dry} and $m_{LH_2}^{dry}$ are the dry masses of each oxidizer and fuel module, respectively (see Table 4.7 for reference). m_{LOX}^{prop} and $m_{LH_2}^{prop}$ are the total propellant masses of oxidizer and fuel, respectively.

Figure 4-23 shows how scaling the size of the propulsion system affects ΔV performance. This data was used to select the best lunar variant design by choosing

the lowest IMLEO configuration. The curve is not linear due to dry mass increases of additional propellant modules required for additional propellant volume. Detailed mass results for the selected configuration are shown in Table 4.11.
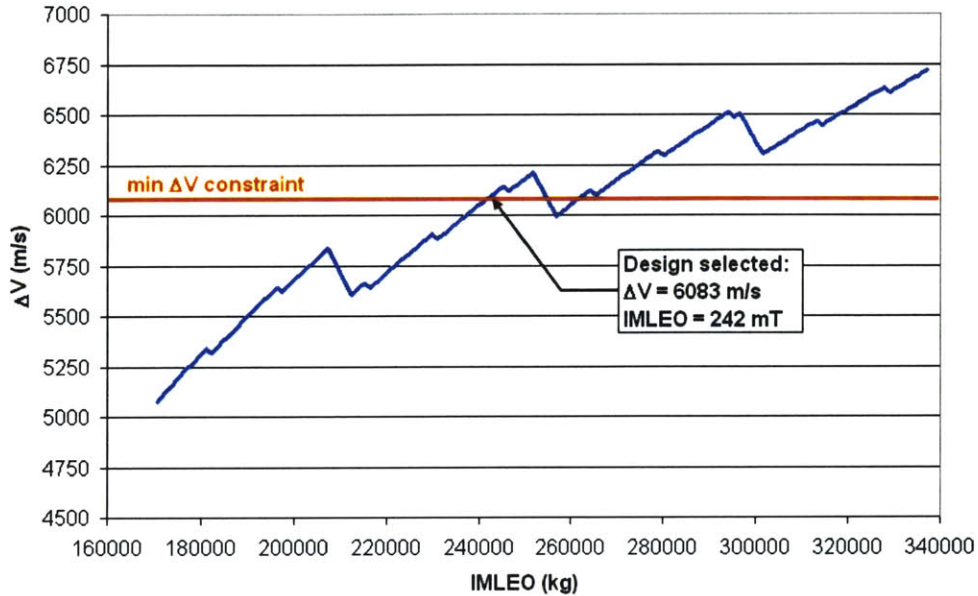

Figure 4-23: Lunar variant TSH vehicle propulsion system scaling ΔV versus IMLEO performance.

Parameter	Description	Oxidizer, LOX	Fuel, LH_2
N_{mod}	Number of modules (m^3)	5	13
$N_{mod} \cdot m^{dry}$	Total dry mass (kg)	22,000	8,190
m^{prop}	Total propellant mass (kg)	155,500	25,900
f_{fill}	Tank fill percentage (%)	95	98

Table 4.11: Mass calculation results for lunar variant propulsion system.

4.8.6 "Mars-back" Design Conclusions

A vehicle used for a Moon exploration mission is created using elements designed for a mission to Mars. The modular design of the TSH vehicle allows for this design extensibility. Significant cost savings potential can result from leveraging spacecraft designs from one set of missions to another in this manner. Although the design

extensibility of one vehicle is shown in this example, this process should be feasible for other vehicles in the architectures presented. In fact, extensibility may be possible between different vehicles for the same mission, an analysis which may be performed in future work. A side-by-side visualization of the TSH vehicles designed for Mars and Moon missions is shown in Figure 4-24.

Total Mass (kg)	
Lunar Variant TSH	242,400
Mars TSH	335,000
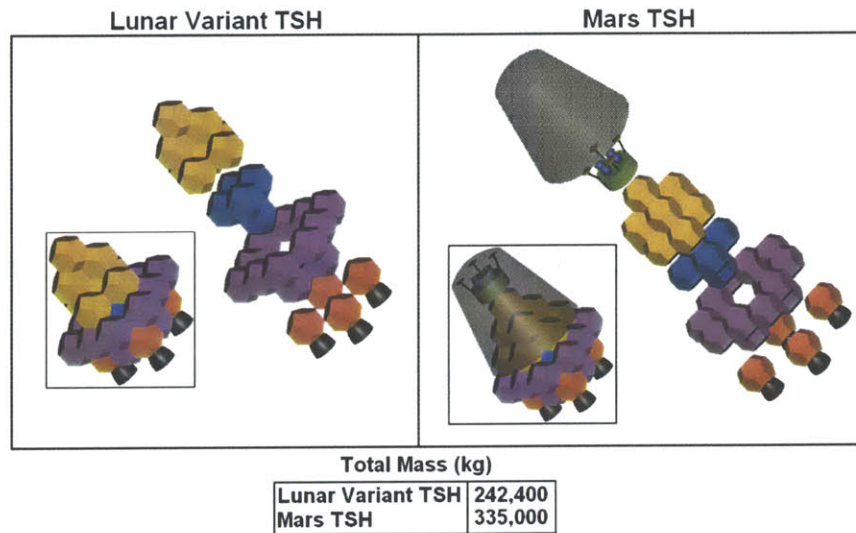
Figure 4-24: Extensible TSH vehicle combinations: Mars and lunar variant TSH configurations.

4.9 Modular Vehicle Stability Benefits

This section highlights several stability benefits of modular spacecraft design. These benefits are improved pitch stability, improved landing stability, and reduced thrust inaccuracy due to misalignment of the thruster and center of gravity.

4.9.1 Pitch Stability

First, assume the linear and modular spacecraft are spin stabilized about the axes shown in Figure 4-26. In order to be stable in pitch, the spin axis of the spacecraft must be the axis of maximum moment of inertia (MOI) [54]. While neither the linear

143

or modular Mars exploration spacecraft designs from Section 4.7 are spin stabilized about their axis of maximum MOI (Y-axis), the relative difference in magnitude between the maximum MOI and the other moments of inertia for each spacecraft differs significantly. The MOI directions are shown in Figure 4-26 and the resulting principal moments of inertia of each spacecraft are shown in Table 4.12.

Moment of Inertia	Linear Design $(kg \cdot m^2)$	Modular Design $(kg \cdot m^2)$
I_x	1.63×10^7	8.28×10^6
I_y	1.63×10^7	8.72×10^6
I_z	1.61×10^6	4.23×10^6

Table 4.12: Mass calculation results for lunar variant propulsion system.

From Table 4.12, it is shown that the maximum principal moment of inertia axis for each spacecraft is in the Y-direction. However, the relative magnitude difference between the maximum principal moment of inertia and the other principal moments of inertia is significantly smaller for the modular spacecraft than the linear stack design. This means that while both spacecraft are unstable in pitch, the modular spacecraft is not as unstable as the linear stack design. In fact, a modular spacecraft could be assembled in a pancake shape in which it would indeed be able to be spin stabilized about the maximum principal moment of inertial. This is infeasible with linear stack design concept due to the payload dimension limitations of the launch vehicle fairing.

For vehicles in inertial flight mode, as assumed in this analysis, the radius vector in the body-fixed coordinate system can be described as follows in Equation 4.36. A revolution angle Θ, corresponding to true anomaly, is introduced to describe the changing radius vector throughout an orbit. See Figure 4-25 for the coordinate system description of inertial flight mode.

$$\hat{R} = \begin{bmatrix} \sin \Theta \\ 0 \\ -\cos \Theta \end{bmatrix} \tag{4.36}$$

Assuming each spacecraft is in an inertial flight mode while in a circular orbit
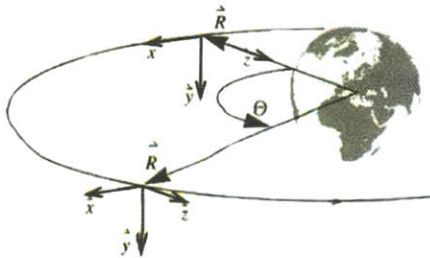
144

Figure 4-25: Body-fixed coordinate system and inertial flight attitude [55].
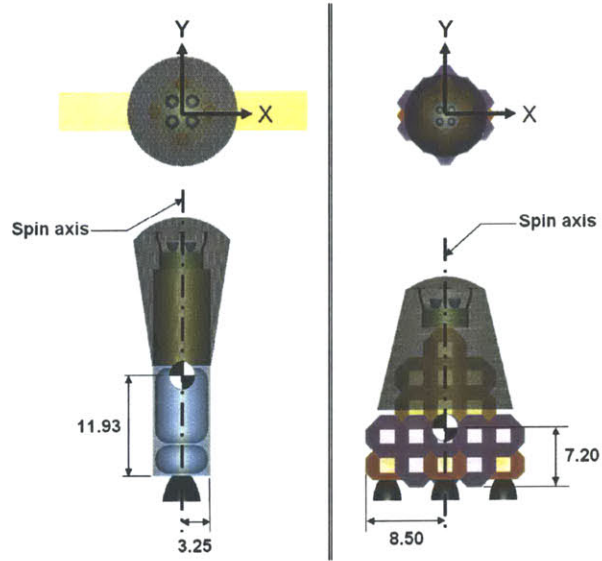

Figure 4-26: Linear and modular Mars TSH configurations with coordinate systems, spin axes, and moment arms labeled.

in LEO, the stability performance of each vehicle can be visualized as shown in Figure 4-27 [50]. Based on the results in Figure 4-27, with respect to gravity gradient disturbance torques, both the linear and modular spacecraft are stable in yaw and roll but are unstable in pitch. The modular design is favorable because it more closely approximates a spherical-shaped spacecraft (located at the origin).

4.9.2 Landing Stability

An important factor in the landing stability of a spacecraft is the height of the spacecraft center of gravity from the bottom of the landing structure. The smaller this dimension, the less "top heavy" the lander. The reduction in this dimension has the benefit of improving the stability of the lander by reducing the likelihood of the spacecraft toppling over during or after landing. A rough landing or high winds may cause the center of gravity of the lander to shift such that it may not be between the landing legs, causing the spacecraft to topple over. However, a lower center of gravity will reduce the chances of encountering this toppling condition. As seen in Figure 4-26, the modular spacecraft has a smaller center of gravity height (7.20 meters) than
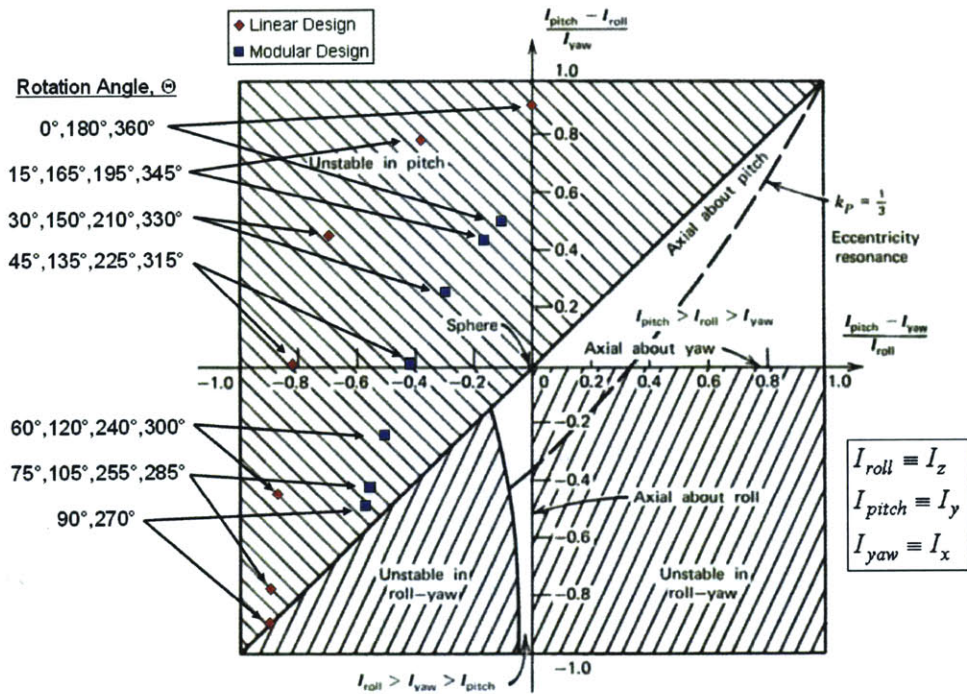
Figure 4-27: Gravity gradient stability regions with linear and modular spacecraft stability performance overlayed.

the linear design (11.93 meters). The modular spacecraft design concept allows a wide array of configuration options for reducing this height as opposed to the long, cylindrical configuration of the linear stack concept.

4.9.3 Thruster Misalignment

A third benefit to the configuration options provided by the modular spacecraft design concept is the ability to reduce the penalty associated with a thrust line misalignment with the center of gravity. If the thruster is misaligned, the thrust line does not pass directly through the center of gravity of the spacecraft. The burn error resulting from this misalignment requires that corrective propulsive maneuvers are performed to keep the spacecraft on the desired trajectory. The ability to reduce the distance between the thrust wall and spacecraft center of gravity modular design concept using the truncated octahedron (shown in Figure 4-26) helps reduce the distance of the center

146

of gravity and the thrust line, helping reduce the burn error associated with thrust line misalignment. The geometrical benefit is shown in Figure 4-28.
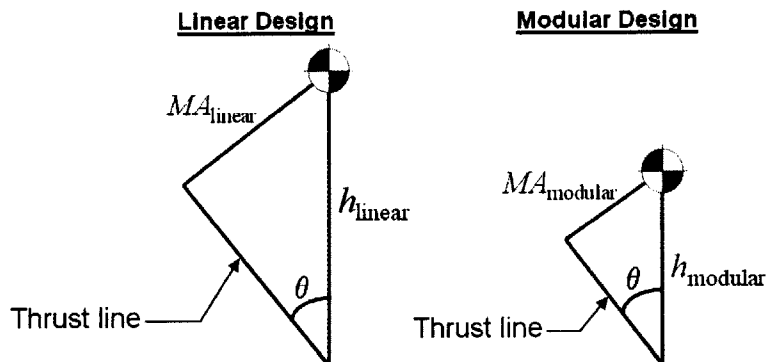

Figure 4-28: Thrust line distance from center of gravity for linear and modular spacecraft designs resulting from thrust misalignment angle, Θ.

In Figure 4-28, MA_{linear} and $MA_{modular}$ are the distances between the thrust lines and centers of gravity for the linear and modular vehicle designs, respectively. Also, h_{linear} and $h_{modular}$ are the distances between the centers of gravity and the thrust walls of the linear and modular vehicle designs, respectively. From Figure 4-28, it is clear that $MA_{modular}$ is less than MA_{linear}. The resulting torque on the spacecraft from the misalignment is also reduced accordingly.

4.10   Chapter 4 Summary

The truncated octahedron is an efficient, modular geometry for potential use in human space exploration systems. This convex polyhedron approaches the volumetric efficiency of the sphere, but has no voids when closely packed (ideally). In fact, the truncated octahedron is claimed to be the three-dimensional solid that has the largest volume/surface-area ratio, while still being close-packing. The number of reconfigurations allowed, on the other hand significantly exceeds those of the cylinder and the cube. The launch stowage efficiency is somewhat reduced compared to cylindrical structures, but it is unclear whether this is a real disadvantage in cases where launch mass is the driving constraint. The modularity and reconfigurability provided by the

147

truncated octahedron also allows for significant stability performance improvements. The mass penalty in designing a modular version of a Mars transfer and surface habitat vehicle compared to a "point design," linear stack concept, was found to be approximately 25%.

For future space exploration, the benefits of modular, reconfigurable spacecraft design are:

- Enhancing mission flexibility: spacecraft could be reconfigured to complete new tasks

- Economic benefits (non-recurring and recurring cost savings)

- Extensible spacecraft design, facilitating an affordable, "Mars-back" approach for architecting an affordable and sustainable space exploration system

Both truncated octahedra and cylinders are capable of exhibiting modularity. However, the greater number of interfaces, and hence physical configurations, enabled by truncated octahedra make the shape uniquely suited for architecting spacecraft with complex functional flows and incidental interactions, architecture being the manner in which the functions of a product are mapped to its physical modules. To architect spacecraft with complex functional flows with cylinders requires many more cylinders to embody the functional elements, introducing wasted space, increasing launch costs, and increasing the complexity of the system.

Even for spacecraft whose functional flows are not complex, the greater number of interfaces and configurations permit designers greater flexibility in drawing module boundaries. The greater number of interfaces and configurations also facilitate a greater ease of extensibility associated with bus modularity.

The benefits due to the geometry and modularity of the truncated octahedron are not possible without penalties. A mass penalty is incurred from modularization. Spacecraft complexity is increased due to the increased number of module interconnections. This complexity will likely require sophisticated control systems to be used for autonomous rendezvous and docking of the various spacecraft modules. In addition, initial design cost of a modular space exploration system may be more expensive

148

than an "optimized" system. However, "optimality" over the entire space exploration system lifecycle may favor the modular design approach.

Chapter 5

Conclusion

This chapter will summarize the main points of this thesis and address future work. Recommendations are given for flexible structural design based on the work in this thesis. A general flow diagram for flexible structural design is presented.

5.1 Design Recommendations

Based on the experience doing flexible structural design in this thesis, a set of important design recommendations are listed here.

1. **Consider many different sets of structural design requirements:** At the beginning of a flexible structural design process, consider many different sets of structural design requirements that are traditionally not considered simultaneously and are designed as separate structures. The flexible structure will be designed to accommodate all of these considered requirements.

2. **Consider designing for backwards compatibility:** Designing for backwards compatibility, such as the "Mars back" design concept may provide many benefits that are not obvious at first glance (see Section 4.8).

3. **Use a tool to help explore a broad design space:** A tool such as an optimization algorithm or spreadsheet will help find regions of flexible structural

design feasibility. From this feasible set of designs, a designer, optimization algorithm, or both can select the "best" design.

4. **Start from many initial designs:** When performing flexible structural design optimization start from many different initial designs. This allows the design space to be explored broadly.

5. **Optimize for the worst case objective:** If multiple requirements are considered in the design and optimization process, it is recommended to optimize for the worst case objective function of the set for each iteration. This tends to improve the overall objective functions of the designs.

5.2   Flexible Structural Design Process

Figure 5-1 shows a flow diagram for the process of structural design for flexibility.

The first step in the design process is to clearly define the set of requirements being considered. This should include the objective functions to be considered, target values for each, if available, as well as definitions of other requirements such as load cases, boundary conditions, and materials to be used.

The second step involves optimization and design. Based on a selected design for a particular iteration, feasible structural design configurations are found for each set of design requirements. These feasible design configurations are then evaluated according to specified objective functions. The worst case objective function is used as the system objective result for each iteration and the cycle repeats again until satisfactory objective results are obtained.

The end result of this process is a set of structural components with the capability to be reconfigured to satisfy a set of design requirements. The benefit of this resulting structural design is cost savings due to the reconfigurability, modularity, and extensibility properties of the design. This result has been shown for applications of individual components, simple structural systems, and a complex system of structures.

Requirements Definition:

1. Set objective function(s): cost, structural performance, or other goals
2. Define load cases, dimensions, boundary conditions, connectivity, materials, etc.

Optimization and Design:

1. Choose a structural design of a set or sets of components for consideration
2. Create feasible structural design configurations using set of components for each set of design requirements
3. Evaluate each design configuration according to defined objective function(s)
4. Use worst objective function result for output to optimizer for next iteration
5. Repeat iterative process until desired results achieved for the objective function(s)

Results:

A set of *modular, reconfigurable, extensible, and affordable* structural components with capabilities beyond a single, custom-designed structure
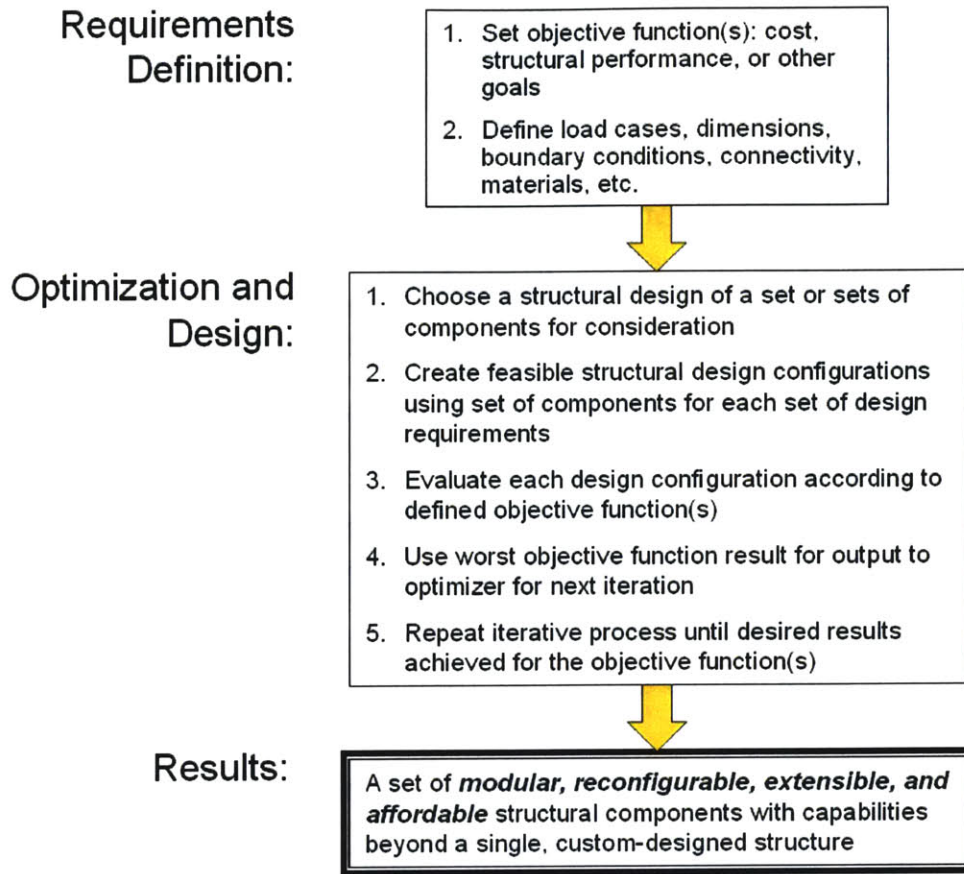
Figure 5-1: Flexible structural design flow diagram.

5.3 Future Work

5.3.1 Structural Component Shape Optimization Considering Performance and Manufacturing Cost

Future work will include implementing the adaptive weighted sum (AWS) method developed by de Weck and Kim [27] for the generic structural part example. This method may allow for the generation of a well-distributed Pareto frontier for the example. The bicycle frame example results will be improved by including the bicycle frame joints in the design space by allowing their shapes to be optimized. Additional future work will include performing topology optimization in which the number of curves are considered as design variables and the creation and merging of holes is

153

allowed. Finally, the method will be applied to more complex structures and a new manufacturing cost model will be implemented. Potential manufacturing process cost models could include milling and stamping.

5.3.2 Multidisciplinary Structural Subsystem Topology Optimization for Reconfigurability

Future work on this topic will involve applying this structural design optimization methodology to more realistic and more complex structures. Some structural design applications include military bridges and modular bookshelf structures. A parking structure which can accommodate additional levels is another potential application of this design methodology. Finally, inner loop optimization will be used to create a true double-loop optimization method used to improve an objective function such as assembly time which depends on structural configuration.

5.3.3 The Truncated Octahedron: A New Concept for Modular, Reconfigurable Spacecraft Design

Future work to be performed to further refine the truncated octahedron concept will be composed of several items. First, additional investigation of extensibility benefits of spacecraft design using the truncated octahedron concept will be performed. Spacecraft design extensibility for different vehicles and missions will be studied. Also, application of this concept to the NASA Space Exploration Initiative [12] will be done by generating requirements, creating conceptual designs, and performing trade offs to assess the benefits of this concept.

Additional items include the design of standardized interfaces between truncated octahedron-shaped modules, the application of the rod, ring, and "sphere" structural combinations to overall space exploration mission contexts, and manual and autonomous methods for construction and reconfiguration of modules in space.

Bibliography

[1] Airline Deregulation Act of 1978. Public Law 95-504, 92 Stat. 1705.

[2] Swiss military imagery archive, http://zem.dev.imagefinder.ch.

[3] The reference mission of the NASA Mars exploration study team. NASA Special Publication 6017, July 1997.

[4] Integrated Modeling of Optical Systems (IMOS), rel. 5.0,. Jet Propulsion Laboratory, California Institute of Technology, Pasadena, California, 2000.

[5] Omax Make: Precision velocity controller, ver. 3.2. Omax Corporation, Kent, Washington, 2001.

[6] Omax Layout, software package, ver. 6.2. Omax Corporation, Kent, Washington, 2002.

[7] Ansys, ver. 8.1, educational edition. ANSYS, Inc., Canonsburg, Pennsylvania, 2004.

[8] Medium girder bridge components. U.S. Army Field Manual, FM 5-212, 2004.

[9] R. Abbott and M. Aceves. Self-engaging connector system for robotic outposts and reconfigurable spacecraft. In *Proceedings of the 2002 IEEE Aerospace Conference*, volume 5, pages 2165–2170, Piscataway, New Jersey, 2002.

[10] National Aeronautics and Space Administration. Apollo 11 press kit. NASA Public Affairs Office, 1969.

[11] National Aeronautics and Space Administration. NASA systems engineering handbook. SP-610S, June 1995.

[12] National Aeronautics and Space Administration. The vision for space exploration. NP-2004-01-334-HQ, February 2004.

[13] E. Antonsson and J. Cagan (Editors). *Formal Engineering Design Synthesis.* Cambridge University Press, 2001.

[14] S. Baily, R. R. Nelson, and W. B. Stewart. Interface standards for spacecraft as a means of enhancing on-orbit servicing. In *Proceedings of the 18th Annual Electronics and Aerospace Systems Conference,* pages 351–355, Piscataway, New Jersey, 1985.

[15] C. Y. Baldwin and K. B. Clark. Managing in an age of modularity. *Harvard Business Review,* 75(5):84–93, September 1997.

[16] M. O. Bendsøe and N. Kikuchi. Generating optimal topologies in structural design using a homogenization method. *Computer Methods in Applied Mechanics Engineering,* 71(2):197–224, November 1988.

[17] President G. W. Bush. A renewed spirit of discovery: The President's vision for U.S. space exploration, January 2004.

[18] United States Congressional Budget Office (CBO). A budgetary analysis of NASA's new vision for space exploration, September 2004.

[19] O. Cetin, K. Saitou, S. Nishigaki, T. Amago, and N. Kikuchi. Modular structural component design using the first order analysis and decomposition-based assembly synthesis. In *Proceedings of the International Mechanical Engineering Congress and Exposition,* New York, New York, November 2001.

[20] K. H. Chang and P. S. Tang. Integration of design and manufacturing for structural shape optimization. *Advances in Engineering Software,* 32(7):555–567, July 2001.

[21] E. F. Crawley. The CDIO syllabus: A statement of goals for undergraduate engineering education. MIT Department of Aeronautics and Astronautics, Source: http://www.cdio.org, May 2002.

[22] E. F. Crawley. Introduction to (space) system architecture: Architecture and value. MIT 16.89 Course Notes, Spring 2004.

[23] E. F. Crawley and O. de Weck. Space mission extensibility. Presentation at NASA Headquarters, October 2003.

[24] E. F. Crawley, E. M. Greitzer, S. E. Widnall, S. R. Hall, and et. al. Reform of the aeronautics and astronautics curriculum at MIT. *ASEE Journal of Engineering Education*, 83(1):47–56, January 1994.

[25] M. Daniels and B. Saavedra. The conestoga launch vehicle - a modular approach to meeting user requirements. In *Proceedings of the 15th International Communications Satellite Systems Conference*, San Diego, California, February–March 1994.

[26] O. de Weck, R. de Neufville, and M. Chaize. Enhancing the economics of communications satellites via orbital reconfigurations and staged deployment. American Institute of Aeronautics and Astronautics, AIAA-2003-6317, 2003.

[27] O. de Weck and I. Y. Kim. Adaptive weighted sum method for bi-objective optimization. In *Proceedings of the 45th AIAA/ASME/ASCE/AHS/ASC Structures, Structural Dynamics, and Materials Conference*, Palm Springs, California, April 2004.

[28] O. de Weck and K. Willcox. 16.888 multidisciplinary system design optimization course notes. Massachusetts Institute of Technology, spring 2004.

[29] F. Dietrich. The Globalstar satellite cellular communication system: Design and status. American Institute of Aeronautics and Astronautics, AIAA-98-1213, 1998.

[30] A. W. M. Dress, D. H. Huson, and E. Molnár. The classification of face-transitive periodic three-dimensional tilings. *Acta Crystallographica*, A49:806–817, 1993.

[31] Wikpedia: The Free Encyclopedia. NASA Budget. http://en.wikipedia.org/wiki/NASA_Budget.

[32] 16.89 Space Systems Engineering. Paradigm shift in design for NASA's new space exploration initiative. Massachusetts Institute of Technology, June 2004.

[33] J. Enright, C. Jilla, and D. Miller. Modularity and spacecraft cost. *Journal of Reducing Space Mission Cost*, 1(2):133–158, 1998.

[34] A. Ertas and J. Jones. *The Engineering Design Process*. Wiley Publishers, 1993.

[35] R. W. Farquhar, D. W. Dunham, Y. Guo, and J. V. McAdams. Utilization of libration points for human exploration in the sun-earth-moon system and beyond. In *Proceedings of the 54th International Astronautical Congress of the International Astronautical Federation*, Bremen, Germany, September-October 2003.

[36] P. Fortescue and J. Stark. *Spacecraft Systems Engineering*, page 161. John Wiley and Sons, Chichester, West Sussex, England, second edition, 1995.

[37] C. E. Fossa. An overview of the Iridium low earth orbit (LEO) satellite system. In *Proceedings of IEEE 1998 National Aerospace and Electronics Conference*, pages 152–159, July 1998.

[38] E. Fricke, A. Schulz, S. Wenzel, and H. Negele. Design for changeability of integrated systems within a hyper-competitive environment. In *Proceedings of the INCOSE Colorado 2000 Conference*, Denver, Colorado, March 2000.

[39] W. Frisina. Close-pack modules for manned space structures. *Journal of Spacecraft and Rockets*, 22(5):583–584, 1985.

[40] W. Frisina. Modular spacecraft. *Journal of Aerospace Engineering*, 7(4):411–416, October 1994.

[41] B. Grossman, Z. Gurdal, G. J. Strauch, W. M. Eppard, and R. T. Haftka. Integrated aerodynamic/structural design of a sailplane wing. *Journal of Aircraft*, 25(9):855–860, September 1988.

[42] C. A. Hartke. The illinois bees and apiaries program photo gallery. http://www.agr.state.il.us/programs/bees/pages/bee_with_honeycomb.htm.

[43] O. P. Harwood and R. W. Ridenoure. A universal orbital docking and berthing system. In T. R. Meyer, editor, *The Case for Mars IV: The International Exploration of Mars, Mission Strategy and Architectures*, volume 89, pages 613–630. American Astronautical Society, San Diego, California, 1990.

[44] E. J. Haug, K. K. Choi, and V. Komkov. *Design sensitivity analysis of structural systems*. Academic Press, San Diego, California, 1986.

[45] W. Hofstetter. Extensible modular landing systems for human moon and mars exploration. Master's thesis, Technische Universität München, 2004.

[46] W. M. Hollister, E. F. Crawley, and A. R. Amir. Unified engineering: A twenty year experiment in sophomore aerospace education at MIT. In *AIAA 32nd Aerospace Sciences Meeting and Exhibit*, Reno, Nevada, January 1994.

[47] C. Huang and A. Kusiak. Modularity in design of products and systems. *IEEE Transactions on Systems, Man, and Cybernetics - Part A: Systems and Humans*, 28(1):66–77, January 1998.

[48] S. J. Isakowitz, J. B. Hopkins, and Jr. J. P. Hopkins. *International Reference Guide to Space Launch Systems*. American Institute of Aeronautics and Astronautics, Reston, Virginia, 2004.

[49] C. D. Jilla and D. W. Miller. Multi-objective, multidisciplinary design optimization methodology for distributed satellite systems. *Journal of Spacecraft and Rockets*, 41(1):39–50, January-February 2004.

[50] M. H. Kaplan. *Modern Spacecraft Dynamics and Control.* John Wiley and Sons, New York, New York, 1976.

[51] I. Y. Kim and B. M. Kwak. Design space optimization using a numerical design continuation method. *International Journal for Numerical Methods in Engineering*, 53(8):1979–2002, 2002.

[52] J. Koski. Multicriteria truss optimization. In W. Stadler, editor, *Multicriteria Optimization in Engineering and in the Sciences*, pages 263–307. Plenum Press, New York, New York, 1988.

[53] K. Lee. *Principles of CAD/CAM/CAE Systems.* Addison Wesley, 1999.

[54] P. Likins. Spacecraft attitude dynamics and control – a personal perspective on early developments. *Journal of Guidance*, 9(2):129–134, March-April 1986.

[55] E. Messerschmid and R. Bertrand. *Space Stations: Systems and Utilization.* Springer, Berlin, Germany, 2004.

[56] J. H. Mikkola and O. Gassmann. Managing modularity of product architectures: Toward an integrated theory. *IEEE Transactions on Engineering Management*, 50(2):204–218, May 2003.

[57] M. M. Mikulas and J. T. Dorsey. An integrated in-space construction facility for the 21st century. In G. V. Butler, editor, *The 21st Century in Space*, volume 70, pages 75–92. American Astronautical Society, San Diego, CA, 1990.

[58] J. Miller, J. Guerrero, D. Goldstein, and T. Robinson. Spaceframe: Modular spacecraft building blocks for plug and play spacecraft. In *Proceedings of the 16th Annual AIAA/USU Conference on Small Satellites*, Logan, Utah, August 2002.

[59] G. W. Morgenthaler. A cost trade-off model for on-orbit assembly logistics. In *Proceedings of the 4th AIAA/SOLE Space Logistics Symposium*, pages 503–524, Washington D.C., 1991.

[60] S. A. Nelson, M. Parkinson, and P. Papalambros. Multicriteria optimization in product platform design. *Journal of Mechanical Design*, 123(2):199–204, June 2001.

[61] J. Olsen. Motion control with precomputation. Assignee: Omax Corporation, U.S. Patent 5,508,596, 1996.

[62] AIAA Technical Committee on Multidisciplinary Design Optimization (MDO). White paper on current state of the art. American Institute of Aeronautics and Astronautics, January 1991.

[63] C. Pantelides and S. Ganzerli. Design of trusses under uncertain loads using convex models. *Journal of Structural Engineering*, 124(3):318–329, March 1998.

[64] C. Park, W. Lee, W. Han, and A. Vautrin. Simultaneous optimization of composite structures considering mechanical performance and manufacturing cost. *Composite Structures*, 65(1):117–127, July 2004.

[65] R. C. Parkinson. Space platform - a new approach to space operations. In *Proceedings of the 36th Congress of the International Astronautical Federation*, Paris, France, 1985.

[66] R. C Parkinson. Why space is expensive - operational/economic aspects of space transport. *Journal of Aerospace Engineering*, 205(G1):45–52, 1991.

[67] A. Petro. Transfer, entry, landing, and ascent vehicles. In W. J. Larson and L. K. Pranke, editors, *Human Spaceflight Mission Analysis and Design*, pages 403–404. McGraw Hill, New York, New York, 1999.

[68] 16.981 Advanced Special Project. NASA concept evaluation and refinement study. Massachusetts Institute of Technology, fall 2004.

[69] M. Rais-Rohani and Z. Huo. Analysis and optimization of primary aircraft structures based on strength, manufacturability, and cost requirements. In *Proceedings*

of the 44th AIAA/ASME/ASCE/AHS/ASC Structures, Structural Dynamics, and Materials Conference, pages 1112–1124, Norfolk, Virginia, April 2003.

[70] R. Roy. Cost engineering: What, why, and how? In R. Roy and C. Kerr, editors, *Decision Engineering Report Series*. Cranfield University, Cranfield, United Kingdom, 2003.

[71] A. Schulz and E. Fricke. Incorporating flexibility, agility, robustness, and adaptability within the design of integrated systems. In *Proceedings of the IEEE/AIAA 18th Digital Avionics Systems Conference*, St. Louis, Missouri, October 1999.

[72] P. J. Sellers. The next manned Earth-to-orbit vehicle (ETOV): What do we need and when do we need it? White paper available from: PJ Sellers, code CB, NASA/JSC, Houston, TX 77058, 2003.

[73] Seven Cycles. Bicycle manufacturer. http://www.sevencycles.com/.

[74] Lt. Col. J. Shoemaker. Orbital express space operations architecture. http://www.darpa.mil/tto/programs/oe.html.

[75] P. Singh and J. Munoz. Cost optimization of abrasive waterjet cutting systems. In *Proceedings of the 7th American Water Jet Conference*, pages 191–204, Seattle, Washington, August 1993.

[76] C. Smithies, M. Meerman, A. Wicks, A. Phipps, and M. Sweeting. Microsatellites for affordable space science: Capability and design concept. In *Proceedings of the 53rd International Astronautical Congress*, Paris, France, October 2002.

[77] J. Sobieszczanski-Sobieski and R. T. Haftka. Multidisciplinary aerospace design optimization: Survey of recent developments. In *Proceedings of the AIAA 34th Aerospace Sciences Meeting and Exhibit*, Reno, Nevada, January 1996.

[78] D. V. Steward. *Systems Analysis and Management: Structure, Strategy, and Design*. Petrocelli Books, Inc., Princeton, New Jersey, 1981.

[79] K. Suzuki and N. Kikuchi. A homogenization method for shape and topology optimization. *Computer Methods in Applied Mechanics Engineering*, 93(3):291–318, December 1991.

[80] Boeing Integrated Defense Systems. Delta iv heavy growth options for space exploration. http://www.boeing.com/defense-space/space/bls/d4heavy/docs/delta_growth_options.pdf.

[81] D. Tcherniak and O. Sigmund. A web-based topology optimization program. *Structural and Multidisciplinary Optimization*, 22(3):179–187, October 2001.

[82] J. S. Tyll, M. A. Eaglesham, J. A. Schetz, M. Deisenroth, and D. T. Mook. An MDO design methodology for the concurrent aerodynamic/cost design of MAGLEV vehicles. In *Proceedings of the 6th AIAA, NASA, and ISSMO Symposium on Multidisciplinary Analysis and Optimization*, pages 501–513, Reston, Virginia, September 1996.

[83] K. Ulrich and K. Tung. Fundamentals of product modularity. In *ASME Issues in Design Manufacture/Integration*, volume 39, pages 73–79, Atlanta, Georgia, December 1991.

[84] S. Vogel. *Cats' Paws and Catapults*. W. W. Norton and Company, London, England, 1998.

[85] S. Wakayama and I. Kroo. Subsonic wing design using multidisciplinary optimization. In *Proceedings of the 5th AIAA/NASA/ISSMO Symposium on Multidisciplinary Analysis and Optimization*, pages 1358–1368, Panama City, Florida, September 1994.

[86] A. Weigel and D. Hastings. Measuring the value of designing for uncertain future downward budget instabilities. *Journal of Spacecraft and Rockets*, 41(1):111–119, January-February 2004.

[87] D. Weiner. Personal communication, November 2003.

[88] E. W. Weisstein. B-spline. MathWorld–A Wolfram Web Resource. http://mathworld.wolfram.com/B-Spline.html, 1999.

[89] D. A. Whelan, E. A. Adler, S. B. Wilson, and G. Roesler. The darpa orbital express program: Effecting a revolution in space-based systems. In B. J. Horais and R. J. Twiggs, editors, *Small Payloads in Space*, pages 121–128. International Society for Optical Engineering, Bellingham, Washington, 2003.

[90] D. Wingo. *Moonrush: Improving Life on Earth with the Moon's Resources*. Apogee Books, Burlington, Ontario, Canada, 2004.

[91] J. Wong. Literature survey and analysis for the truncated octahedron concept. MIT Undergraduate Research Opportunity White Paper, Summer 2004.

[92] B. Woolford and R. L. Bond. Human factors of crewed spaceflight. In W. J. Larson and L. K. Pranke, editors, *Human Spaceflight Mission Analysis and Design*, pages 149–150. McGraw Hill, New York, New York, 1999.

[93] R. J. Yang and C. H. Chuang. Optimal topology design using linear programming. *Computers and Structures*, 52(2):265–275, July 1994.

[94] L. Zadeh. Optimality and non-scalar-valued performance criteria. In *IEEE Transactions on Automatic Control*, pages 59–60, 1963.

[95] J. Zeng. *Mechanisms of Brittle Material Erosion Associated with High-pressure Abrasive Waterjet Processing*. PhD thesis, University of Rhode Island, Department of Mechanical Engineering and Applied Mechanics, 1992.

[96] J. Zeng and T. Kim. Parameter prediction and cost analysis in abrasive waterjet cutting operations. In *Proceedings of the 7th American Water Jet Conference*, pages 175–189, Seattle, Washington, August 1993.

[97] J. Zeng, T. Kim, and R. Wallace. Quantitative evaluation of machinability in abrasive waterjet machining. In *Precision Machining: Technology and Machine Development and Improvement at the Winter Annual Meeting of The American*

Society of Mechanical Engineers, pages 169–179, Anaheim, California, November 1992.

[98] J. Zeng, J. Olsen, and C. Olsen. The abrasive water jet as a precision metal cutting tool. In *Proceedings of the 10th American Water Jet Conference*, pages 829–843, Houston, Texas, August 1999.

[99] J. P. Zolésio. The material derivative (or speed) method for shape optimization. In *Optimization of Distributed Parameter Structures*, pages 1089–1151. Sijthoff & Noordhof, The Netherlands, 1981.

Appendix A

Innovative Modern Engineering Design and Rapid Prototyping Course: A Rewarding CAD/CAE/CAM Experience for Undergraduates

Il Yong Kim, Olivier de Weck, William Nadir, Peter Young and David Wallace

Department of Aeronautics and Astronautics and Engineering Systems Division

Massachusetts Institute of Technology

Cambridge, Massachusetts 02139

A.1 Abstract

This appendix reproduces a new undergraduate design course in the Department of Aeronautics and Astronautics at MIT. This course combines design theory, lectures and hands-on activities to teach the design stages from conception to implementation. Activities include hand sketching, CAD, CAE, CAM, design optimization, rapid prototyping, and structural testing. The learning objectives, pedagogy, required re-

sources and instructional processes as well as results from a student assessment are discussed. This paper is added as a supplement to this thesis because (1) I worked as a teaching assistant for the course and helped create the project and (2) "systems thinking" in structural design must begin with engineering education.

A.2 Introduction

A recent survey of undergraduate students in the Department of Aeronautics and Astronautics at MIT has shown that there is a desire for training in modern design methods using state-of-the-art CAD/CAE/CAM technology and design optimization. Individual students have suggested the addition of a short and intense course in rapid prototyping, combined with design optimization. The specific reference from the student survey is paraphrased here:

> *"The CDIO [conceive-design-implement-operate] initiative has been well received by undergraduates, who have thoughtful suggestions for improvements. Some feeling of imbalance between fundamentals and other skills. Offerings in CAD/CAM, machining, fabrication desired."*

The intent of this course is to respond to this perceived gap, while exploiting synergies with other engineering departments that have articulated similar needs. We have developed an intense 6-credit-unit IAP (independent activities period)1 course that takes students through the conception, design, and implementation of a single, complex structural component. This activity supports the learning objectives of the Conceive-Design-Implement-Operate (CDIO) initiative [24], [21], [46] and leverages the latest technologies in computer-assisted design, analysis, optimization, and rapid prototyping. The novelty of this course lies in its combination of rapid prototyping with design optimization in order to demonstrate the complementary capabilities of humans and computers during the design process.

The overall learning objective of this activity is for students to develop a holistic view of and initial competency in engineering design by applying a

combination of human creativity and modern computational methods and tools to the synthesis of a complex structural component.

This goal can be mapped onto the following learning objectives of the CDIO syllabus [21]:

- Core Engineering Fundamental Knowledge: **solid mechanics and materials**

- Advanced Engineering Fundamental Knowledge: **computational techniques**

- Engineering Reasoning and Problem Solving: **modeling**

- Personal Skills and Attitudes: **creative thinking**

- Conceiving and Engineering Systems: **modeling systems and ensuring goals can be met**

- The Design Process: **execute appropriate optimization in the presence of constraints**

- Implementing: **hardware manufacturing process**

- Implementing: **test, verification, validation, and certification**

This paper first offers a description of the course, focusing on its structure and flow (Section A.3). Next, the target student population (Section A.4) and required resources (Section A.5) will be discussed. The design project, including the requirements levied on the students, is the subject of Section A.6. In Section A.7, we explain how design optimization can be incorporated in such design courses. An overview of the student deliverables (Section A.8), assessment results (Section A.9) and conclusions (Section A.10) round out the paper.

A.3 Course Description

The goal of the course is to provide the students with an opportunity to conceive, design, and implement products quickly and effectively, using the latest rapid prototyping methods and CAD/CAE/CAM technology. This is meant to be an intense

and satisfying experience that emphasizes the chain of design steps shown in Figure A-1.
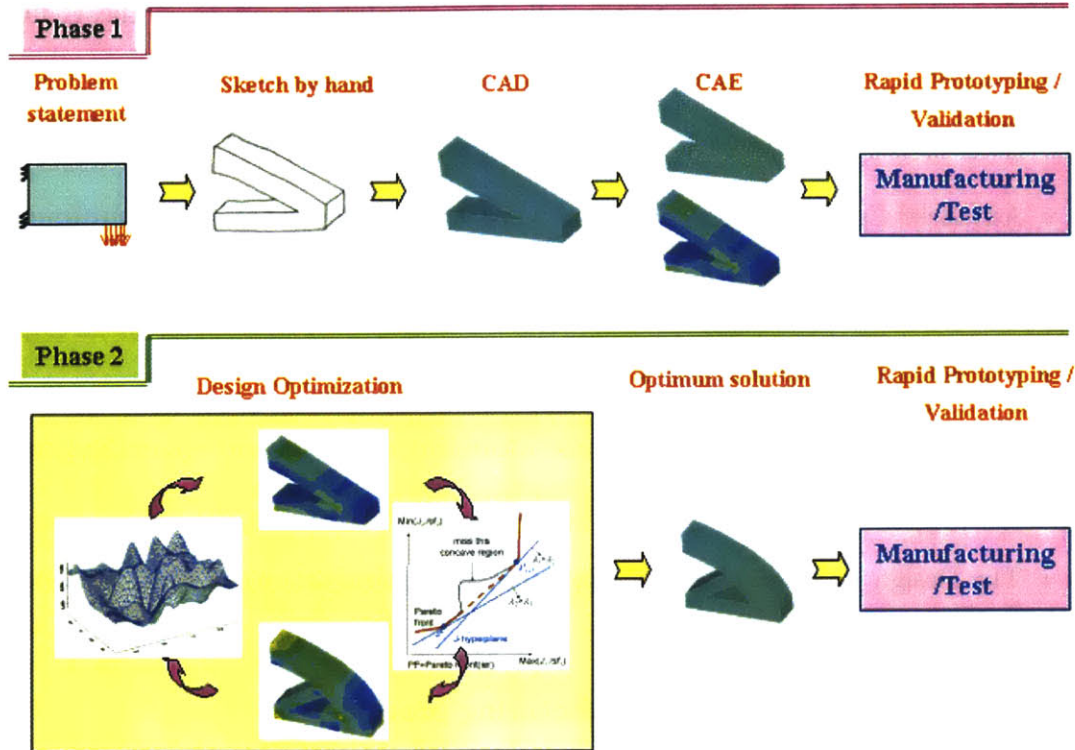
Figure A-1: Engineering Design and Rapid Prototyping: course pedagogy.

A.3.1 Course Pedagogy and Concept

Fundamental engineering design principles and procedures are introduced and in some cases reviewed during the first week [34], [53], [13]. The idea of structuring the course in two phases is rooted in the following cognitive progression:

In the **first phase**, the students are presented with solution neutral requirements and constraints for a structural component. Teams of two students are formed and each team receives slightly different requirements (see Section A.6). A creative process of hand sketching is followed by computer aided design (CAD) and analysis (CAE). This helps the students ascertain that their Phase 1 design will theoretically meet the

170

requirements. After some manual iteration, the part specification is implemented on water jet cutting equipment. The prototype is subjected to structural testing in the laboratory to verify the validity of the predictions as well as requirements compliance.

The **second phase** takes the Phase 1 manual design as an input and improves the solution via design optimization. In effect, the earlier manual solution is used as an initial condition for the design optimization step. This is what ties Phases 1 and 2 together. The students conduct design optimization using either commercial or faculty-provided software. The optimum solution obtained is modeled as a CAD model, and again computer numerically controlled (CNC) equipment is used to fabricate the improved component. The optimized component is compared with the hand-designed one, and conclusions are drawn.

The course concludes with student presentations culminating in a "Critical Design Review," and potentially a competition, which includes results from testing of the initial and optimized designs. This side-by-side comparison helps produce several educational insights:

- Understanding of the predictive accuracy of CAE modeling versus actual test results

- Understanding of the relative improvement that computer optimization can yield relative to an initial, manual solution

- Illustration of the capabilities and limitations of the human mind and digital computer during design and manufacturing

A.3.2 Course Flow

The course plan starts by exposing the students to the design process, its phases, and the importance of properly formulated requirements. An introduction to state-of-the-art CAD/CAE/CAM environments is given during the first week. Initial hands-on activities include hand sketching, creating engineering drawings, and CAD Modeling. Due to the time limitations of this IAP course, compromises have to be made with

respect to the breadth and depth of some of the topics that are covered. Emphasis is placed on successfully completing the various steps of the design process, rather than understanding all the details of the methods and tools used along the way. Assumptions outlined in Section 5 limit the complexity of this undertaking in order to avoid overwhelming the students and to ensure that they focus on the learning objectives. A flowchart of the class activities, which includes student deliverables, is shown in Figure A-2.
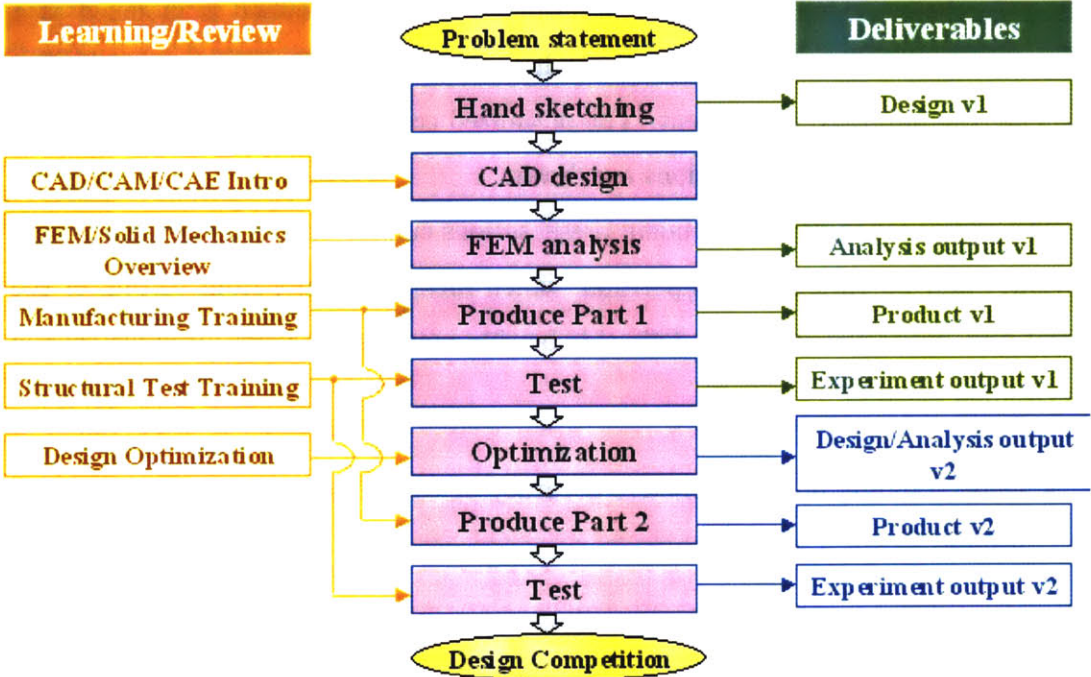
Figure A-2: Flowchart of Engineering Design and Rapid Prototyping class.

Figure A-3 shows the detailed course schedule. Each class consists of a lecture on theory (1 hour and 30 minutes) directly followed by a hands-on activity (1 hour and 30 minutes). The first seven classes constitute Phase 1, and the remaining four classes make up Phase 2. Two sessions are devoted to design optimization because of its complexity. Other activities in Phase 2, such as CAD modeling, manufacturing, and testing, can be done quickly because students have already acquired most of these skills in Phase 1. Two guest lectures provide the students with opportunities to learn

172

about current practices and challenges in industry.

Week		Monday	Wednesday	Friday
1	Lecture	L1 – Introduction (de Weck)	L2 – Hand Sketching (Wallace)	L3 – CAD modeling (Kim, de Weck)
	Hands-on activities	Tour - Design studio - Machine shop - Testing area	Sketch Initial design	Make a 2-D CAD model (Solidworks) Nadir
2	Lecture	L4 – Introduction to CAE (Kim)	L5 – Introduction to CAM (Kim)	L6 – Guest Lecture 1 (Bowlett) Rapid Prototyping
	Hands-on activities	FEM Analysis (Cosmos)	Water Jet Intro machine shop Omax (Weiner, Nadir)	Make part version 1
3	Lecture	Martin Luther King Jr. Holiday – no class	L7 – Structural Testing (Kim, de Weck)	L8 – Design optimization (Kim)
	Hands-on activities		Test part ver. 1 (Kane)	Introduction to Structural Optimization Programs
4	Lecture			L9 – Guest Lecture 2 (Sobieski) Multidisciplinary Optimization
	Hands-on activities	Carry out design optimization	Manufacture part ver. 2 Test part ver. 2	Final Review (de Weck, Kim)

Figure A-3: Course schedule.

A.4 Student Target Population

The initial offering of the class was limited to 18 students, broken down into 9 teams of two students each. Because the class is laboratory oriented, such a small number of students is preferable. In addition, the number of seats in the Design Studio and the capacity of the machine shop are inherently limited. The target level were seniors (4th year) and juniors (3rd year) who already have basic knowledge of mechanics, engineering mathematics, and design. The course is targeted primarily to undergraduate students with special emphasis on Aerospace and Mechanical Engineering.

This course is offered as an elective and seeks to attract students who want to:

1. Experience the conceive-design-implement-operate process for a single, complex component using the latest CAD/CAE/CAM technology.

2. Understand the subtleties of complementary human design abilities and computer strengths in optimization.

173

3. Understand the predictive accuracy of CAE modeling versus actual laboratory test results.

4. Obtain 6 units of credit without imposing additional scheduling constraints during the regular semesters.

A.5 Resources

We use MATLAB as a general computing environment for this course. The Solid-Works and Cosmos package is used for CAD design and finite element analysis, respectively. All the lectures and computer-based hands-on activities are performed in a Design Studio (Figure A-4a). This concurrent engineering facility is comprised of 14 networked CAD/CAE workstations that are used for complex systems design and optimization. An abrasive waterjet cutter with OMAX CAM software is used for rapid prototyping in the department's machine shop (Figure A-4b). We have manufactured a dedicated testing fixture to enable fast testing, as shown in Figure A-4c.

(b) Abrasive water-jet cutting machine
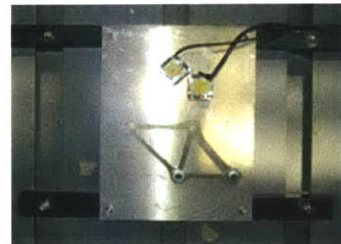
(c) Fixture for testing (test article installed)

(a) Design studio

Figure A-4: Design studio, abrasive waterjet, and fixture for testing.

A.6 Project Description

This section describes the design project that was used during the initial offering (2004). The project is limited to a single structural component with medium complexity (some boundary conditions, one single-load case, some functional surfaces, and forbidden zones given). The maximum part dimensions are approximately 12" x 12" x 0.5". No assemblies, machines, or mechanisms were produced. The part complexity might be modified in future years as we learn more about feasibility, student ability, and time constraints. We limited the design task to two dimensions. This significantly simplified hand sketching and CAD modeling. The parts still had to fulfill three-dimensional requirements (e.g. first natural frequency).
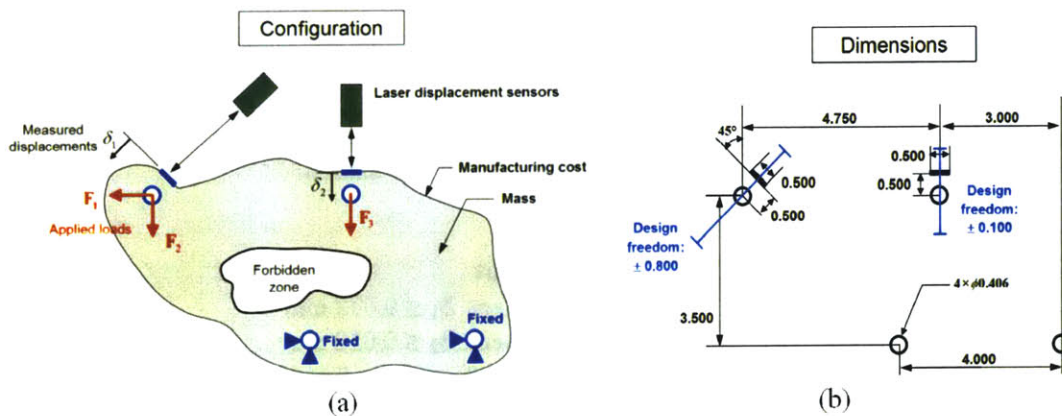
Figure A-5: Configuration and dimensional design requirements.

Figure A-5 shows the configuration and dimensions associated with the design requirement. The requirement is based on a simplified bicycle frame model. The lower two holes are fixed, and three loads F1, F2 and F3 are applied to the two upper holes (Figure A-5a). These forces represent the fork and saddle loads. A fixture with two laser sensors was fabricated and used for structural testing, see Figure A-4c, in order to obtain measurements of the displacements, δ_1 and δ_2.

The class had nine teams of two students each. Every team carried out a surrogate bicycle frame design for a different hypothetical market segment. The nine market segments were as follows: **Consumer division**: Family economy, Family deluxe,

Cross over, City bike, **Specialty division**: Racing, Mountain, BMX, and Acrobatic, **Motor division**: Motor bike. During the last week of the course, the students visited a leading, local bicycle frame manufacturer [73], where they saw first hand that designing products based on the needs of differentiated market segments is very relevant in the real world. Load magnitude, design requirements, and design priorities vary according to the market segment.

A sample requirement, which is handed to students in the first week, is given below in Figure A-6.

Market Segment: *Family Economy*

(a) Market Description
This bicycle is to be designed for the mass consumer market. The expected sales volume is 100,000 per year. The requirements of affordability, excellent performance/cost ratio and low weight are most important to be successful in this market.

(b) Requirements

Manufacturing Cost (C):	$C \leq \$3.6$/part
Performance (δ_1, δ_2, f_1):	Displacement $\delta_1 \leq 0.078$ mm
	Displacement $\delta_2 \leq 0.012$ mm
	First natural frequency, $f_1 \geq 195$ Hz
Mass (m):	$m \leq 0.27$ lbs
Surface Quality (Q):	$Q \geq 2$
Load Case (F):	$F1 = 50$ lbs / $F2 = 50$ lbs / $F3 = 100$ lbs

The part has to conform to the interface requirements and geometrical boundary conditions shown in this document. This requirement cannot be waived.

(c) Priorities
Low manufacturing cost is the first priority for this product. Next, the customer prefers a low weight product, and thirdly, structural performance should be as high as possible. These priorities are shown in the Ishii-matrix below:

Figure A-6: Sample design requirements.

Attribute	Constrain	Optimize	Accept
Cost	■		
Performance			■
Mass		■	

Figure A-7: Ishii's matrix for design requirements.

A.7 Design Optimization

The students conducted structural topology optimization, based on a pixel-like approach. We utilized web-based optimization that was developed by Tcherniak and Sigmund [81]. This optimization software can solve two-dimensional problems with rectangular design domains with a maximum number of 1000 design cells. If a cell has a density of one, it means material should be used in the cell. Compliance is used as the objective function, and the constraint is the volume fraction. This topology optimization is used to determine improved design layouts. Because the design requirements in Section A.6 have other performance metrics, it is not possible to use this software for optimization considering all of our performance metrics of interest. For future years, we intend to develop an optimization environment that is easy to use and complements the web-based tool. Optimum designs cannot (yet) automatically be imported to CAD software. When optimum solutions are obtained, students must interpret them and create CAD designs on their own. Figure A-8 shows the graphical user interface (GUI) of the web-based optimization software and a sample optimization result.

A.8 Student Deliverables

The entire set of deliverables produced by one of the student teams (Team 5: Racing) is shown in Figure A-9. Note, that their hand sketch is different from their CAD model in Phase 1 because a design improvement occurred based on several FEM simulations. In Phase 2, topology optimization found a rough optimum design from which a more refined CAD design was created.
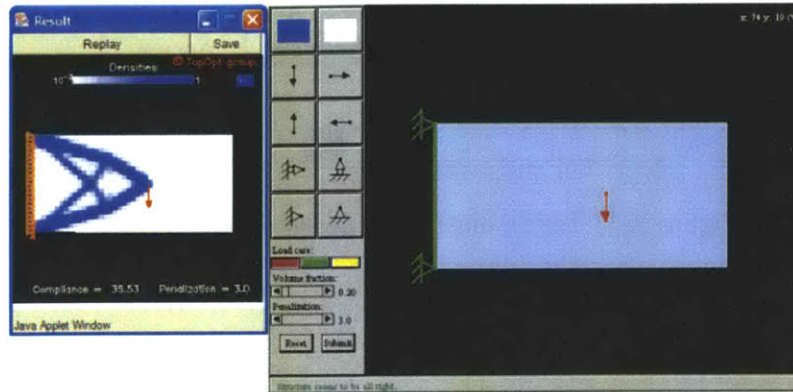
Figure A-8: Web-based structural topology optimization (GUI and sample solution).

Figure A-10 shows deliverables by all teams. The first four bicycle frames (T1–T4), which belong to the consumer division, feature rather simple, slender designs because low manufacturing cost and low mass were important design priorities for them. On the other hand, structural performance metrics were more important for bicycle frames in the specialty and motor divisions (T5–T9). This resulted in more complex, costlier and generally heavier designs obtained by this second group of teams. The variety of the proposed designs is noteworthy.

The performance of each student team's design is shown in Figure A-11. All designs in the consumer division (T1–T4) lie in the region where manufacturing cost is low. Bicycle frames in the specialty division (T5–T8) generally have larger mass and natural frequency, at the expense of higher manufacturing cost. These designs have lower displacements, which do not appear in this plot. The Motor division (T9 student team) had to deal with a rectangular, forbidden zone as shown in Figure A-10. Figure A-11 also shows the position of a baseline design, which was constructed by faculty and staff and revealed to the students only at the beginning of Phase 2.

Figure A-11 was debated extensively during the final design review. This gave the students a deeper appreciation for the relationship between their design decisions (part configuration and topology, design features, sizing) and the resulting attributes of their product: structural performance, mass and manufacturing cost. At the end of this course, the students were able to articulate the merits of one topology over

178

Phase 1

Problem Statement ➡ Sketch ➡ CAD Model ➡ CAE ➡ Rapid Prototyping
Validation

Phase 2

Design Optimization (Trimming!) ➡ CAD Model V2 ➡ CAE V2 ➡ Rapid Prototyping V2
Validation V2
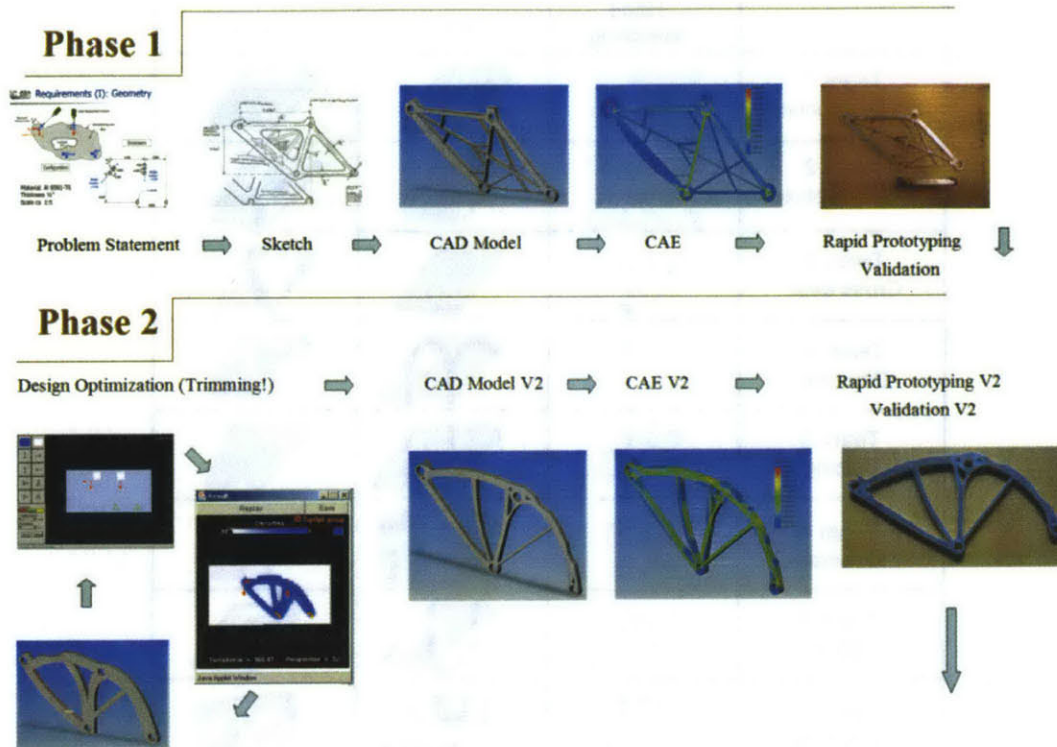
Figure A-9: Hand-sketching, CAD, CAE, and manufacturing deliverables by Team 5.

the other, promote and defend the virtues of their own designs as well as debate the trade offs and necessary choices between design objectives.

A.9   Course Evaluation

In the last week of the course, an anonymous course evaluation was conducted. The survey consisted of a brief introductory tutorial followed by 5 sections containing questions that needed to be answered by multiple choice as well as essay responses. Ten out of nineteen students participated in the survey. A sample of results from the survey is in Figure A-12.

Some of the **students' comments** were:

> "This course is an excellent idea, and fills a serious need in the undergraduate program, keep developing it, and keep up the good work."

179

	Hand sketching	Ver. 1	Ver. 2
Team 1 Family economy			
Team 2 Family deluxe			
Team 3 Cross over			
Team 4 City bike			
Team 5 Racing			
Team 6 Mountain			
Team 7 BMX			
Team 8 Acrobatic			
Team 9 Motor bike			

Figure A-10: Hand-sketches and manufactured parts (versions 1 and 2) by all teams.

"The course was great. I really enjoyed the fact that we manufactured the part and tested it."

"I think this was an extremely useful class, and I hope it continues because I think that I've learned how to use programs that I will continue to use in the department, and I've gotten some experience in the machine shop, which I could not have had otherwise."

Suggestions for improvement included among others:

"Have each team tackle a more significantly different design challenge."

"Provide for more input from classmates on the design process (semi-formal design reviews before a board of your peers)."
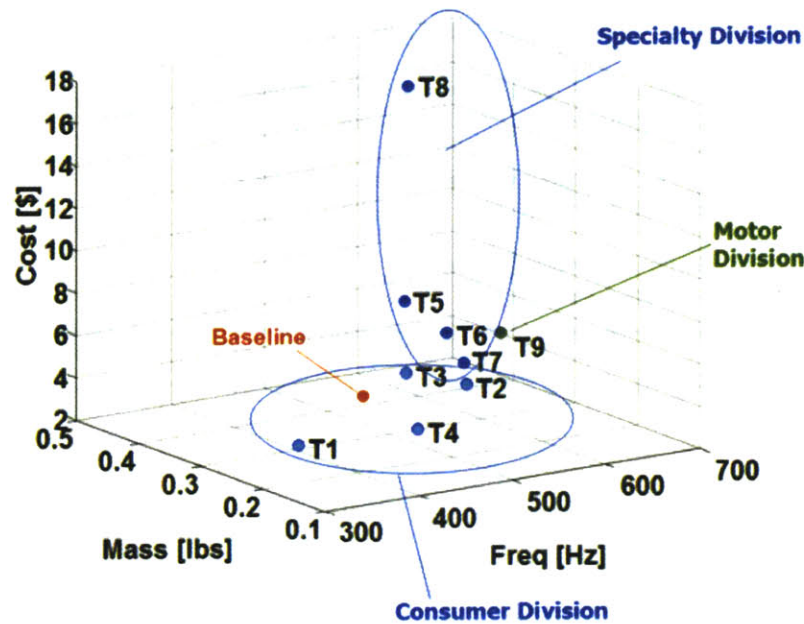
Figure A-11: Product attribute overview, T1-9 refers to the student teams.

"Make the design slightly more challenging of a problem. If not more challenging, I would have liked to have had the ability to think of a more innovative solution."

"Changing the testing procedure slightly. The testing inaccuracies were frustrating, and it would also have been better to sign up in advance for a time to test the part Version 1."

A.10 Discussions and Conclusions

This paper presented a new design course for undergraduate students. The main learning objective of this course is for students to develop a holistic view of and initial competency in engineering design by applying a combination of human creativity and modern computational methods and tools to the synthesis of a structural component. Lectures and hands-on activities are integrated for each phase of the course. Activities include hand sketching, CAD design, finite element analysis, CAM manufacturing,
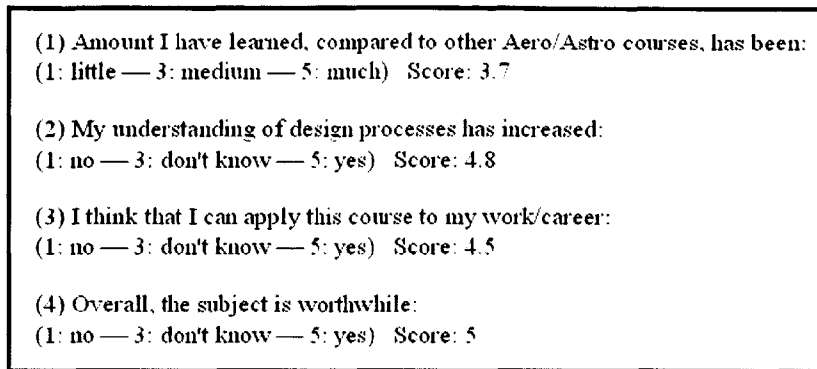
```
(1) Amount I have learned, compared to other Aero/Astro courses, has been:
(1: little — 3: medium — 5: much)   Score: 3.7

(2) My understanding of design processes has increased:
(1: no — 3: don't know — 5: yes)   Score: 4.8

(3) I think that I can apply this course to my work/career:
(1: no — 3: don't know — 5: yes)   Score: 4.5

(4) Overall, the subject is worthwhile:
(1: no — 3: don't know — 5: yes)   Score: 5
```

Figure A-12: Sample of course survey results.

structural testing, and design optimization. Nine different design requirements were given according to each team's hypothetical market segment.

Overall responses from students were very positive. They benefited mainly from the fact that design activities were presented and executed as a coherent stream. Most students may not have experienced the design process in this way before. Allowing the students to carry their design through two iterations, rather than only one, was a crucial element of the pedagogy. Based on the results of the initial offering, it was decided to integrate this course into the permanent MIT course catalog.

For most teams, the testing results did not agree well with static finite element simulation results. Likely error sources included the boundary conditions as well as relative compliance between fixture and test article. Improving testing accuracy is a primary task for future years. Improving interactions between teams and early peer review are other areas of improvement. Methods of quantitative assessments and benchmarking of these students against those without design experience would also be beneficial in fine tuning the learning objectives and course procedures.

A.11   Acknowledgments

This course was made possible thanks to a grant by the alumni sponsored Teaching and Education Enhancement Program (Class of '51 Fund for Excellence in Education,

Appendix B

Future Launch Vehicle Performance

Figure B-1 is used to set the upper size and payload mass constraints for the modularization analysis performed in Section 4.7. An upgraded Delta IV Heavy launch vehicle with the capability included in the "Delta IV Heavy Upgrade Classes" section of Figure B-1 was selected as the launch vehicle to consider for the modularization analysis. This launch vehicle has a payload fairing diameter of 6.5 meters and a payload capability to LEO of 40,000 kilograms.
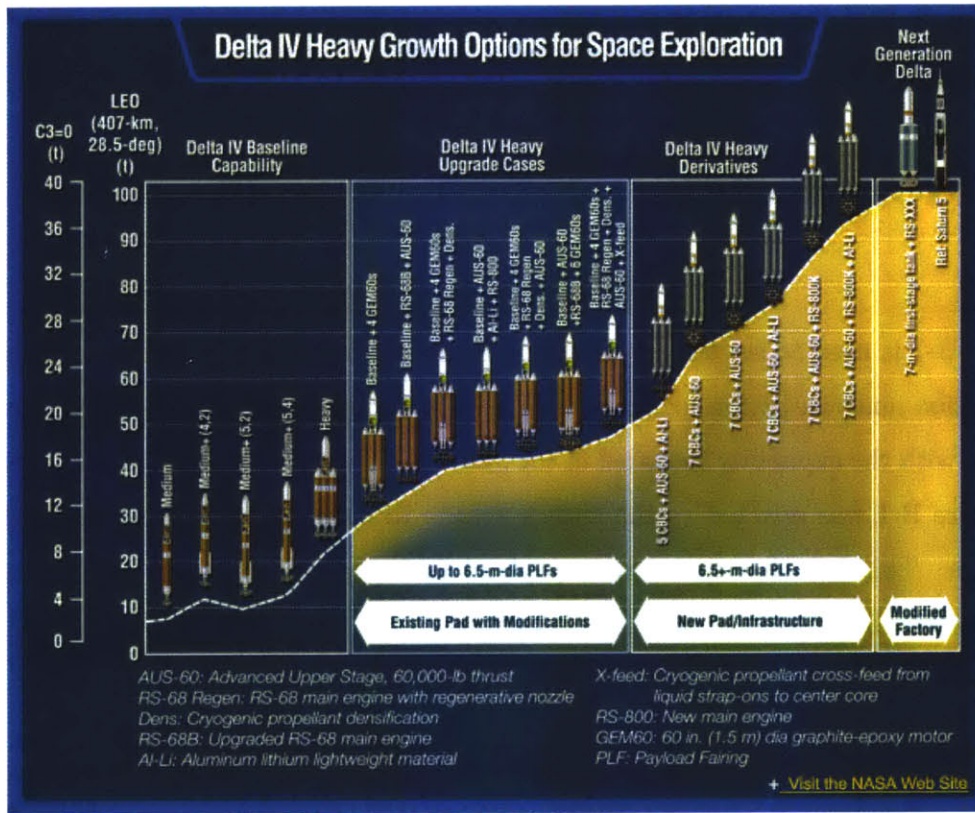
Figure B-1: Delta IV launch vehicle growth options [80].

3429-32